

**STUDY OF ELECTRONIC, STRUCTURAL AND
MAGNETIC PROPERTIES OF THE
DISORDERED SOLIDS**

THESIS SUBMITTED FOR THE DEGREE OF
DOCTOR OF PHILOSOPHY (SCIENCE)

IN

PHYSICS (THEORETICAL)

BY

AMBIKA PRASAD JENA

DEPARTMENT OF PHYSICS
UNIVERSITY OF CALCUTTA

SEPT., 2014

To the Family (Immediate & Extended) . . .

*For Encouragements throughout the Endeavour,
For Continuous push for tenacity,
For Instilling the Culture.*

Acknowledgements

“ Far better an approximate answer to the *right* question, which is often vague, than an *exact* answer to the wrong question, which can always be made precise.”

– John Tukey

At the final stage of this mental *odyssey* of mine, a little pause for a look back to relish is worth sustaining. This journey, as I remember it, has been quite tumultuous; crisis as a characteristic of the juvenile phase of life. At times steps has faltered and ideas got blurred by heedless thoughts. But during this, a constant source of inspiration that continued motivating me from the very beginning and through out, has come from my supervisor Abhijit Mookerjee (Professor Emeritus), to whom, I would like to express my sincere indebtedness for being more than generous with his expertise and precious time, and reasons not just confined to that for academics only. His persistence and scientific brilliance has enlightened me while always fascinated me is his humanly gentleness, something of him that is hard to fathom until having a direct interaction with him.

During these years *S.N. Bose National Centre for Basic Sciences* (SNBNCBS), Kolkata, India had been like a ‘second home’ – With all its relaxing atmosphere and lush greenery will enrich my treasure box of beautiful memories to cherish. I thank all its comprising members and congratulate them for upbringing and maintaining such a nice work place and productive research atmosphere. Their kind and *unbureaucratic* support and tireless willingness to help made the completion of my work an agreeable experience.

I sincerely thank Prof. Biplab Sanyal, Uppsala for his critical helps, discussions and suggestions during some parts of my research. I’m thankful to Prof. P. Mahadevan and Prof. T. SahaDasgupta, members of my annual review committee at SNBNCBS, for their suggestions and advices on research and approach to the field.

I am heartily thankful to my seniors and friends, who have shared a lots of quality time for my concerns, for sometimes entertaining, sometimes improvising and sometimes making me stronger for the hard realities of life by confrontations. And all at the end had been my pleasurable benefits. I could not have worked with a nicer and supporting group of fellows, that includes MoshourDa, MitaliDi, ShreemoyeeDi, RudraDa, GopiJi, Prashant, Rajeev and Tanumoy. Including but not limited to them are all those seniors and friends, few of them are strong coupling measures to this time-line of my life, few supported, few sustained and a few corroborated my dreams, who I don’t name here not inadvertently but deliberately as I fall sort of pages and my words lag my emotions – Thank you all to fit into my niche.

Last but not the least, I thank CSIR, India for in part financial support for the research.

— A.P. Jena,
Kolkata.

Publications

1. Study of disorder-order transitions in $\text{Fe}_x\text{Al}_{1-x}$ binary alloys using the augmented space recursion based orbital peeling technique.

Ambika Prasad Jena, Moshour Rahman, Abhijit Mookerjee
Physica B - Condensed Matter, Vol. 406, No. 20, pp. 3810-3815, 2011
DOI: 10.1016/j.physb.2011.06.075

2. Study of the effect of short ranged ordering on the magnetism in FeCr alloys.

Ambika Prasad Jena, Biplab Sanyal, Abhijit Mookerjee
Journal of Magnetism and Magnetic Materials, Vol. 349, pp. 156-158.
DOI: 10.1016/j.jmmm.2013.08.016

3. Study of the effect of magnetic ordering on order-disorder transitions in binary alloys.

Ambika Prasad Jena, Biplab Sanyal, Abhijit Mookerjee
Journal of Magnetism and Magnetic Materials, Vol. 360, pp. 15-20.
DOI: 10.1016/j.jmmm.2014.01.042

4. Effect of short range ordering on the magnetism in disordered FeAl alloy.¹

Tanmoy Ghosh, Ambika Prasad Jena, Biplab Sanyal, Hirosuke Sonomura, Takashi Fukuda, Tomoyuki Kakeshita, P.K. Mukhopadhyay, Abhijit Mookerjee
Journal of Alloys and Compounds, Vol. 613, pp. 306-311.
DOI: 10.1016/j.jallcom.2014.05.113

¹Not Included Explicitly in Present Thesis

Contents

Acknowledgements	iv
Publications	v
List of Tables	viii
List of Figures	ix
1 Introduction	1
1.1 Disordered binary alloys	2
1.2 Statistical Analysis	4
1.3 Main Objectives of the Present Study	5
1.4 Organization of the thesis	6
2 A Brief Rundown of Electronic Structure Claculations	7
2.1 Wave function Approach	11
2.2 Density Functional Theory(DFT)	13
2.2.1 Kohn-Sham Equation	14
2.3 General Band Structure Methods	17
2.4 Linear Muffin-Tin Orbital Method	18
2.4.1 Korringa, Kohn and Rostoker Method	22
2.4.2 Linearisation of MTO for Materials	24
2.5 The Recursion Technique	26
3 Study of Disordered Alloys	31
3.1 Introduction	31
3.2 Theories for the Study of random disordered alloys systems	33
3.2.1 Supercell Method	33
3.2.2 Mean-field Theory	34
3.2.3 Configuration Avearging	36
3.2.4 Augmented Space Recursion	37
3.2.5 Mathematical description of the configuration space	38
3.2.6 The augmented space theorem	40
3.2.7 Augmented space theorem for binary alloy	43
3.3 Effective pair Exchange interactions	45

3.4	Statistical Analysis	53
3.4.1	Ordering Energy	54
3.4.2	Monte Carlo Simulation	55
3.4.2.1	Detailed Balance	57
3.4.3	Glauber dynamics	59
3.4.4	Kawasaki dynamics	61
3.4.5	Finite Size Effect	62
3.4.6	Boundary Conditions	63
3.4.7	Code Implementation and practicalities	63
3.5	Results and Discussion	66
3.5.1	Density of states	66
3.5.2	Pair Energies and stability analysis	68
3.5.3	Monte Carlo simulation	73
3.6	Conclusion & Future Plans	74
4	Short Range Ordering in FeCr Alloys	76
4.1	Treatment of Short-range Ordering	77
4.2	Cluster Expansion	79
4.2.1	Notes on Generation of SQS	82
4.3	Computation of Magnetic Exchange Interactions	83
4.4	Results and Discussion	84
4.5	Conclusions & Future Plan	87
5	Inter-biasing of Multiple Ordering in Alloys	88
5.1	Mean-field Analysis	89
5.1.1	Mean-Field Solution	94
5.2	Computation of Exchanges	95
5.3	Inadequacies of Mean-field calculations	97
5.4	Monte Carlo Set up	98
5.5	MC Results	99
5.6	Conclusion & Future Plans	100
	References	101

List of Tables

3.1	Weights for different neighbouring shells for seven different bcc based equi-atomic superstructures.	70
-----	---	----

List of Figures

1.1	Schematic presentation of different types of disorders	3
2.1	Model of muffin-tin potential and overlapping spheres	19
3.1	Equilibrium phase diagram of $\text{Fe}_x\text{Al}_{1-x}$	32
3.2	DO_3 and derived superstructures for $\text{Fe}_x\text{Al}_{1-x}$	32
3.3	More DO_3 derived superstructures for $\text{Fe}_x\text{Al}_{1-x}$	33
3.4	Augmented space map for a square lattice	41
3.5	DOS for CrTi by ASR	46
3.6	DOS for $\text{Mo}_{50}\text{Nb}_{50}$, $\text{Mo}_{50}\text{V}_{50}$ and $\text{Mo}_{50}\text{W}_{50}$ by ASR	47
3.7	DOS for FeAu by ASR	48
3.8	DOS for $\text{Fe}_x\text{Al}_{1-x}$ by ASR	49
3.9	Phase space simple and importance sampling in MC	58
3.10	Skew-periodic boundary condition	64
3.11	Magnetisation of Ising model by MC	65
3.12	Partial and total DOS for $\text{Fe}_{50}\text{Al}_{50}$ by ASR compared with SQS	67
3.13	Pair energy functions against energy for $\text{Fe}_{50}\text{Al}_{50}$	68
3.14	EPI calculated for $\text{Fe}_x\text{Al}_{1-x}$ as function of $ \vec{R}_n $, for $x=0.25,0.5$ and 0.75 .	69
3.15	Ordering energies for seven bcc based super-structures for FeAl	69
3.16	The plane bounded by the lines (00h) and (kk0) in reciprocal space within the bcc Brillouin zone	70
3.17	$V(\vec{k})$ for $\text{Fe}_{25}\text{Al}_{75}$ shown as \vec{k} varies on the plane bounded by (top) (100) and (001) lines and (bottom) (001) and (110) lines	71
3.18	(left panels) $V(\vec{k})$ variation shown on the plane bounded by (001) and (110) in reciprocal space (top) 50-50 composition (bottom) 75-25 composition (right panels) projection of the left panel onto the plane bounded by (001) and (110) with contours.	72
3.19	Monte Carlo results for $\text{Fe}_{50}\text{Al}_{50}$ showing transition around $T_C = 1250^\circ\text{C}$.	73
3.20	Monte Carlo simulation of magnetic interactions for $\text{Fe}_{50}\text{Al}_{50}$ showing a paramagnetic stability for temperature as low as $T_C = 95^\circ\text{K}$	74
4.1	Schematic representation of short range ordering (left) Random binary alloy (middle) Positive correlation (right) Negative correlation	78
4.2	Schematic presentation of randomness of a small sqs cell(non-shaded) embodying average correlations of several apparently non-random configurations(shaded cells)	79

4.3	Illustration of ‘figures’ in a 2D lattice showing some pairs, triplets, and quadruplets with symmetric similitude in same colour	81
4.4	(left panel) Nearest neighbor exchange energies. Fe-Fe exchanges are much stronger compared to Fe-Cr and Cr-Cr exchanges over the entire concentration range. (right panel) Fe-Fe exchange as a function of distance.	85
4.5	Temperature variation of the Order parameter (left) for strongly ferromagnetic $Fe_{75}Cr_{25}$ shows equivalent natures for Monte Carlo runs from generated random structures and the adapted method of Monte Carlo simulation on SQS structures. For both structures super-cells of 1024 sites were considered. (right) For $Fe_{25}Cr_{75}$ the agreement is less than the previous case.	85
4.6	(Top left panel) Effect of SRO on the temperature variation of magnetization for the alloy $Fe_{50}Cr_{50}$. (Top right panel) Effect of SRO on the temperature variation of susceptibility. (Bottom left panel) Variation of T_C with SRO for the 50-50 alloy. (Bottom right panel) The variation of T_C with composition, and comparison with experimental data [Bur+83].	86
5.1	The mean-field behaviour of magnetic and chemical order parameters coupled. One of 50-50 alloy constituent is non-magnetic. (left panel) V is fixed and J is varied. Increasing J suppresses order-disorder transition temperature T_0 . (right panel) Here J is fixed and V is varied. With increasing V the magnetic critical temperature T_c is elevated.	93
5.2	Here both the constituents are magnetic. We show the behavior of the coupled magnetic and chemical order parameters at two compositions (left) 40-60 and (right) 60-40.	95
5.3	(left) Estimates of the nearest neighbour exchange energies $J^{QQ'}(R_0)$ and $V(R_0)$ for FeCo alloys obtained from the Lichtenstein formula implemented within the LMTO-CPA. (right) The spatial extent of the exchange energies.	96
5.4	(left) Finite size effect of two order parameters with system size $Fe_{50}Co_{50}$. (right) The shift of the ordering temperature caused by magnetic ordering for $Fe_{50}Co_{50}$	97
5.5	Defining atomic and spin variables in MC	98
5.6	(left) Two bumps in total energy for $Fe_{50}Co_{50}$ corresponding to two peaks in the specific heat which in turn indicates the two transitions taking place. (right) Variation of the Magnetic and Ordering transition temperatures of $Fe_{50}Co_{50}$ with composition. The experimental data has been taken from HANSEN [Han65] and OYEDELE and COLLINS [OC77].	99

Acronyms

ASF	Augmented Space Formalism
ASR	Augmented Space Recursion
bcc	Body Centred Cubic
CPA	Coherent Potential Approximation
DFT	Density Functional Theory
fcc	Face Centred Cubic
GPM	Generalized Perturbation Method
KKR	Korringa-Kohn-Rostocker
LDA	Local Density Approximation
LMTO	Linear Muffin-Tin Orbital
OP	Orbital Peeling
SQS	Special Quasi-Random Structure
SRO	Short-range Ordering
TB-LMTO	Tight-binding linear muffin-tin orbital

Introduction

An integral part of modern society development or ancient man's survival has understandably been centred on Metals, Metalloids and inter-metallics, since time immemorial, largely on account of their properties like strength, durability and tunability. Social developments and advancement has continuously bargained only for finer and sophisticated replenishments of increasing human needs. These requirement based tuning of the material characteristics from a limited set of elements in the periodic table has become possible by mixing them for different combinations, understanding their nature and manoeuvring for usages. The basic understanding, however, had very limited scope, in a era prior to the quantum mechanics and related theoretical developments, being the technicality was not instrumental enough to deal with the microscopic details of materials. It is easily observed that the multiphase mixtures are perplexed enough to follow the whatsoever purview of mixing. Alloy formation has been a technologically important sector which seeks and fortifies the theoretical understanding needed for the purpose of their processing and designing so as to impart their performance. The continuous efforts on theoretical part, specially, the post-quantum concepts corroborated by emergent computational power has provided tangible explanations for widely available experimental data. And together with all, the field has been ever blooming.

In a detailed understanding, it is often natural to expect environmental and force-field perturbations in the materials. Ideal smoothness and flawlessness qualities hardly sustain, rather various types of disorders creep in, and as a matter of fact disorder becomes the most *natural* order of arrangements to be expected. These deviations from idealness play crucially. All of these properties in the alloys stem from the chemical structure and magnetic interactions of the system. "The analysis involve two steps: a quantum mechanical determination of interactions in the solid and minimisation of the free energy expression obtained by the techniques of statistical mechanics." [Ber+88] Addressing these developments, we carried out the electronic structure calculations,

and correspondingly the chemical and magnetic properties analysis of random alloys which consequently enabled us to theoretically understand and reason the experimentally available phase diagrams.

1.1 Disordered binary alloys

After the eventful success in Quantum mechanics and its verifiable predictability one has a very little problem in understanding the mechanism of solid formation and the consequential dynamics involved. But typical to nature, the subtlety arises from various interactions and driving potentials like thermal agitation, concentration gradient etc. So what we encounter in our day-to-day life is not perfectly disciplined arrays of atoms filling an underlying lattice of some ordered structure, for which a concept of an abstract space, the reciprocal space comprised of the Bloch's basis, is completely broken to explain any of the electronic structure effects. The loss of translational symmetry, however, is not unique to this situation. Rather, the analysis of many non-disordered systems, like clusters (confined systems), surfaces (even for a ordered alloy) have the same kind of theoretical difficulties.

Disorder in solids, around the realm of crystalline structure, can be categorised, broadly, into two types: structural and substitutional. The manifestation of the disorder by the disruption of the topology of the lattice is known as the structural disorder, the description of which involves calculations of forces and movements of ions. The substitutional disordering is rather based on the chemical properties of the alloy acting on longer time scale. In substitutional disorder the underlying lattice remains unchanged, only the sites of which are randomly occupied by different species of atoms. In Fig.1.1, schematically shown 2D model of ordered and different disordered patterns. Although both types of disorder are often relevant, In this thesis we shall address only substitutional disordering due to chemical or magnetic instabilities. We will explore theoretical techniques applicable to these scenario. We have specifically looked into the binary alloys A_xB_{1-x} , where A and B are the constituent elements with corresponding concentrations x and $(1 - x)$ respectively.

To deal such kinds of disorder, configuration averaging of physical quantities is the most important and difficult part. This difficulty is overcome by introducing mean-field theories [ES76; Fau82; Pra92] . In these approaches, the disordered system is replaced by a lattice periodic effective medium, with *effective atoms* occupying lattice

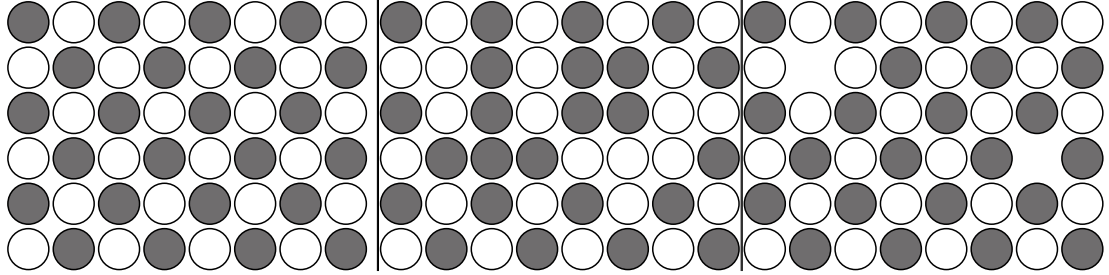


Figure 1.1: Schematic presentation of order and disorder by chemical substitution and vacancy formation leading to structural deformation

sites. The Coherent Potential Approximation is one of the most successful technique to evaluate the configuration averaging [Sov70]. However it is single-site mean field approximation. It cannot accurately take into account the local correlations leading to clustering or short-ranged order. Neither can it deal with disorder in the off-diagonal part of the Hamiltonian that arises, for example, when there is a large difference in the band widths of the constituents. With the realization of the need to go beyond the CPA, several attempts have been reported. Among them, the Travelling cluster approximation and Augmented Space Formalism (ASF) [Moo73a; Moo73b] are the only approaches which have been proved to be analytic, while preserving the conservation laws and sum rules. The ASF is originally developed in the tight binding framework provides self-consistent cluster coherent potential approximation in which one can go beyond CPA in the systematic way. The ASF, therefore, is a generalization of the CPA. We can introduce such approximations that short-ranged correlations are included and the essential properties like positive definite spectral densities and, in cases of homogeneous disorder, lattice translation symmetry of averaged quantities are all preserved. ASF is one of alternatives suggested for CPA because it goes beyond standard mean-field approximations to consider randomness not only at a site but also in its near neighbourhood.

In this thesis we have used both ASF and CPA in our calculations. The ordering effect in disordered alloys is studied using the Generalized Perturbation Method(GPM) [Tur+88]. The expansion coefficients are small energy differences of large magnitudes. We have chosen the Orbital Peeling(OP) method to accurately obtain such small energy differences. The GPM mapped our problem on to an effective Ising model for doing magnetic phase analysis of disordered systems under consideration.

The exchange interaction energy is also computed from CPA Green's function by Liechtenstein formulation [AHS99; Lie+87] using magnetic force theorem. For this,

Tight Binding Linear Muffin-tin Orbital Green Functions(TB-LMTO-GF) code is employed which works under the frame work of CPA technique.

1.2 Statistical Analysis

An accurate quantitative treatment of finite temperature instabilities of the alloy systems remains a challenge for the discussed *ab-initio* theories. From the exchange interactions so obtained, that bear the chemical signature of the atoms, the statistical properties of the system with atoms distributed on the underlying lattice has to be characterised. The mean-field analysis is, as always, necessary for the correct trend identification, though it has its own limitations, specially in both low and high limits of temperature. Spin wave theory for magnetic interactions are useful in low temperature regime where the quantum effects are prevalent. The alloy systems we carried out the studies on, as will see in proceeding discussions, have Ising type magnetic characters. The chemical composition of a binary alloy has already one-to-one correspondence with Ising model. Explicit cluster variation calculations are relatively laborious for the improvements over mean-field results. Instead, we have used rigorous computational numerical method widely used now-a-days, the Monte Carlo simulation to get results closer to the experiments. We employed several alterations to optimize the simulation by benefiting from modern computational architectures. The short-range ordering or the local chemical ordering of some alloys in some compositions become prominently active. Pure simulation is blind to this effect. We propose an assembled method of using Special Quasi-Random Structure (SQS) with Monte Carlo simulations to capture and quantify this effect.

Different types of interactions are analysed differently. But the fact remains that they have directly or indirectly, originated from the same electron cloud sitting on atoms of the alloy. We extend the mean-field analysis, in this light, to combine the different chemical and magnetic exchanges to govern a single dynamics. The increase in complexity, however, limits the approximations heavily. Motivated by the qualitative mean-field results, we expanded the Monte Carlo simulation for this coupled Hamiltonian and studied the dynamics.

1.3 Main Objectives of the Present Study

The main aim of the present thesis is to study the electronic and magnetic properties of disorder binary solids and the phase stabilities emerging from these properties. We carried forward the Tight-binding linear muffin-tin orbital (TB-LMTO) based Augmented Space Recursion (ASR) calculations. In conjunction with the Orbital Peeling (OP) method the exchanges interaction strengths of magnetic and atomic pairs were calculated. Disorder averaging based on the Coherent Potential Approximation (CPA) in LMTO basis was also considered in some cases for magnetic force theorem based Liechtenstein formulation to calculate the exchange interactions. And then we used several mean-field based approaches and Monte Carlo simulations and its ameliorations to deal with specific cases of alloys with signatures of theoretical complications. The work largely involved computational developments and computations. The objective of this thesis, on the outset, can be summarised like this:

- I. To study the electronic structure and magnetic properties of ordered alloys. Employing different methods of configuration averaging techniques to find ergodic properties.
- II. To study the atomic interactions of the alloy components by indirect methods to energy differences as to say, counting poles and zeroes of the Greenian or introducing small perturbations within the limits of magnetic force theorem or by a brute force cluster decomposition approaches.
- III. To study the phase change behaviours of alloys using the parametric information obtained by aforementioned *ab-initio* calculations. We use several direct mean field approaches to testify the experimental agreement. Then we step in to developing a fast Monte Carlo code with several programmatic tweaks to better use modern computer architecture. And use that for our ongoing phase transitions studies.
- IV. To study the role of Short-range Ordering (SRO) effect in alloy phase transitions from a statistical point of view. We contrived a method using Monte Carlo simulation algorithms and Special Quasi-Random Structures (SQSs) to obtain satisfactory insight.
- V. To study the inter-dependence chemical and magnetic phase-fields and the cumulative result on the phase diagram of alloys having suitable interaction strengths.

Owing to the limits of mean-field approaches, again we re-frame our Monte Carlo code for this coupled transitions and compare with experiments.

1.4 Organization of the thesis

The thesis has been organized as follows:

- I. In **Ch.2**, we shall briefly discuss, before delving into the studies carried in this thesis, the necessary theoretical framework of electronic structure calculations for solids.
- II. **Ch.3** deals with the development of inter-atomic exchange calculations and their analysis in the context of $\text{Fe}_x\text{Al}_{1-x}$ alloys. We'll discuss about the development of a rigorous Monte Carlo code with many possible optimisations to enhance the speed of the simulation. We'll standardise the results and compare with other calculations.
- III. In **Ch.4**, we discuss the aspect of the local ordering in disordered alloys quantitatively in terms of SRO and its effect. We shall bring in the SQS approach into the Monte Carlo simulations to account for SRO effects in alloys. We focus on the *FeCr* alloy system for its long standing experimental literature highlighting this effect recursively.
- IV. The existing chemical and magnetic phase transitions of an alloy may happen to come close enough to show some inter-dependence in terms of shifting in transition temperature. Starting from an Ising like coupled Hamiltonian we will look in to the problem and will then make some accurate numerical treatments by combined Monte Carlo simulations in **Ch.5**.

A Brief Rundown of Electronic Structure Calculations

Because a solid contains large number of electrons and nuclei in mutual interactions, the dynamics of these particles in general can not be considered separately. The interactions between the particles are Coulombic and their dynamics is in the regime of quantum mechanics. This produces a set of equations to solve that is increasingly tedious with the increase in system size and ultimately prohibitive for modelling an actual chunk of solid. We need some kind of decoupling scheme based on judicious assumptions so that the problem is manageable, yet the theory is congruous with the observed phenomena. Recent developments in the field of computation has a biasing effect on these theoretical evolutions. The conceptual efforts in the reduction of the problem has geared towards the better suitability of *computation*. Among the multitude of such approaches, we will start from the historic Hartee-Fock theory and then discuss aspect beyond the one electron approximation, in particular the Density Functional Theory (DFT) which has been unsurpassably successful for the ground-state properties of solids. Some of the classic texts, like that of GROSSO and PARRAVICINI [GP00] and MARTIN [Mar04] etc. among many others, provide extensive discussions and exhaustive references on the topic. Here, firstly we describe about the electronic properties of many electron system and the electronic band structure calculations. Our focus is on the specialized case of existence of disorder in the materials and appropriate methodologies necessary to model them. So our discussion would mainly go in that line to form a basis of the present study of electronic and magnetic properties of the *disordered binary alloys*.

Introduction

In the last decade many calculations on disordered alloys, based on semi-empirical tight binding Hamiltonian, have been reported. In spite of its encouraging success the electronic structure calculations based on the semi-empirical tight-binding Hamiltonian has some underlying approximations which are often unjustified [Pet72]. It calls the need for first principle theories of disordered alloy systems. During the last few years it has become clear that DFT in the Local Density Approximation (LDA) provides a sound and feasible, *ab-initio* theoretical basis for calculating ground state properties of pure metals and ordered compounds. A number of electronic structure methods within the frame-work of DFT-LDA exists in literature. While Korringa-Kohn-Rostoker(KKR) method [Kor47; KR54] and the Augmented Plane Wave(APW) method [Sla37] provide the most accurate electronic structure descriptions of solid, their energy linearised versions, *Linearized Muffin-Tin Orbital(LMTO)* method [AJ84] and the *Linearized Augmented Plane Wave(LAPW)* method [And75] are also widely applied because of their better computer tractability compared to their parent methods. The successful theoretical tools for understanding the electronic properties of disordered alloys is based on these first-principle electronic structure techniques in conjunction with mean field approaches like single site Coherent Potential Approximation(CPA)[Sov67]. Augmented space formalism (ASF) introduced by MOOKERJEE [Moo73a], within the framework of tight-binding LMTO, coupled with the recursion method of HAYDOCK, HEINE, and KELLY [HHK72] is another method which intrinsically does multi-site configuration averaging.

In the sections to follow, we will start our discussion with a theory capable enough to handle the atomic interactions, and yield some useful physical properties out of the available macroscopic knowledge of the system. Then off course, with all its limitations and restrictions, we would extend to the high temp regime where a statistical analysis is necessary for studying the room temperature behaviour.

Electronic structure determination

In the microscopic regime, the quantum mechanical laws are abided by the virtue of a fundamental equation, known as the Schrödinger wave equation:

$$\hat{\mathcal{H}}\Psi = E\Psi; \quad , \hat{\mathcal{H}}\Psi = i\hbar\frac{\partial\Psi}{\partial t}, \quad (2.1)$$

where $\hat{\mathcal{H}}$ is the Hamiltonian of the system that identifies the type of the system and $\Psi \equiv \Psi(\vec{r}, t)$ is known as the *wave function* of the system which contains all the information about the particular state of the system. However simple may the equation look, for many-body systems, it becomes immediately intractable, due to the high degrees of freedom involved, as soon as one tries to solve them. So without potential and scientific approximation it is of no use to give material properties of many electron systems.

The Hamiltonian for an interacting ensemble of M nuclei having N electrons reads in absence of any external potential, in atomic units, as

$$\hat{\mathcal{H}} = \underbrace{-\frac{1}{2} \sum_i^N \nabla_i^2}_{\hat{T}_e::\text{KE of Electrons}} - \underbrace{\frac{1}{2} \sum_I^M \frac{\nabla_I^2}{M_I}}_{\hat{T}_N::\text{KE of Nuclei}} - \underbrace{\sum_i^N \sum_I^M \frac{Z_I}{r_{iI}}}_{\hat{V}_{ext}::\text{Ion-El. Int. En.}} + \underbrace{\sum_i^N \sum_{j>i}^N \frac{1}{r_{ij}}}_{\hat{V}_{int}::\text{EL-El Int. En.}} + \underbrace{\sum_{I>J}^M \frac{Z_I Z_J}{r_{IJ}}}_{\hat{V}_{NN}::\text{Ion-Ion Int. En.}}, \quad (2.2)$$

where atomic units are used (*i.e.*, $\hbar = m_e = 1$), the symbols have their usual meanings and lowercase and uppercase indices are used, respectively, for electronic and nuclear labels. The distances, for example, are defined like: $r_{ij} = |\vec{r}_i - \vec{r}_j|$, $r_{i,I} = |\vec{r}_i - \vec{R}_I|$ and $r_{I,J} = |\vec{R}_I - \vec{R}_J|$. Hence the terms \hat{V}_{II} and \hat{V}_{eI} are the Coulomb interactions between the ion-ion and between the electrons and ions. r_{ij} is the distance between the i^{th} and the j^{th} electron. The terms \hat{V}_{ext} makes the term inseparable. The energy terms related to the spin and magnetic moments of the particles in the interaction are omitted.

This equation is exactly solvable for H-atom. And variational or perturbative approach give very close results for smaller systems like the three body problem of He^+ . The analytical solution of this equation is tedious and almost impossible for larger systems though the mathematical solution of it for single atom and very small molecules are available. In order to solve this equation analytically some reasonable and well controlled approximations has to be done so that we can be able to handle most of the systems exist in nature.

Born-Oppenheimer Approximation The equation 2.2 is complex to solve because it deals with a large number of interacting ions and electrons. For a truly many body systems ($Z \geq 4$ as a rule of thumb) the very first approximation is the reputed *Born-Oppenheimer*(BO) approximation[BO27] which basically stems from the quantum adiabatic theorem. Roughly speaking, the theorem states that a physical system remains in its instantaneous *eigenstate* if a given perturbation is acting on

it slowly enough and if there is a gap between the eigenvalue and the rest of the Hamiltonian's spectrum.[BO27; Wik14] So the adiabatic theorem in quantum theory helps decoupling the Hamiltonian and its perturbative component, if the switch-on of the energy difference is sufficiently slow. This *adiabatic* condition characterized by gradual change in the external conditions is satisfied due to very different masses involved here. Since ions are much heavier than electrons ($m_e : M_I :: 1 : 1836$ for Hydrogen atom), they move much slower compared to electrons so that the ionic motion is instantaneously responded by the electronic motion. In essence these degrees of freedom can be decoupled and the electronic properties can be calculated by assuming that the ions are fixed to a particular configuration(frozen ion-core). This is the Born-Oppenheimer approximation, also known as the *adiabatic approximation*, within which one necessarily solves only the electronic part of the Hamiltonian with parametrised ionic positions.

Following this approximation, the kinetic energy of ions can be neglected and the ion-ion interaction is assumed to be constant. The constant term is called **Madelung energy** and is calculated classically. So under B-O approximation, the many-body Hamiltonian for a system of N interacting electrons moving in the field of fixed ion cores can be expressed as,

$$\hat{\mathcal{H}}_{\text{BO}} = \hat{T} + \hat{V} + \hat{V}_{\text{ext}}.$$

$\hat{\mathcal{H}}_{\text{BO}}$ is the Born-Oppenheimer Hamiltonian with KE \hat{T} , electron-electron interaction energy \hat{V} and the only system specific potential energy \hat{V}_{ext} . The total energy of the system so obtained, at the zero temperature, where all phonon modes are in the ground state, is a sum of electron and nuclear Zero point energies.

$$\hat{\mathcal{H}} = -\sum_{i=1}^N \frac{\nabla_i^2}{2m} - \frac{1}{2} \sum_{i,I} \frac{1}{|\vec{R}_I - \vec{r}_{ij}|} + \sum_{i>j} \frac{1}{|\vec{r}_i - \vec{r}_j|} \quad (2.3)$$

The wave function may then be written in a separable form $\chi(\{\vec{R}_I\})\psi(\{\vec{r}_i\}|\{\vec{R}_I\})$. Thus, the Schrödinger equation for the electrons (for a given position of the ion cores $\{\vec{R}_I\}$) can be written as:

$$\left[-\sum_{i=1}^N \frac{\nabla_i^2}{2m} + V_{eI}(\{\vec{r}_i\}|\{\vec{R}_I\}) + \frac{1}{2} \sum_{i,j} \frac{1}{r_{ij}} \right] \psi(\{\vec{r}_i\}|\{\vec{R}_I\}) = E_e(\{\vec{R}_I\})\psi(\{\vec{r}_i\}|\{\vec{R}_I\}) \quad (2.4)$$

It's admittedly an inordinate simplification, nonetheless, the remained is a many-

body *eigen* value problem where “many” is quantitatively of the order of Avogadro’s number (\mathcal{N}_a). Several methods have been developed in order to reduce this equation to an approximate but much simpler set of equations. The most widely used one uses the spirit of Classical mechanics of transforming many-body problem into effective single body problem.

Single-Particle Approximation

The problem in trying to solve the Eqn. 2.4 is posed by the number of variables involved. Moreover, the interpretation of the solution is a ‘difficult’ problem itself. To quote Feynman “The trouble with quantum mechanics is not only in solving the equations, but in understanding what the solutions mean.” Attempts to solve these problems due to the immensely large number of variables and lack of easy interpretation has led to the development of newer and advanced approaches. Efforts have been put, therefore, to develop an effective single-particle picture, in which the system of interacting electrons can be mapped into a system of non-interacting quantum mechanical particles that approximates the behaviour of the original system. Two distinct approaches have been put forward in this direction: wave function approach and density functional theory.

2.1 Wave function Approach

Numerical solution of multi-variable quantum problems poses as its main difficulty, the electron-electron Coulombic interactions that tie all the variables together. Some of the major variational methods, like Hartree method, Hartree-Fock approximation, Cluster variation method etc. are based on the mean-field approach to this potential experienced by electrons.

The Hartree method [Har28a; Har28b; Har28c; Har29] is one of the first approximations that tried to deal with these complexities by expressing the many-body wave function as a product of independent single-electron functions $\{\phi_i(\vec{r}_i)\}$.

$$\psi_H(\vec{r}_1, \vec{r}_2, \dots, \vec{r}_n) = \phi_1(\vec{r}_1)\phi_2(\vec{r}_2) \dots \phi_n(\vec{r}_n)$$

The single electron wave function $\phi_i(\vec{r})$ can be obtained by minimizing the total energy

subjecting to normalization condition,

$$\int \phi_i^* \phi_i dr = 1$$

The Hartree approximation is a straightforward task to calculate the variational lowest energy. However, the Hartree wave function has a very important shortcoming; It ignores the anti-symmetric characteristic of the all electron wave functions. Anti-symmetry attributes fermionic wave-function a change of sign under odd permutations of the electronic variables. This approximation can only take into account the electron-electron Coulomb repulsion in a mean-field way, but it neglects the exchange and correlation properties completely.

The approximation that overcomes the non-inclusion of the antisymmetric character of electronic wave function is the Hartree Fock theory, introduced by FOCK [Foc30]. The wave function in this approximation is expressed in terms of single Slater determinant [Sla37] of N spin-orbitals, as

$$\psi_{\text{HF}} = \frac{1}{\sqrt{N!}} \begin{vmatrix} \phi_1(\vec{r}_1, s_1) & \phi_2(\vec{r}_1, s_2) & \cdots & \phi_n(\vec{r}_1, s_n) \\ \phi_2(\vec{r}_2, s_1) & \phi_2(\vec{r}_2, s_2) & \cdots & \phi_n(\vec{r}_n, s_n) \\ \vdots & \vdots & & \vdots \\ \phi_n(\vec{r}_n, s_1) & \phi_n(\vec{r}_n, s_2) & \cdots & \phi_n(\vec{r}_n, s_n) \end{vmatrix} \quad (2.5)$$

Now the Hamiltonian in the Hartree-Fock approximation can be expressed in terms of $\phi_i(\vec{r})$ as,

$$\left(\frac{\nabla^2}{2} + V_{\text{ext}} + V_H + V_x \right) \phi_i = \varepsilon_i \phi_i$$

The first two terms are the kinetic energy and the electron-ion potential energy. The third term, or the *Hartree* term, is simply the electrostatic potential arising from the charge distribution of N electrons. This term includes an unphysical self-interaction of electrons when $j = i$. This term is subdued by the fourth, or *exchange* term. This term results from the inclusion of the Pauli principle and the assumed determinantal form of the wave function. The effect of exchange is for electrons of like-spin to avoid each other. Each electron of a given spin is consequently surrounded by an “exchange hole”, a small volume around the electron which the like-spin electrons avoid. V_x is difficult to derive in practice because it is non-local and related to the interaction between all electrons in the system. In agreement with the variational principle, the Hartree-Fock energy E_{HF}^0 is higher than the exact ground state energy E_{exact}^0 of

the many body system and the difference $E_{\text{exact}}^0 - E_{\text{HF}}^0$ is called the correlation energy. Hartree-Fock(HF) Approximation does not include the electron correlation part to the multi-electron wave function, which plays an important role in the electronic structure and binding of many solids. In spite of the importance and achievements of the Hartree-Fock approximation, corrections beyond it are often considered due to the fact that a single determinantal state, even with the best possible orbitals, remains in general a rather poor representation of the complicated ground state wave function of a many-body system. Extended versions of HF emerges from systematic and *well-defined* improvements to the original approximation and hence believably more precise. But these one-electron approximations and their extended versions that rely on mixing of the many-electron wave functions are extremely computationally intensive and scale badly(with 4th to 6th power of the increasing number of electrons) with the system size.

2.2 Density Functional Theory(DFT)

By the time while wave-function approaches were continuously being improved and generalised, a all total different approach to the problem had formally evolved with the possibility of a density description of many-electron systems, leading to the so called Density Functional Theory (DFT). Although the first DFT, viz. The Thomas Fermi method has existed since 1927, the birth of modern DFT has been through the formal proof of two theorems by HOHENBERG and KOHN [HK64](HK) in 1964. This developed the quantum mechanics of many-electron systems in reduced space by establishing density as the basic variable, hence totally bypassing the wave function. The first theorem showed a **one-to-one** correspondence between the ground state electron density $\rho(\vec{r})$ of an interacting many-electron bound system and the external potential $V_{\text{ext}}(\vec{r})$ while the second theorem expressed the total energy represented by the Hamiltonian as a functional of the density. A given $\rho(\vec{r})$ determines the corresponding potential V_{ext} uniquely, or at most up to an ‘uninteresting’ additive term. If $v(\vec{r})$ is fixed, the Hamiltonian and hence the wave functions are also fixed by the density $\rho(\vec{r})$. Since the wave function is a functional of density, the energy functional $E_V[\rho]$ for a given ion-core-electron potential $V_{eI}(\vec{r})$ is a unique functional of density. It can also be directly proved that this energy functional assumes a minimum value for the true density. Following the HK theorem, the energy functional can be expressed in the form as,

$$\begin{aligned}
E^{(\text{HK})}[\rho] &= \langle \Psi | \hat{T} + \hat{V} | \Psi \rangle + \langle \Psi | V_{\text{ext}} | \Psi \rangle \\
E^{(\text{HK})}[\rho(r); v_{\text{ext}}] &= T[\rho(r)] + V_{ee}[\rho(r)] + \int v_{\text{ext}}(\vec{r}) \rho(\vec{r}) \, d\vec{r} \\
&= F_{\text{HK}}[\rho] + \int \rho(\vec{r}) V_{\text{ext}}(\vec{r}) \, d\vec{r}. \tag{2.6}
\end{aligned}$$

The energy functional $E^{(\text{HK})}[\rho(\vec{r}); v_{\text{ext}}]$, which exists and is unique, is minimal at the exact ground state density and its minimum gives the exact ground state energy of the many-body electron system corresponding to v_{ext} . Here $F_{\text{HK}}[\rho] = T[\rho(\vec{r})] + V_{ee}[\rho(\vec{r})]$ is the universal (*i.e.*, it doesn't depend on v_{ext}) Hohenberg-Kohn functional for any many-electron system. If F_{HK} can be assumed approximately, by Rayleigh-Ritz variational method $E^{\text{HK}}[\rho]$ can be minimized to the ground state energy wrt the ground state density $\rho(\vec{r})$. Unfavourably $F_{\text{HK}}[\rho]$ is not known explicitly and must be approximated appropriately.

Though HK theorem gives a one-to-one correspondence between $\rho(\vec{r})$ and the ground state wave function ψ_0 , it had few limitations, like (a) there is no prescription to determine ψ_0 for a given ρ_0 , (b) it is not applicable to degenerate state. In a rather generality, the V-representability of the density $\rho(r)$ can be avoided. In a series of papers, LEVY [Lev79] and LIEB [Lie83] introduced an alternative definition of the HK theorems. This is a two step minimization, where instead of considering the full N-particle Hilbert space for the trial density, the search is constrained only to the space of trial wave functions that give the density $\rho_0(\vec{r})$.

2.2.1 Kohn-Sham Equation

Hohenberg-Kohn theorem does not suggest a way of approximating the HK functional and in turn to calculate the ground state density. One method of approach to this problem is that by KOHN and SHAM [KS65]. Kohn-Sham equations are obtained by minimizing the energy functional 2.6 with respect to $\rho(\vec{r})$. They introduced a wave function basis Ψ_i , with

$$\rho(\vec{r}) = \sum_i^N \Psi_i^*(\vec{r}) \Psi_i(\vec{r}), \tag{2.7}$$

where N is the number of electrons, serves necessarily as a constraint from the physicality of the system. The orthonormalization of the Kohn-Sham wavefunctions is

expressed as

$$\int \Psi_i^*(\vec{r})\Psi_j(\vec{r}) d\vec{r} = \delta_{ij} .$$

The Hohenberg Energy functional is re-expressed in terms of the Hartree energy and exchange-correlation energy as:

$$E[\rho] = T[\rho] + V_H[\rho] + V_{XC}[\rho] + V_{ext}[\rho]$$

Variation in energy is a result of the variation in the density of the electron.

$$\delta E[\rho(\vec{r})] = \delta \sum_{ij} \epsilon_{ij} \int \Psi_i^*(\vec{r})\Psi_j(\vec{r}) d\vec{r},$$

where Lagrange multipliers ϵ_{ij} ensure the ortho-normality of wave functions. Minimization of this equation wrt $\rho(\vec{r})$ subject to the constraint of normalized density, as given by Eqn.(2.7), leads to the Euler equation for the direct calculation of density. The essence of the problem now is to obtain an expression for the energy functional in terms of density which has the general form

$$\left[\hat{T} + \hat{V}_H + \hat{V}_{XC} + \hat{V}_{ext} \right] \Psi_i(\vec{r}) = \epsilon_i \Psi_i(\vec{r}). \quad (2.8)$$

This set of *Schrödinger like* equations, is called as the **Kohn-Sham**(KS) equations. $T_s[\rho]$ is the kinetic energy of a system of non-interacting particles. The other part of the exact kinetic energy functional $T[\rho]$ is the contribution from the electron-electron interaction energy other than the classical electrostatic contribution. This difference $T[\rho] - T_s[\rho]$ constitutes the non-classical component what is known as the exchange-correlation (xc) energy functional $E_{xc}[\rho]$. Thus E_{xc} is simply the sum of the error made in treating the electrons classically and in the error made in using a non-interacting kinetic energy. We note at this point that the nomenclature in general use and also used in the present context, exchange-correlation (xc) energy functional is quite misleading for as stated above the E_{xc} contains an element of the kinetic energy and is not the sum of the exchange and correlation energies. The differential of E_{xc} in the point ρ is the exchange-correlation functional $\hat{V}_{XC} = \frac{\partial E_{xc}}{\partial \rho}$ where the density ρ is given by

$$\rho(\vec{r}) = \sum_{i=1}^N |\psi(\vec{r})|^2 ,$$

ψ_i being the N lowest eigen function of the KS equation.

This set of non-linear equations (the Kohn-Sham equations) describes the behaviour of non-interacting “electrons” in an effective local potential. For the exact functional, and thus exact local potential, the “orbitals” yield the exact ground state density and corresponding energy. The Kohn-Sham approach gives an exact correspondence of the density and ground state energy of a system consisting of non-interacting Fermions within the Born-Oppenheimer approximation. The correspondence of the charge density and energy of the many-body and the non-interacting system is only exact if the exact functional is known. Every terms in the Kohn-Sham Hamiltonian is known, in principle, except the exchange-correlation term, which we do not know and have no way of systematically approaching. However the functional is universal - it does not depend on the materials being studied. For any particular system we could, in principle, solve the Schrödinger equation exactly and determine the energy functional and its associated potential.

The simplest one of several available approximations to the exchange-correlation energy is the Local-Density Approximation(LDA) in which one constructs E_{xc} from the exchange-correlation energy per atom at \vec{r} in an inhomogeneous electron gas $\varepsilon_{xc}(\rho(\vec{r}))$, which is given by that of the homogeneous electron gas with the density ρ i.e., $E_{XC} \approx \int \rho(\vec{r})\varepsilon_{xc}(\rho(\vec{r})) d\vec{r}$. Based on interpolation formulas, LDA is parametrized in several ways to match exact experimental results, like Wigner, Kohn and Sham, Hedin and Lundqvist, Vosko Wilk and Nussair, Pedrew and Zunger. However, this approximation is suitable for systems where the electron density is uniform. Inclusion of spin degree of freedom is quite straight forward which just involves two set of solutions of the KS equation, leading to two electron densities: ρ_{\uparrow} and ρ_{\downarrow} for spin $+1/2$ and $-1/2$. The corresponding approximation for $E_{XC}[\rho_{\uparrow}, \rho_{\downarrow}] \approx \int \rho(\vec{r})\varepsilon_{xc}(\rho_{\uparrow}, \rho_{\downarrow}) d\vec{r}$ is known as the Local Spin-Density Approximation (LSDA). There has been several improved approaches in approximating the real form of the term E_{xc} , even beyond LDA like Generalized Gradient Approximation (GGA), meta GGA etc., all of which vary very little but improve results significantly. For the maturation of these related algorithms, taken with the substantial developments in computing, last decades have witnessed explosive growth in the use of DFT methods in material sciences.

2.3 General Band Structure Methods

The distribution of electrons and hence the change in density often determines the success of the method applied. A strongly bound electron to the nucleus can not be treated same way as a comparatively weakly bound electron responsible for chemical bonding and other properties like optical, thermodynamic etc. In order to solve the single-particle Kohn-Sham and to obtain the *eigenvalues* (band structure) and *eigenfunctions*, a number of methods have been introduced. These are based on approaches using either reciprocal or real space and applicable to both finite systems such as molecules or clusters as well as extended systems such as disordered solids, surfaces and interfaces. In the discussions above we have ignored the practical inconvenience of using a single-electron wave function constructed out of the complete set of wave functions. There are various types of basis sets reported and we have to choose an appropriate basis set to expand the single-particle wave-functions. The existent several choices of approximating the wave function bases set, all aiming at being computationally efficient in addition to agreeing with the physical behaviours of the actual wave functions for the given problem, fall, in general, into one of the two approaches. (i) The first describes the wave function in terms of matching partial waves, more suitable for periodic crystalline systems. The basis set is non-linearly energy dependent resulting a matrix equation that demands, especially for rapidly varying electron core densities, huge computational resources. These methods include cellular method [PK59], Augmented Plane Wave (APW) method [Lou67] and the Korringa-Kohn-Rostocker (KKR) Green's function method [Kor94]. (ii) While the second uses a linear combination of fixed energy independent basis functions such as atomic orbitals like tight binding method using Linear Combination of Atomic Orbitals (LCAO) type basis [SK54], orthogonalized plane wave (OPW) method that uses a set plane waves orthogonalized to core states within a pseudo-potential scheme. The plane wave basis set is inherently suitable for periodic lattices (systems obeying the Bloch's theorem) whereas the localized basis set is suitable for molecules, clusters etc. Though it takes less computational time, a judicious choice of appropriate basis set is crucial. For example within the muffin tin approximation to the potential, a fixed basis set can be constructed from partial waves and their (first \Rightarrow LMTO, $N^{\text{th}} \Rightarrow$ NMTO) energy derivatives. This is commonly known as the *linear methods* of ANDERSEN [And75]. It is the most suitable in our analysis and we'll continue the discussion on the TB-LMTO basis set and the formulation.

2.4 Linear Muffin-Tin Orbital Method

Muffin tin orbitals (MTOs) aim to provide a minimal basis of accurate meaningful orbitals which are constructed from the Kohn-Sham Hamiltonian. The tight binding linear muffin-tin orbital (TB-LMTO) method is a specific implementation of density functional theory within the local density approximation (LDA) [Skr85]. In the discussion of this part we will closely follow that of the excellent book on the topic *The LMTO method: muffin-tin orbitals and electronic structure* by SKRIVER [Skr11]. In this method there is no shape approximation to the crystal potential, unlike methods based on the atomic-spheres approximation (ASA) where the potential is assumed to be spherically symmetric around each atom. For mathematical convenience the crystal is divided up into regions inside muffin-tin spheres, where Schrödinger equation is solved numerically, and an interstitial region. In all LMTO methods the wave functions in the interstitial region are Hankel functions. Each basis function consists of a numerical solution inside a muffin-tin sphere matched with value and slope to a Hankel function tail at the sphere boundary. The so-called multiple-kappa basis is composed of two or three sets of s, p, d, etc. LMTOs per atom. The extra variational degrees of freedom provided by this larger basis allow for an accurate treatment of the potential in the interstitial region.

Muffin-Tin Potential The first approximation in using atomic sphere method, is that the potential in the crystal has a local spherical symmetry and extremity at potential in interstitial space. This approximation is called Atomic Sphere Approximation(ASA) cf. Fig.2.1. So in effect, the solid is divided into a group of Wigner-Seitz spheres so that we only need to sum up the energies in each Wigner-Seitz cell. In practice one has to increase the size of the atomic spheres used by Muffin Tin potential or add, if necessary, new “vacuum” spheres to the interstitial region so that the total volume of all the spheres equals that of the solid cell. As the sphere can not fill the space, some interstitial space in which the Kinetic energy is completely neglected and some overlapping region (up to around 18%) are tolerated.

The basic assumption of muffin-tin orbital is that in the neighbourhood of an ion-core the potential seen by the electron in a solid is not very different from that of the atomic ion-core. This neighbourhood is spherically symmetric with radius S centred at R . In the interstitial region the potential is flat, called Muffin-Tin Zero (V_{MTZ}).

Inside the muffin-tin of R^{th} atomic sphere of radius S , the spherically symmetric

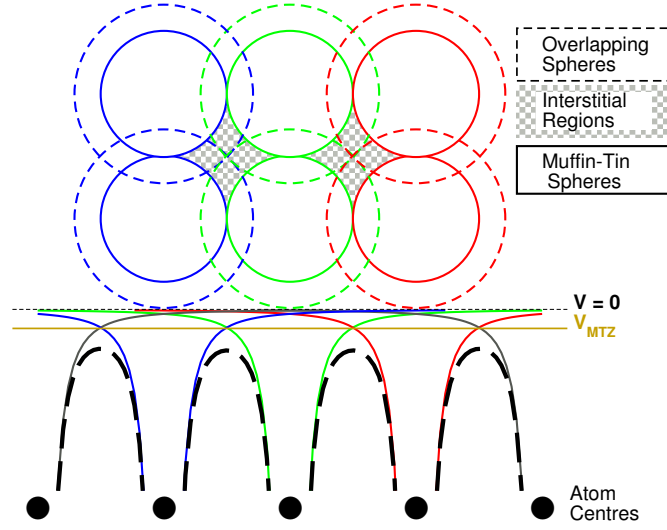


Figure 2.1: Model of muffin-tin potential and overlapping spheres

potential at any point \vec{r} is defined as

$$V_{\text{MT}}(\vec{r} - \vec{R}) = \begin{cases} v(|\vec{r} - \vec{R}|) - V_{\text{MTZ}} & r \leq S \\ 0 & r \geq S \end{cases} \quad (2.9)$$

Thus Hamiltonian can be rewritten as:

$$H = \nabla^2 + \sum_{\vec{R}} V_{\text{MT}}(|\vec{r} - \vec{R}|) - \kappa^2 + E \quad (2.10)$$

where κ is the kinetic energy in the extended region, $\kappa^2 = E - V_{\text{MTZ}}$. The single-electron wave function can be expressed in any basis, call it MT orbitals $\{\chi(\vec{r} - \vec{R})\}$ here, as

$$\Psi(\vec{r} - \vec{R}) = \sum_i C_i \chi_i(\vec{r} - \vec{R})$$

The Boundary conditions satisfied by the wave-function construct the set of MT-Orbitals. In single-site approximation, one considers a single sphere in the whole space, these boundary conditions are: (a) $\{\chi(\vec{r} - \vec{R})\} \rightarrow (\text{finite})$ as $(\vec{r} - \vec{R}) \rightarrow 0$, (b) $\{\chi(\vec{r} - \vec{R})\} \rightarrow 0$ as $(\vec{r} - \vec{R}) \rightarrow \infty$ (c&d) logarithmic derivative of $\{\chi(\vec{r} - \vec{R})\}$ must be continuous at the sphere boundary. And in addition, by the rotational invariance or the spherical symmetric nature of the potential, the solution is separable in to radial ($\psi_l(|\vec{r} - \vec{R}|)$)

and angular components :

$$\Psi(\vec{r} - \vec{R}) = \sum_{lm} \psi_l(|\vec{r} - \vec{R}|) Y_l^m(\widehat{\mathbf{r} - \mathbf{R}}).$$

Inside the interstitial region ($r \geq S$), the potential is a level shifting constant (V_{MTZ}) which can be set to zero in Eqn.2.10 so that it is just a Laplace equation. This leads to the well-known radial form of Laplace Equation:

$$\left[-\frac{d^2}{dr^2} + \frac{l(l+1)}{r^2} \right] r\psi_l(E, r) = 0 \quad (2.11)$$

This has been solved numerically for radial solution $\psi_l(E, r)$ written in terms of Bessel function (regular solution) and Hankel function (irregular solution).

In the atomic sphere, the radial part of the one-particle Schrödinger equation has the form

$$\left[-\frac{d^2}{dr^2} + \frac{l(l+1)}{r^2} + v(\vec{r}) - E \right] r\psi_l(E, r) = 0 \quad (2.12)$$

Solution of this equation is analysed in the asymptotic limit, *i.e.*, behaviour for $r \rightarrow 0$, where $v(\vec{r}) - E$ can be dropped and we get two solutions, the regular one $\psi_l(E, r) \propto r^l$ and the irregular one $\psi_l(E, r) \propto r^{-l-1}$. Under physical requirement that inside the atomic sphere the MTO should remain finite, only regular solution is retained as $r \rightarrow 0$.

The complete wave function is thereby given as:

$$\psi_L(\epsilon, \kappa, \vec{r}) = {}^l Y_L(\hat{\mathbf{r}}) \begin{cases} \psi_l(\epsilon, \vec{r}) + \kappa \cot(\eta_l(\epsilon)) j_l(\kappa r) & r \geq S \\ \kappa \eta_l(\kappa r) & r \leq S \end{cases} \quad (2.13)$$

with MT basis set

$$\chi_L^{\text{MTO}}(\epsilon, \kappa, \vec{r}) = {}^l Y_L(\hat{\mathbf{r}}) \begin{cases} \psi_l(\epsilon, \vec{r}) + \kappa \cot(\eta_l(\epsilon)) j_l(\kappa r) & r \leq S \\ \kappa \eta_l(\kappa r) & r \geq S \end{cases} \quad (2.14)$$

where S is the muffin-tin sphere radius. j_l and η_l are the spherical Bessel functions

and the spherical Neumann functions, respectively, defined as

$$j_l(\kappa r) \rightarrow \begin{cases} \frac{(\kappa r)^l}{(2l+1)!} & \kappa r \rightarrow 0 \\ \frac{\sin(\kappa r + \frac{l\pi}{2})}{\kappa r} & r \rightarrow \infty \end{cases}, \quad \eta_l(\kappa r) \rightarrow \begin{cases} -\frac{(2l-1)!}{(\kappa r)^{2l+1}} & \kappa r \rightarrow 0 \\ -\frac{\cos(\kappa r + \frac{l\pi}{2})}{\kappa r} & r \rightarrow \infty \end{cases}. \quad (2.15)$$

It's evident that j_l is regular both at origin and at ∞ , whereas η_l is regular at ∞ only and diverges at the origin. This yields a bound state envelop function which is real, and regular both inside (since $j_l(\kappa r)$ is regular at origin) and outside (since $\eta_l(\kappa r)$ is regular at infinity) the sphere. The inclusion of $j_l(\kappa r)$ in the single particle basis set includes the effect of neighbours so that the minimal basis set is capable of describing the full system.

The wave function at energy E can be written as

$$\psi_j(\vec{k}, \vec{r}) = \sum_{lm} b_{Rlm}^{jk} \psi_{Rl}(E, |\vec{r} - \vec{R}|) {}^l Y_l^m(\widehat{\mathbf{r} - \mathbf{R}}) \quad (2.16)$$

where b_{Rlm}^{jk} is the expansion coefficient of the partial wave, Y_l^m is a spherical harmonics, l is a phase factor (phase conventions used for spherical harmonics as of 'The Theory of Atomic Spectra' [CS35]). Wigner and Seitz [WS34] suggested the spherically symmetric potential to extend until the boundary of atomic polyhedron. The wave functions in solid is then expressed as Bloch sum

$$\psi_j(\vec{k}, \vec{r}) = \sum_R e^{i\vec{k} \cdot \vec{R}} \sum_{lm} b_{lm}^{jk} \delta(\vec{r} - \vec{R}) \psi_l(E; |\vec{r} - \vec{R}| {}^l Y_l^m(\widehat{\mathbf{r} - \mathbf{R}})) \quad (2.17)$$

where $\delta()$ inside atomic sphere is unity and zero outside. Though this cellular method turned out to be too tough for applying boundary conditions, it gave rise to KKR (named after Korringa, Kohn and Rostoker) (and LMTO) method and Wigner-Seitz rule of energy band. Slater in his Augmented Plane-wave(APW), inscribed a muffin-tin(MT) sphere in each atomic sphere. Inside the sphere, the potential is spherically symmetric and wave functions are expanded as Wigner-Seitz partial wave. KORRINGA [Kor47] and later KOHN and ROSTOKER [KR54] expand the MT spheres similar to cellular and APW. The interstitial potential is flat and wave functions are expanded as phase shifted spherical wave. Boundary conditions are expressed as condition for self-consistent multiple scattering between the MT spheres. ANDERSEN [And75] *linearised*

this method which is one of the most used method of solving the KS equation.

2.4.1 Korringa, Kohn and Rostoker Method

In the KKR-ASA, muffin-tin(MT) and interstitial region is divided into overlapping atomic spheres (AS's). The total volume of the AS's thus equals the total crystal volume. Any point \vec{r} in the space is denoted by (\vec{r}, R) , where R is the index for th AS and $\vec{r} = (r, \hat{r}) = (r, \theta, \phi)$ ($r < R$) is the vector denoting the position in each AS. R denotes the radius of AS and here ϕ is azimuthal angle.

Starting point for KKR is a fixed basis set of energy dependent muffin-tin orbitals(MTO) defined as

$$\chi_{lm}(E, \vec{r}) = {}^l Y_l^m(\hat{r}) \begin{cases} \psi_l(E, r) + p_l(E)(r/S)^l & r < S \\ (S/r)^{l+1} & r > S \end{cases} \quad (2.18)$$

where $\psi_l(E, r)$ is the solution of radial Schrödinger's equation inside an atomic sphere of radius S . Y_l^m are standard spherical harmonic. This muffin-tin orbital(MTO) is regular, continuous and differentiable over all space. The potential function $p_l(E)$ and normalization of $\psi_l(E, r)$ require continuity and differentiability at the sphere boundary with the boundary condition

$$p_l(E) = \frac{D_l(E) + l + 1}{D_l(E) - 1},$$

where,

$$D_l(E) = \frac{S}{\psi_l(E, S)} \left. \frac{\partial \psi_l(E, \vec{r})}{\partial r} \right|_{r=S}$$

is the logarithmic derivative function of the wave function at the sphere radius.

The tail of the orbital $(S/r)^{l+1}$ has a portion $r > S$ that for one sphere will overlap into the neighbouring spheres and the tails from the surrounding spheres will spill into the current sphere(cf. same, the way potential overlaps in Fig.2.1). The tail of the orbital is the solution of Poisson's equation $\nabla^2 X = 0$ and has zero kinetic energy. So, the tail centred at R can be expanded as Bloch sums around the origin of their

respective spheres in terms of phase shifted spherical harmonics:

$$\sum_{\vec{R} \neq 0} \exp(i\vec{k} \cdot \vec{R}) \left(\frac{S}{|\vec{r} - \vec{R}|} \right)^{l+1} {}^l\hat{Y}_l^m(\vec{r} - \vec{R}) = \sum_{l'm'} \frac{-1}{2(2l'+1)} \left(\frac{r}{S} \right)^{l'} {}^{l'}Y_{l'}^{m'}(\hat{\mathbf{r}}) S_{l'm',lm}^{\vec{k}} \quad (2.19)$$

where the expansion coefficients $S_{l'm',lm}^{\vec{k}}$ are the canonical structure constant of the lattice, converge inside the sphere of nearest neighbour.

As the Bloch theorem is applicable to the crystal lattice, the linear combination of Bloch sums of the MTOs (Eq. 2.18)

$$\sum_{lm} a_{lm}^{j\vec{k}} \sum_{\vec{R}} e^{i\vec{k} \cdot \vec{R}} \chi_{lm}(E, \vec{r} - \vec{R})$$

is a solution to the Schrödinger's equation (Eq. 2.8) where \vec{R} represents the lattice vectors and $a_{lm}^{j\vec{k}}$ are the expansion coefficients. But the first term of MTO ${}^lY_l^m(\hat{\mathbf{r}})\psi_l(E, \vec{r})$ is already a solution of eqn. 2.8 and is the one-centre expansion with origin at \vec{r} . For any other sphere, therefore, the term is

$$\sum_{lm} a_{lm}^{j\vec{k}} Y_l^m(\hat{\mathbf{r}}) \psi_l(E, \vec{r}).$$

provided tails from all other spheres cancel the potential function, p_l , that exists in the current sphere in the term

$$\sum_{lm} a_{lm}^{j\vec{k}} {}^lY_l^m(\hat{\mathbf{r}}) p_l(E) \left(\frac{r}{S} \right)^l,$$

where $a_{lm}^{j\vec{k}}$ is the expansion coefficient of MTO. From eqn. 2.19, the condition for this tail cancellation is

$$\sum_{lm} \left[P_l(E) \delta_{ll'} \delta_{mm'} - S_{l'm',lm}^{\vec{k}} \right] a_{lm}^{j\vec{k}} = 0 \quad (2.20)$$

where P_l is the slightly modified potential function defined as

$$P_l(E) = 2(2l+1) \frac{D_l(E) + l + 1}{D_l - 1} \quad (2.21)$$

Solution of secular form of eqn. 2.20 gives eigenvectors $a_{lm}^{j\vec{k}}$ iff

$$\det \left[P_l(E) \delta_{ll'} \delta_{mm'} - S_{l'm',lm}^{\vec{k}} \right] = 0 \quad (2.22)$$

This is the secular determinant of KKR-ASA approach. The potential function P is dependent on energy and the structure constant matrix is dependent on the k -vectors of the crystal, thus give rise to a $E \sim \vec{k}$ relation or the band structure.

2.4.2 Linearisation of MTO for Materials

The MTOs are energy dependent and we need to circumvent this by energy linearisation by performing a Taylor expansion of radial solution inside an atomic sphere centered at R . Andersen's method of linearisation [AJ84; AK71] shows that the basis can be written as

$$\chi_{RL}^{\alpha}(\vec{r}_R) = \phi_{RL}(\vec{r}_R) + \sum \dot{\phi}_{R'L'}^{\alpha}(\vec{r}_{R'}) h_{R'L',RL}^{\alpha} \quad (2.23)$$

where the functions $\dot{\phi}_{R'L'}^{\alpha}(\vec{r}_{R'})$ are linear combinations of the ϕ 's and their energy derivatives $\dot{\phi}$ and given by

$$\dot{\phi}_{R'L'}^{\alpha} = \dot{\phi}_{R'L'}^{\alpha} + \phi_{R'L'} o_{R'L'}^{\alpha} \quad (2.24)$$

here, $o_{R'L'}^{\alpha}$ is overlap matrix and the Hamiltonian matrix h^{α} are defined as,

$$h^{\alpha} = C^{\alpha} - \epsilon_{\nu} + (\Delta^{\alpha})^{1/2} S^{\alpha} (\Delta^{\alpha})^{1/2}. \quad (2.25)$$

where C^{α} and Δ^{α} are the diagonal **potential parameter matrices** defined as

$$C^{\alpha} = \epsilon_{\nu} - \frac{P^{\alpha}(\epsilon_{\nu})}{\dot{P}^{\alpha}(\epsilon_{\nu})}, \quad \text{and} \quad (\Delta^{\alpha})^{1/2} = \frac{1}{\dot{P}^{\alpha}(\epsilon_{\nu})} \quad (2.26)$$

These are called **band centre** and **band width** respectively. They depend on the potentials inside the atomic spheres, the atomic sphere volume and the representation (α) chosen. Whereas the S matrix is a structure matrix which depends on the representation (α) and the lattice geometrical arrangement of the atomic sites. In terms of canonical structure matrix S^0 and the representation specified by an orbital diagonal matrix α , S^{α} is given by

$$S^{\alpha} = S^0 (\mathbf{1} - \alpha S^{\alpha})^{-1}.$$

In the recursion calculations to follow, it is practical to work with an orthonormal sparse representation known as the γ representation. The Hamiltonian in γ representation which is correct up to second order in $(E - E_\nu)$ is given by,

$$H^{(2)} = E_\nu + h^\gamma . \quad (2.27)$$

In this representation the overlap matrix is a unit, diagonal in RL representation whose value is determined by the logarithmic derivative of ϕ at the muffin-tin sphere boundary, and therefore it fulfils the orthogonality condition required in the recursion purpose. However, the structure matrix itself is intrinsically random in this representation, therefore, it is useful to rewrite the Hamiltonian in terms of a most-localised (or β) representation. h^γ can be expanded in terms of any other representation α as

$$h^\gamma = h^\alpha - h^\alpha o h^\alpha - \dots . \quad (2.28)$$

The set $\alpha = \beta$ is characterized by a set of screening parameters, found numerically by ANDERSEN and JEPSEN [AJ84]. These site independent constants are: $\beta_s = 0.3458$, $\beta_p = 0.0530$, $\beta_d = 0.0107$ and for $l \geq 3$, $\beta_l = 0$. LMTO, together with this screening parameters is called the tight-binding (TB-)LMTO in which the structure factor S^β is exponentially decaying short-ranged. For this, even for s and p bands, consideration of interactions up to the second neighbour also produce quite accurate results. The power series 2.28 truncated after the first order term along with Eq. 2.27 give rise to the first order tight-binding Hamiltonian

$$H^{(1)\beta} = C^\beta + (\Delta^\beta)^{1/2} S^\beta (\Delta^\beta)^{1/2} . \quad (2.29)$$

This is a two-centre *sparse* Hamiltonian correct up to first-order in $(E - E_\nu)$. Inclusion of higher terms in Eq. 2.28 is quite straightforward as each term in second and subsequent terms in the expansion are themselves two-centred and sparse. To achieve the self consistency, a correction term, named *combined correction* is also attached. The corresponding (corrected) Hamiltonian is given by

$$H^\beta = C^\beta + (\Delta^\beta)^{1/2} S^\beta (\Delta^\beta)^{1/2} - \kappa^2 + v_0 \delta_{\kappa^2 h^\beta} \quad (2.30)$$

2.5 The Recursion Technique

Bloch's theorem [Blö29] has rigid requirements of lattice translational symmetry by which the dimensionality of infinite matrix Hamiltonian representation is reduced essentially to $2l_{max} + 1$. So in the problems of systems with surfaces or randomness one has to resort with suitable alternative techniques. The recursion technique, introduced by HAYDOCK, HEINE, and KELLY [HHK72] (details given in [Moo02]) is one such alternative that expands the solution to the Schrödinger equation in a sequence of increasingly de-localised functions and obtains the Green functions associated with the secular equation. And in turn, obtain useful physical properties like magnetisation density, moment, charge transfer, band energy, Fermi energy.

A finite cluster of atoms around a central atom is divided into shells. The Green function of the resolvent of this cluster of atoms is expanded in terms of a continued fraction whose levels are the direct consequential of the number of shells of the cluster accounted. Considering $|0\rangle$ to be a general orbital on which the solutions are to be projected, the recursion method uses the electronic Hamiltonian $\hat{\mathcal{H}}$ to generate a sequence of orbitals $|1\rangle, |2\rangle, \dots |n\rangle, \dots$ which are the successively less-localized. These orbitals are related to one another by $\hat{\mathcal{H}}$ according to the three-term recurrence relation,

$$\hat{\mathcal{H}}|n\rangle = \alpha_n|n\rangle + \beta_{n+1}|n+1\rangle + \beta_n|n-1\rangle \quad (2.31)$$

where $|-1\rangle$ is taken to be zero, and the dependence of these orbitals on position, spin and other coordinates has not been considered for simplicity. The projection of the solution onto $|0\rangle$, the projected density of states (PDOS), is the singular part of a solution to the above recurrence, namely the continued fraction,

$$G(E) = \frac{1}{E - \alpha_0 - \frac{\beta_1^2}{z - \alpha_1 - \frac{\beta_2^2}{z - \alpha_2 - \frac{\beta_3^2}{z - \alpha_3 - \frac{\beta_4^2}{\ddots}}}}} \quad (2.32)$$

Now, the parameters $\{\alpha_n, \beta_n\}$ need to be determined.

The construction of the three term recurrence relation and its solution as a con-

tinued fraction can be carried out either analytically or numerically; the only real difference being whether the parameters $\{\alpha_n, \beta_n\}$ can be expanded as functions of n . In analytic, applications, the electronic states are mapped onto systems of orthogonal polynomials which satisfy the same recurrence as the Hamiltonian. When this happens, the PDOS is the weight distribution for the polynomials, and the eigenstates of the Hamiltonian can be expanded in the polynomials. In such cases, the mathematical properties of the many known polynomial systems can be applied to physical problems. Otherwise, the $\{\alpha_n, \beta_n\}$ can be computed using some basis for the $\{n\}$.

In a numerical approach to recursion, the orbitals $\{n\}$ must be expanded in some basis which should be as similar to the recursion orbitals as possible. Though the recursion orbitals are not known beforehand, which is why the numerical approach is essential, still a good choice of basis helps a lot. The best basis is the one for which the Hamiltonian is most sparse, *i.e.*, has most of the matrix elements zero. It is seen that this criterion is usually achieved by functions similar to the valence orbitals of atoms, not necessarily orthogonal, but decaying exponentially at large distances. Another essential requirement for the choice of basis is that it should be easy to calculate the matrix elements of the Hamiltonian. This is facilitated by the use of a two-centre approximation (involving a two-centre integral). The tight-binding approximation is such an approximation [Ehr80, pp. 129-215]. It gives very simple parametrization of the Hamiltonian matrix elements for various orientations of the orbitals and atoms. The assumption behind tight-binding is that there are negligible contributions from the potential centred on one atom to Hamiltonian matrix elements for hopping from an orbital centred on a second atom to an orbital centred on a third atom. The d -electrons in transition metals are sufficiently localized for this approximation to work well, but fails quantitatively for less localized valence electrons such as the s - and p -electrons.

In the recursion approach Haydock devised a scheme to transform the basis in such a way that the Hamiltonian of the system has a tri-diagonal form. A new orthonormal basis set $|n\rangle$ in which the Hamiltonian is tri-diagonal is constructed by the three term recurrence formula mentioned earlier. The first recursion orbital $|0\rangle$, is assumed to have a normalization of unity, and is the one on which the states are to be projected. Thus this orbital plays a significant role in determining the specific physical property and the new state $|1\rangle$ takes the form as,

$$\beta_1|1\rangle = \hat{\mathcal{H}}|0\rangle - \alpha_0|0\rangle \quad (2.33)$$

The whole set of orthonormal states are generated by the following three term recurrence relation:

$$\beta_{n+1}|n+1\rangle = \hat{\mathcal{H}}|n\rangle - \alpha_n|n\rangle - \beta_n|n-1\rangle \quad (2.34)$$

α_n and β_n are the coefficients to orthogonalize $\hat{\mathcal{H}}|n\rangle$ to the preceding vectors $|n\rangle$, $|n-1\rangle$ and β_{n+1} is the coefficient to normalize $|n+1\rangle$ to unity. β_0 is assumed to be unity. In the new basis, the Hamiltonian matrix elements are,

$$\{n|H|n\rangle = \alpha_n ; \{n-1|H|n\rangle = \beta_n \text{ and } \{n|H|m\rangle = 0 \quad (2.35)$$

In this new representation, the Hamiltonian has the following tri-diagonal form,

$$\begin{pmatrix} \alpha_0 & \beta_1 & 0 & 0 & 0 & 0 & 0 \\ \beta_1 & \alpha_1 & \beta_2 & \ddots & 0 & 0 & 0 \\ 0 & \beta_2 & \alpha_2 & \beta_3 & \ddots & 0 & 0 \\ 0 & \ddots & \beta_3 & \alpha_3 & \beta_4 & \ddots & 0 \\ 0 & 0 & \ddots & \ddots & \ddots & \ddots & 0 \\ 0 & 0 & \dots & \dots & \dots & \dots & 0 \end{pmatrix} \quad (2.36)$$

The above transformation can be graphically represented as the transformation of a d-dimensional system to a semi-infinite linear chain. $\{\alpha_n\}$ and $\{\beta_n\}$ are represented as the on-site term and the coupling between two sites.

As we have discussed earlier since for systems where the lattice symmetry breaks down, we can not apply Bloch's theorem, so we take recourse to an alternative approach to calculate the electronic properties instead of solving Schrodinger equation. In this approach, properties are extracted from the corresponding Green function of the system which is defined as the resolvent of the Hamiltonian :

$$G(z) = (zI - H)^{-1}$$

In the recursion method, we use the same approach and calculate the diagonal elements of the Green function which is directly related to the density of states, spectral functions, structure factors etc. and most of the material properties follow thereafter. The starting state of recursion is then :

$$|0\rangle = |R, \alpha\rangle$$

where R indicates the position of the R -th unit cell and α the Cartesian direction.

The diagonal element of the Green function by definition is,

$$G_{00}(E) = \{0|(EI - H)^{-1}|0\} = \frac{M_1(E)}{M_0(E)} = \frac{1}{G_1(E)}$$

where M_0 and M_1 are the determinant of the matrix $(EI - H)^{-1}$ (represented in the new basis $\{|n\rangle\}$) and the determinant of the matrix obtained from the original matrix by deleting the first row and column respectively.

Using Cauchy's expansion theorem,

$$\begin{aligned} M_n(E) &= (E - \alpha_n)M_{n+1} - \beta_{n+1}^2 M_{n+2} \\ G_{n+1} &= E - \alpha_n - \frac{\beta_{n+1}^2}{G_{n+2}} \end{aligned} \quad (2.37)$$

This suggests that it is possible to express the Green function as a continued fraction expansion characterized by a set of coefficients,

$$G_{00}(E) = \frac{1}{E - \alpha_0 - \frac{\beta_1^2}{E - \alpha_1 - \frac{\beta_2^2}{E - \alpha_2 - \frac{\beta_3^2}{E - \alpha_3 - \frac{\beta_4^2}{\ddots}}}}} \quad (2.38)$$

where the coefficients $\{\alpha_n\}$ and $\{\beta_n\}$ are the ones appearing in the tri-diagonal matrix H .

In any practical calculation we can go only up to a finite number of steps, consistent with our computational process. This limits the number of atoms that can be modelled, and also implies that one is always studying a finite system. The terminating continued fraction obtained in this process yields a number of isolated bound states, appropriate for a finite cluster. For most purpose this is an unphysical approximation to the problem under investigation and one needs to overcome these finite size effects by the embedding the cluster in an infinite medium. Mathematically a suitable terminator should be appended to the continued fraction so as to obtain a Green function with a branch cut, rather than a set of simple poles. Several terminators are available in the literature which reflect the asymptotic properties of the continued fraction expansion of the Green function accurately. The advantage of such a termination pro-

cedure is that the approximate resolvent retains the analytic properties of the Green function, called the Herglotz properties which are as follows :

- All the singularities of $G(z)$ lie on the real z -axis.
- $\Im[G(z)] > 0$ when $\Im(z) < 0$ and $\Im[G(z)] < 0$ when $\Im(z) > 0$.
- $G(z) \rightarrow 1/z$ when $\Re(z) \rightarrow \infty$ along the real axis. Terminator preserves the first $2n$ -moments of the density of states exactly.

In case the coefficients converge, *i.e.*, if $|\alpha_n - \alpha| \leq \epsilon$, and $|\beta_n - \beta| \leq \epsilon$ for $n \geq N$, we may replace $\{\alpha_n, \beta_n\}$ by $\{\alpha, \beta\}$ for all $n \geq N$. This is called the square terminator in which the asymptotic part of the continued fraction may be analytically summed to obtain :

$$T(E) = (1/2) \left(E - \alpha - \sqrt{(E - \alpha)^2 - 4\beta^2} \right)$$

which gives a continuous spectrum $\alpha - 2\beta \leq E \leq \alpha + 2\beta$. This is the most commonly used terminators. However, since the terminator coefficients are related to the band edges and widths, a sensible criterion for the choice of these asymptotic coefficients is necessary, so as not to give rise to spurious structures in our calculations. If calculations up to a large N is not possible, carrying out the terminator approximation after N steps ensures that the first $2N$ moments of density of states are exact and asymptotic moments are also accurately reproduced [LN87]. BEER and PETTIFOR [BP84] suggested a sensible criterion: given a finite number of coefficients, we must choose $\{\alpha, \beta\}$ in such a way so as to give, for this set of coefficients, the minimum bandwidth consistent with no loss of spectral weight from the band. The terminator proposed by them is useful when the convergence of the coefficients is either oscillatory or slow. Several other terminators have been suggested by MÜLLER and VISWANATH [MV93] for different asymptotic distributions of $\{\beta\}$ s, for example, the terminator with an exponential tail for $\beta_n \rightarrow n$ or the terminator with a Gaussian tail suitable when $\beta_n \rightarrow n^2$.

It is observed that the recursion coefficients are weakly energy-dependent. Therefore, recursion can be carried out on equispaced energy “seed” points and the intermediate points found by interpolation.

Study of Disordered Alloys

3.1 Introduction

$\text{Fe}_x\text{Al}_{1-x}$ is a classical inter-metallic alloy system widely used as high temperature structural and functional material both in scientific applications and technology. With the variation of the composition and their heat treatments, the alloy shows different magnetic and physical properties [Wan+91]. It has been verified to have conspicuous disordered meta-stable states existing over the range of compositions [Gia95]. In addition, the commonness of this alloy has attracted considerable theoretical attempts in understanding of its stabilities. Studies include that based on mean-field Bragg-Williams treatment [Has80; SO80] of the free energy, cluster variation method by GOLOSOV, TOLSTIK, and PUDAN [GTP76], extensive comparative study of the model bcc with Monte Carlo (MC) simulations, Kikuchi cluster variation method within tetrahedron approximation and BW approximations by CONTRERAS-SOLORIO et al. [CS+88] and DÜNWEIG and BINDER [DB87]. With a short-range interaction conjecture, even the small spin-glass region has been tried by models using magnetic moment extrapolation and an imposed artificial competition between Fe-Fe ferromagnetic and, presumably, Al mediated anti-ferromagnetic super-exchange [SW80]. All such models using parametrised interaction parameters, without having any electronic structure input, have captured only the gross details of the system. In this alloy, the tendencies of constituting Fe and Al atoms, to occupy wrong lattice sites limit the formation of vacancies or complex structures and result in a chemical disordered state. We will focus in sections to follow about theoretical framework and developments concerned with the study of this type of chemical disordering.

The parent structure of $\text{Fe}_x\text{Al}_{1-x}$ is bcc based (Fig.3.1). Among the three main phases, viz., DO_3 , B2, and A2, of the iron rich side of $\text{Fe}_x\text{Al}_{1-x}$ alloy the A2 structure is short-range ordered random solid solution with the Fe and Al atoms distributed at random in the crystallographic positions of a Body Centred Cubic (bcc) structure

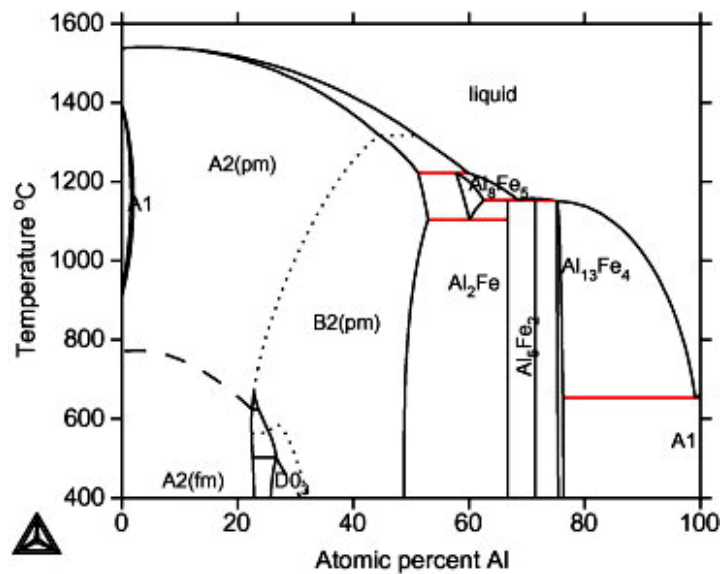


Figure 3.1: Equilibrium phase diagram of $\text{Fe}_x\text{Al}_{1-x}$ from thermodynamic calculations after SUNDMAN et al. [Sun+09]

[Ike+01]. The general DO_3 structure formed from 4 interpenetrating Face Centred Cubic (fcc) lattices A, B, C and D, cf. Fig3.2, can lead to several derived structures based on the occupancies [Pea72]. Note that the DO_3 disorder is rather hard to be differentiated from the L2_1 (Heusler) structure by X-ray imaging; this adds subtlety to the experimental analysis. At temperature below 550°C , between Fe concentrations $x = 65 - 75$ i.e., around the Fe_3Al stoichiometry, DO_3 is the ground state structure in which three sub-lattices are occupied by Fe and one by Al. Around the equi-atomic composition, B2 is the stable state configuration.

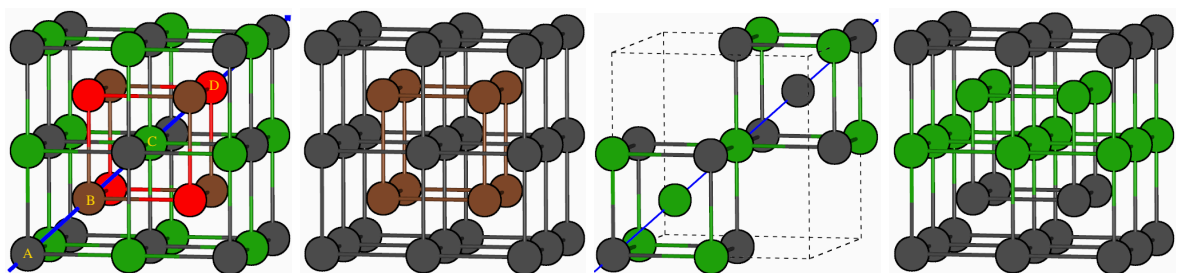


Figure 3.2: (From left) DO_3 Super structure having basis of 4 inter penetrated fcc A,B,C, and D shifted along the body diagonal (blue line) and with origins at $(0,0,0)$, $(.25,.25,.25)$, $(.5,.5,.5)$ and $(.75,.75,.75)$; B2 structure; B32 structure and B11 structure

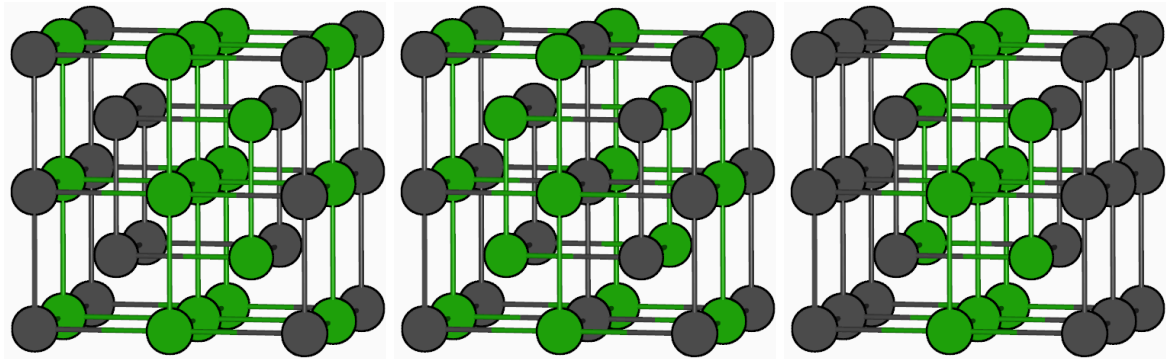


Figure 3.3: (From left) ST1 structure; ST2 structure; ST3 structure

3.2 Theories for the Study of random disordered alloys systems

Alloys are multiphase systems and we want to find out, when and under what conditions, a specific phase becomes favourable for a particular alloy system. Such studies involve determination of the ground states (*i.e.*, stable phases at 0 °K) as a function of the composition and then use of the ground states to construct a temperature-composition phase diagram which indicates the regions of concentration and temperature within which the alloy will exist in a particular phase after it has been allowed to reach thermodynamic equilibrium. In the previous chapter we discussed about the theoretical framework of obtaining electronic properties of ordered materials in the ground state. Naturally forming alloys are often disordered and random. This very first difficulty it poses, is the break down of k -space formalism and inapplicability of Bloch's theorem. Now we need to extend the theoretical frameworks to be able to obtain averaged properties of random alloys which are experimentally observable. To this end, we have only few alternatives.

3.2.1 Supercell Method

Since the translational symmetry is disturbed in random alloys, the first intuitive approach would be to somehow patch the system for making Bloch theorem workable. In one such approach, a bigger cell is constructed out of the unit cell keeping symmetries preserved, and randomness in atomic occupations are introduced in this newly created cell, called the 'supercell'. The supercell now serves as the repeating unit representing the random alloy. The results from the calculations are averaged over

several snapshots to ensure the spatial ergodicity. Though very straightforward, it is both technically demanding and theoretically inconsistent. Extreme concentration ranges additionally more cumbersome to handle in this approach. An extension of this method is to use a statistical ensemble over all the possible configurations or simplified ensembles over a smaller set of representative structures. Known as the *Direct Sampling Method* (DSA) is even more computation demanding.

If the randomness of the alloy can be statistically incorporated in the supercell, then the results of a single shot can do instead of the averaging. These special type supercells, as proposed by Zunger *et al.*, [Zun+90], have zero short-range ordering by construction and so they mimic the randomness of the alloy quite naturally. It shifts the computational requirement from different electronic structure calculations to one-time supercell finding. Finding supercells for odd and extreme concentrations are more difficult now.

3.2.2 Mean-field Theory

Another way of retaining the instrumentality of the Blochs theorem is by replacing the original atoms (Or equivalent) with some *mean/effective medium*. This effective medium accounts for the randomness of the alloy, hence the construction of the effective medium is now the centre place.

The earliest approach in this regard is the Virtual Crystal Approximation (VCA) in which the average potential of the alloy A_xB_{1-x} is the concentration weighted potential of constituting atoms.

$$v_{\text{eff}} = xv_A + (1 - x)v_B. \quad (3.1)$$

This is a very crude approximation, expected to work well when the atoms are very similar to each other.

KORRINGA [Kor47] suggested an improvement of the method by averaging the scattering amplitudes instead of the potential. In quantum mechanical scattering theory, t -matrices represent the scattering amplitude.

$$t_{\text{eff}} = xt_A + (1 - x)t_B. \quad (3.2)$$

This method also had many disagreements with experiments in several cases. Finally came one of the successful effective medium approaches, namely the Coherent Potential Approximation (CPA). Within the CPA the disorder averaged properties of an alloy

are represented by an effective ordered CPA-medium by the virtue of concentration averaged scattering path operator. For a binary system A_xB_{1-x} , then the CPA condition is

$$\tau_{CPA} = x\tau_A + (1 - x)\tau_B. \quad (3.3)$$

By this approximation, substitution of an A(B) atom in place of B(A) atom site in this effective medium should not cause additional scattering. The scattering properties of an A(B) atom embedded in the CPA medium is represented by the component-projected scattering path operators $\tau_{A(B)}$ as

$$\tau_{A(B)} = \tau_{CPA} \left[1 + (t_{A(B)}^{-1} - t_{CPA}^{-1})\tau_{CPA} \right]^{-1}. \quad (3.4)$$

The coupled sets of equations 3.3 and 3.4 are solved iteratively for self-consistency. The dynamics of an electron travelling in an alloy is properly calculated by the amount of scattering it gets from the potential centres. Hence CPA puts forward a major improvement to the theory of random alloys. So far it is the mostly used technique for the electronic structure of the disordered alloys.

The CPA being a single-site approximation cannot take into account the effect at a site of its immediate environment. It needs to be extended to include off-diagonal randomness and short range atomic correlations, and generalised enough to be applied to structurally disordered systems. Several attempts for taking into account the cluster scattering inside CPA medium has been made, for example, Travelling Cluster approximation (TCA) by MILLS and RATANAVARARAKSA [MR78], Molecular CPA(MCPA), Coherent Potential Method(CPM) etc. However, NICKEL and BUTLER [NB73] showed the non-analyticity of multiple-site CPA; that puts a big sign of caution in these approaches. In an attempt to go beyond the single site approximation, de Fontaine *et al.*, suggested a different approach of direct configuration averaging (DCA) [Dre+89; Wol+93]. The effective pair and multi-site interactions were calculated directly in real space for given configurations and the averaging was done in a brute force way by summing over different configurations without resorting to any kind of single-site approximation. Invariably, the number of configurations was finite and convergence wrt the configurations is not yet clearly established.

With the realization of the need to go beyond the CPA, several attempts have been reported which are broadly classified into two categories:

1. Non-self consistent clusters approach which assumed a clusters consisting of a central site and its shell of nearest neighbour(NN) embedded in an effective medium

(e.g., Effective Cluster Medium(ECM) of GONIS et al. [Gon+84]) and

2. Self-consistent cluster approach within which great deal of work has been done, mostly in tight binding models. Among them, Travailing cluster approximation(TCA) [KG76] and the augmented space formalism(ASF) [Moo73a; Moo73b] are the only approaches which have been proved to be analytic, while preserving the conservation laws and sum rules.

3.2.3 Configuration Avearging

As opposed to the cavity field approximations mentioned earlier, there exists an all total different approach to the random alloys problem which works in real space approaches to find out the average properties. Known as the *configuration averaging*, it differs from earlier methods of hand-held averaging by the introduction of a rigorous mathematical formulation that uses an abstract space in par with the space(Hilbert space) in which the Hamiltonian is solved. The idea of taking averages over all possible different states of a system is well understood and commonplace both in quantum mechanics and statistical physics. At finite temperatures, different possible states of a canonical ensemble, for example, are occupied with Boltzmann probabilities and observable physical properties are averages over the ensemble. Similarly, when we wish to measure a given physical observable in a quantum system, the result of the measurement is spread over different possible states with probabilities given by squared amplitudes of the wave function projection onto those states.

In disordered systems also the concept of configuration averaging is central to the study of physical observables of the system. In the realm of quantum mechanics a disordered solid is described by the potential characterized by random parameters. A particular realization of these parameters, either in a given sample (spatial) or at an instant (temporal), is what we call a configuration of the system. The interest in alloys are naturally in the averaged physically measurable quantities: conductivity, susceptibility, electronic density of states etc. It is this set of quantities that one should average over configurations rather than averaging the Hamiltonian or the wave function. A macroscopic system can be partitioned into subsystems, each of which resembles a configuration of the system. A global property which averages over the subsystem is then the same as average over all configurations. This is the basis of *spatial ergodicity* assumption and it must hold in case of configuration averaging.

3.2.4 Augmented Space Recursion

The augmented space formalism introduced by MOOKERJEE [Moo73a] is a conceptually elegant and exact method of configuration averaging. This formalism maps a disordered Hamiltonian described in Hilbert space $\hat{\mathcal{H}}$ onto an ordered Hamiltonian in a much enlarged Hilbert space whose Green function matrix elements correspond to appropriate configurational average of the Green function of the original disordered system. The ordered Hamiltonian is said to be in augmented space which is described as the direct product of the Hilbert space spanned by the original Hamiltonian with the configuration space which spans all possible configurations of the systems. The probability density of a random variable n_R for a bimodal normalized distribution has the following form

$$p(n_R) = x\delta(n_R - 1) + (1 - x)\delta(n_R).$$

Since the probability densities are positive definite functions, they are related to the spectral densities of a positive definite operator $G(n_R)$. That means, the probability density $p(n_R)$ is similar to the density of states of the Hamiltonian. This embarks to modify the Hilbert space of the problem which is characterized by the full configuration space $\Phi = \prod_R \oplus \phi_R$. Now the average of a well-behaved function $f(n_R)$ of the random variable n_R is expressed as :

$$\langle f(n_R) \rangle = \int_{-\infty}^{\infty} f(n_R) p(n_R) dn_R = -\frac{1}{\pi} \text{Im} \int_{-\infty}^{\infty} f(n_R) \langle \uparrow_R | (n_R \mathbf{I} - M_R)^{-1} | \uparrow_R \rangle dn_R$$

where M_R is an operator designed such that its eigenvalues are equal to the functional values of $f(n_R)$. This way the Green function can be averaged to get the configuration averaged properties like DOS etc. of the disordered random alloy.

The ASF is originally developed in the tight binding frame work provides self-consistent cluster coherent potential approximation in which one can go beyond CPA in the systematic way [MP93]. In this method, the effective medium is determined by the self consistency condition that the averaging scattering from all possible configurations of the real cluster embedded in the effective medium be zero. The following sections provides the more detail theoretical description about the augmented space theorem and its mathematical description which is applicable for binary alloys.

3.2.5 Mathematical description of the configuration space

The visualization of configuration space of a set of random variables is most essential to understand the augmented space theorem. This can be done by taking the example of Ising model. The model consists of set of pseudo-spins $\{\sigma_R\}$ arranged on a discrete lattice labelled by R . Each spin σ_R can have two possible states or configurations which are denoted systematically as $|\uparrow_R\rangle$ and $|\downarrow_R\rangle$. The collection of all linear combination of these two states $a|\uparrow_R\rangle + b|\downarrow_R\rangle$ is called configuration space of σ_R denoted as ϕ_R . It is of rank two and is spanned by the states $|\uparrow_R\rangle$ and $|\downarrow_R\rangle$. The set of, say, N points then have 2^N possible configurations each of which can be written as sequence of m -up states and $(N - m)$ -down states. The ordering of this sequence is crucial, since different orderings corresponds to different configurations. The number $N - m$ down states is defined as cardinality of the configuration and the sequence C of sites $R_{i_1}, R_{i_2} \cdots R_{i_{N-m}}$, where the down states sit is called the cardinality sequence of the configuration. For example, the cardinality sequence of a particular configuration of 5 spins: $|\uparrow_1\downarrow_2\downarrow_3\uparrow_4\downarrow_5\rangle$ is 2,3,5 and its cardinality is 3. Another configuration $|\downarrow_1\uparrow_2\downarrow_3\downarrow_4\uparrow_5\rangle$ also has a cardinality 3, but its cardinality sequence is 1,3,4. These two configurations are distinct from each other. Note that the cardinality sequence uniquely describes the configuration and is a very convenient way of labelling the different configurations $|C_k\rangle$, where $k = 1, 2, 3, \dots, 2^N$, of the set of N spins. The configuration space Φ is of rank 2^N and can be written as a *direct product* of the configuration spaces of the individual spins.

$$\Phi = \Pi_R \bigotimes \phi_R$$

The generalization of these ideas when the spins can have $n > 2$ states is quite straight forward. The configuration of an individual spin can be labelled as $|k_R\rangle$, where $k_R = 1, 2, 3, \dots, n$. The rank of ϕ_R is now n , the set of N spins has n^N configurations. The cardinality of the configuration of an individual spin can be defined as the particular k_R and cardinality sequence which uniquely describes a configuration of the set of N spins is the sequence $\{k_1, k_2, \dots, k_N\}$. If we now transform this idea from spins σ_R to the random variables ε_R of the Anderson model, we can immediately visualize the configuration space of the Hamiltonian variables ε_R . When these terms have a binary distribution, their configuration space is isomorphic to the one for collection of Ising spins. Let us now assume that the variable ε_R are independently distributed and the probability density is given by $\rho(\varepsilon_R)$. We shall take into account only those probability densities which have finite moments to all orders. Physically

relevant densities almost all fall in this category. Since the probability densities are positive definite functions, we can always write them as spectral densities of a positive definite operator which is formulated as follows:

$$\rho(\varepsilon_R) = -\frac{1}{\pi} \Im m \langle \emptyset | ((\varepsilon - R + iO)\mathbf{I} - \mathbf{M}_R)^{-1} | \emptyset \rangle = \Im m g(\varepsilon_R + i0) \quad (3.5)$$

If $\rho(\varepsilon_R)$ has a binary distribution, taking the values 0 and 1 with probabilities x and $y = 1 - x$, then a representation of \mathbf{M} is:

$$\begin{pmatrix} x & \sqrt{xy} \\ \sqrt{xy} & y \end{pmatrix}$$

We may interpret this in terms of the configuration space ϕ_R introduced earlier. The configuration space is spanned by the states $|0\rangle$ and $|1\rangle$, which are eigenstates of \mathbf{M}_R with eigenvalues 0 and 1. This is rather similar to the description in quantum mechanics, where an observable taking a random set of values is associated with an operator whose eigenvalues are possible values observed and the states of the system in which the observable takes a particular value corresponds to the related eigenvalue.

The operator \mathbf{M}_R in the configuration space ϕ_R will be associated with the random variable ε_R . The representation of \mathbf{M}_R , shown above, is in a different basis:

$$|\emptyset\rangle = (\sqrt{x}|0\rangle + \sqrt{y}|1\rangle) \quad |R\rangle = (\sqrt{y}|0\rangle - \sqrt{x}|1\rangle)$$

The reason for choosing this particular basis will become clear later. The state $|\emptyset\rangle$ will be called the average state of the system.

For the general probability distribution, we may always find the representation of operator \mathbf{M}_R in similar basis by first expanding the probability density as a continued fraction.

$$g(\varepsilon_R) = -\frac{1}{\pi} \frac{1}{\varepsilon_R - a_0 - \frac{b_1^2}{\varepsilon_R - a_1 - \frac{b_2^2}{\ddots}}}$$

Here, $p(\varepsilon_R) = \Im m g(\varepsilon_R)$.

Since $p(\varepsilon_R) = \Im m g(\varepsilon_R)$ is a positive definite function with finite moments to all orders, $p(\varepsilon_R)$ can be expanded as a convergent continued fraction. The required rep-

representation of the matrix M_i , is given by

$$\begin{pmatrix} a_0 & b_1 & 0 & 0 & \cdots \\ b_1 & a_1 & b_2 & 0 & \cdots \\ 0 & b_2 & a_2 & b_3 & \cdots \\ \cdots & \cdots & \cdots & \cdots & \cdots \end{pmatrix}$$

The average state is defined by $|\emptyset\rangle = \sum_k \sqrt{x_k} |k\rangle$ where k are the random values taken by ε_R with probabilities x_k . The other members of the countable basis $|n\rangle$, in which the above representation of M_R is given, may be obtained recursively from the average state through:

$$\begin{aligned} |0\rangle &= |\emptyset\rangle \\ b_1|1\rangle &= M_R|0\rangle - a_0|0\rangle \\ b_n|n\rangle &= M_R|n-1\rangle - a_{n-1}|n-1\rangle - b_{n-1}|n-2\rangle. \end{aligned}$$

3.2.6 The augmented space theorem

Let us now consider the average of a well-behaved function $f(\varepsilon_R)$ of ε_R . By definition

$$\langle f(\varepsilon_R) \rangle = \int f(\varepsilon_R) p(\varepsilon_R) d\varepsilon_R$$

This equation may be rewritten as:

$$\langle f(\varepsilon_R) \rangle = \oint f(z) g(z) dz$$

The integral is taken over a closed contour enclosing the singularities of $g(z)$ but not any of $f(z)$. We assume here that $f(z)$ is well-behaved, in the sense that it has no singularities in the neighbourhood of a singularity of $g(z)$. We now expanded the function $g(z)$ in the basis of its eigenstates $|\mu\rangle$ of M_i . These may be either discrete or continuous.

This expansion can be written as a Stielje's integral in terms of the spectral density function $\rho(\mu)$ of M_i ,

$$\langle f(\varepsilon_R) \rangle = \int d\rho(\mu) \langle \emptyset | \mu \rangle \left[\oint f(z) (z - \mu)^{-1} \right] \langle \mu | \emptyset \rangle$$

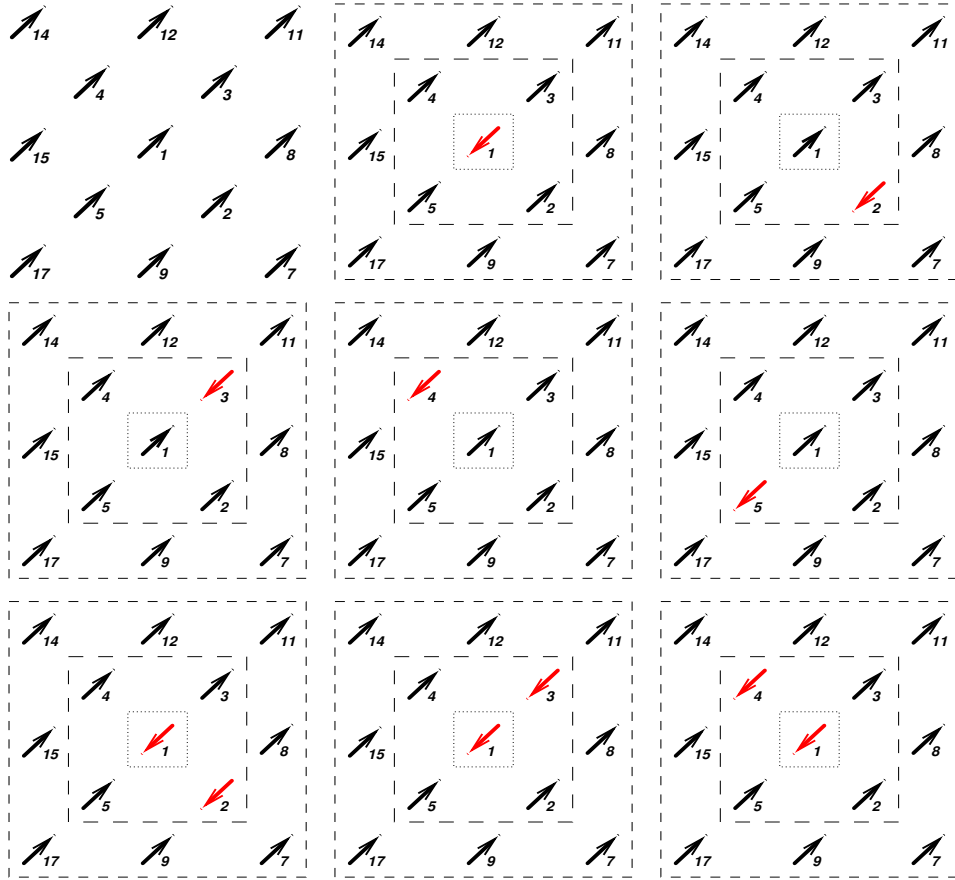


Figure 3.4: Few elements of augmented map for a binary square lattice. Thirteen sites(three shells) shown are initially in real space all having one particular occupation say ‘B’, then shown Z -way down the figure, 6th 10th 13th 16th 18th are all augmented space sites (notice, thus, though these numbers should lie well within the shown shells but are missing in real space enumeration) with single site replaced with an ‘A’ (red and down arrow) followed again by the augmented sites 19th 20th 21st 22nd with two atoms replaced by ‘A’. These combination types rapidly expand and in a mathematically sophisticated way averages over all seemingly important configurations.

$$= \langle \emptyset | \left[\int d\rho(\mu) |\mu\rangle f(\mu) \langle \mu| \right] | \emptyset \rangle$$

The second line requires the function to be well behaved at infinity. The expression in the brackets on the right side of the bottom equation is, by definition, the operator $f(M_R)$. It is the same functional of $f(M_R)$ as $f(\varepsilon_R)$ was of (ε_R) . For example, if $f(\varepsilon_R)$ is ε_R^2 then $f(M_R)$ is M_R^2 . This yields the central equation of the augmented space theorem:

$$\langle f(\varepsilon_R) \rangle = \langle \emptyset | f(M_R) | \emptyset \rangle \tag{3.6}$$

The result is significant, since we have reduced the calculation of averages to one of obtaining a particular matrix element of an operator in the configuration space of the variable. Since we have applied the theorem to a single variable alone, the power of the above theorem is not apparent. Let us now go back to the Anderson model, where we have a set of random variables ε_i which we have assumed to be independently distributed. The joint probability distribution is given by:

$$P(\varepsilon_{R_1}, \varepsilon_{R_2}, \dots, \varepsilon_{R_i}, \dots) = \prod_i p(\varepsilon_{R_i})$$

The generalization of above theorem to averages of functions of the set of random variables is straightforward.

$$\langle f(\varepsilon_R) \rangle = \langle \emptyset | \tilde{f}(\tilde{M}_R) | \emptyset \rangle$$

All operators in the full configuration space Φ will be denoted by *tilde* variables. The operators (\tilde{M}_R) are built up from the operators M_R as:

$$\tilde{M}_R = I \otimes I \otimes I \otimes \dots M_R \otimes I \otimes \dots \quad (3.7)$$

This is the augmented space theorem, proposed by MOOKERJEE [Moo73a; Moo73b].

If we carry out the configuration averaging of, say, green function element.

$$G_{RR}(z) = \langle R | (zI - H(\varepsilon_{R'}))^{-1} | R \rangle$$

The theorem leads to:

$$\langle G_{RR}(z) \rangle = \langle R \otimes \emptyset | (z\tilde{I} - H(\varepsilon_{R'}))^{-1} | R \otimes \emptyset \rangle \quad (3.8)$$

Where

$$\tilde{H} = \sum_R p_R \otimes \tilde{M}_R + \sum_R \sum_{R'} V_{RR'} T_{RR'} \otimes \tilde{I}$$

The power of the theorem now becomes apparent. The average is seen to be particular matrix elements of Green function of an augmented Hamiltonian. This is constructed out of the original random Hamiltonian by replacing the random variables by the corresponding configuration space operators built out of their probability distributions. This augmented Hamiltonian is operator in the augmented space $\psi = \mathcal{H} \otimes \Phi$

where \mathcal{H} is the space spanned by the tight-binding basis and Φ the full configuration space.

3.2.7 Augmented space theorem for binary alloy

As discussed in previous section we can apply recursion method directly on the augmented space without carrying out any mean-field-like approximations. The starting point of the augmented space recursion is the most localized, sparse, tight binding Hamiltonian, derived systematically from the LMTO-ASA theory and generalized to substitutionally disordered random binary alloys:

$$H_{RL,R'L'}^{\alpha(\text{alloy})} = \hat{C}_{RL}^{\alpha} \delta_{RR'} \delta_{LL'} + (\hat{\Delta}_{RL}^{\alpha})^{1/2} S_{RL,R'L'}^{\alpha} (\hat{\Delta}_{R'L'}^{\alpha})^{1/2} \quad (3.9)$$

where $\hat{C}_{RL} = C_{RL}^A n_R + C_{RL}^B (1 - n_R)$; $\hat{\Delta}_{RL}^{1/2} = (\Delta_{RL}^A)^{1/2} n_R + (\Delta_{RL}^B)^{1/2} (1 - n_R)$.

Here R labels the lattice sites and $L = (lm)$ are the compact notation of orbital indices, C_{RL}^A , C_{RL}^B , Δ_{RL}^A and Δ_{RL}^B are the potential parameters of the constituents A and B of the alloy. n_R are the local site occupation variables which randomly take values 1 or 0 according to whether the site is occupied by an A atom or not, with probabilities proportional to the concentrations of the constituents. Hence, the effective non-random Hamiltonian in augmented space can be constructed by replacing the random variable $\{n_R\}$ in Eqn.3.9 by corresponding self-adjoint operators $\{\tilde{M}_R\}$:

$$\begin{aligned} \tilde{H} = & \sum_{RL} (C_{RL}^B \tilde{I} + \delta C_{RL} \tilde{M}_R) \otimes \mathcal{P}_R + \\ & \sum_{RL} \sum_{R'L'} \left((\Delta_{RL}^B)^{1/2} \tilde{I} \delta \Delta_{RL} \tilde{M}_R \right) S_{RL,R'L'}^{\alpha} \times \left((\Delta_{R'L'}^B)^{1/2} \tilde{I} + \delta \Delta_{R'L'} \tilde{M}_R \right) \otimes \mathcal{T}_{RR'}, \end{aligned}$$

where $\delta C_{RL} = (C_{RL}^A - C_{RL}^B)$ and $\delta \Delta_{RL} = ((\Delta_{RL}^A)^{1/2} - (\Delta_{RL}^B)^{1/2})$ and other parameters have their usual meaning. \tilde{I} is the identity operator defined in the augmented space, operation of which, as per normal definition, leaves the state with the augmented configuration as intact. The representations of the operator \tilde{M}_R are given by:

$$\tilde{M}^R = x \mathcal{P}_R^0 + (1 - x) \mathcal{P}_R^1 + \sqrt{x(1 - x)} (\mathcal{T}_R^{01} + \mathcal{T}_R^{10})$$

\mathcal{P}_R^{10} and \mathcal{T}_R^{10} are projection and transfer operators in the augmented space, where each site R is characterized by two states labelled 0 and 1, which may be identified with up and down states of an Ising system.

The augmented Hamiltonian is an operator in a much enlarged space $\Phi = \mathbb{H} \otimes \prod \phi^R$ (the augmented space), where \mathbb{H} is Hilbert space spanned by the countable basis set $\{|R\rangle\}$ (the real space). The enlarged Hamiltonian does *not* involve any random variables but incorporates within itself the full information about the random occupation variable. After the substitution of M_R the augmented Hamiltonian contains the following types of operators :

- a) $\mathcal{P} \otimes \tilde{I}$ and $\mathcal{T}_{RR'} \otimes \tilde{I}$. These operators acting on vector in the augmented space changes only the real space label, but keeps the configuration part unchanged.
- b) $\mathcal{P} \otimes \mathcal{T}_R^{01}, \mathcal{P} \otimes \mathcal{T}_{R'}^{01}, \mathcal{T}_{RR'} \otimes \mathcal{T}_R^{01}$ and $\mathcal{T}_{RR'} \otimes \mathcal{T}_{R'}^{01}$. These operators acting on an augmented space vector may or may not change the real space label. In addition they may also change the configuration at the site R or R' or both. This resembles a single spin-flip Ising operator in the configuration space.
- c) $\mathcal{P} \otimes \mathcal{T}_R^{01} \otimes \mathcal{T}_{R'}^{01}$ and $\mathcal{T}_{RR'} \otimes \mathcal{T}_R^{01} \otimes \mathcal{T}_{R'}^{01}$. These operators may change the real space label, as well as configuration either at site R or R' or both. This resembles a double spin-flip Ising operators in the configuration space.

The diagonal matrix element of the resolvent can now be calculated for this effective Hamiltonian using the recursion method which allows to take into account the effect of the environment of a given site [SDM94; SM96]. The convergence of various physical quantities calculated through recursion with the number of recursion steps and subsequent termination has been studied in great detail [CM01; GDM97]. In the TB Hamiltonian, there is a possibility of having randomness in the site-diagonal potential parameters as well as in the non-diagonal structure matrix (known as the *off-diagonal* disorder). In ASR, the form of the TB-LMTO Hamiltonian is kept intact and the configuration averaging is carried out without having to resort to any single-site approximation, so within ASF both the diagonal and off-diagonal disorder are handled on the same footing. It may be noted that there has been many attempts to utilize ASF in different formalisms of CPA for random alloys like Coherent Cluster approximation (CCA) [Koj85] for high connectivity *Bethe* pseudo-lattice. Another aspect of disorder in alloys is the disorder in structure factor arising out of local lattice distortion due to large size mismatch between components [Bos+92]. The effect of local lattice distortion on the electronic structures of non-isochoric alloys, e.g., CuPd, CuBe, using randomness in the structure matrices $S_{LL'}^{AA}, S_{LL'}^{AB}, S_{LL'}^{BA}$, and $S_{LL'}^{BB}$ in ASR

framework has been studied in detail [SM96]. Finally it may be noted that the increasing accuracy of calculations, as in any numerical implementation, pays back with high computation demands. To account for this issue, local symmetries of the augmented space can be used to reduce the Hamiltonian and carry out the recursion on a reduced subspace of much lower rank [Sah+03].

Electronic density of states of various binary disordered systems are calculated. For all the compounds, unless otherwise mentioned, experimental lattice parameters as compiled into International Crystal Structure Database(ICSD) are used. We first see the dos (Fig. 3.5) for Titanium based alloy CrTi, markedly known for its high tensile properties and corrosion resistance. With the increase in *Cr*-concentration, *Ti* states get more de-localised. The spin-resolved dos showing perfect moment cancellation, validates the calculations with experimental observations. Few more non-magnetic binary alloy examples shown in Fig.3.6 include *MoNb*, *MoV* and *MoW*. *Mo* states are quite similar for *Nb* and *V* solvents whereas in the *Mo*₅₀*W*₅₀ solution the DOS of *Mo* and *W* are almost same up to minor differences due the difference in chemical properties of 4*d* and 5*d* electrons. In case of magnetic alloy system *FeAu* in Fig. 3.7, the *Fe*-states near the Fermi Energy contribute mostly to the electronic properties and the Fermi level shifts resulting higher moment with the increasing *Fe*-concentration. And finally we show the density of states for *Fe*_{*x*}*Al*_{1-*x*} system in Fig. 3.8. The detailed features will be discussed in latter sections.

3.3 Effective pair Exchange interactions

Ab-initio Hamiltonian with configuration averaging enable us to calculate the disordered properties of alloys. To obtain the phase properties, we need to evaluate the exchange interaction energies, which govern the dynamics. The chemical exchanges hold the constituents together to form the alloy while the magnetic exchanges manifests the magnetism by maintaining a stable magnetic ground state. These Effective multi-site interactions which vary slowly with temperature, compete with the thermal agitation and results in a spectrum of different regions called the phase diagram of the alloy. These interactions can either be inferred experimentally, determined within phenomenological theories or obtained as the result of fitting procedures in specific statistical models.

In order to understand the onset of ordering in random alloys, one needs a deriva-

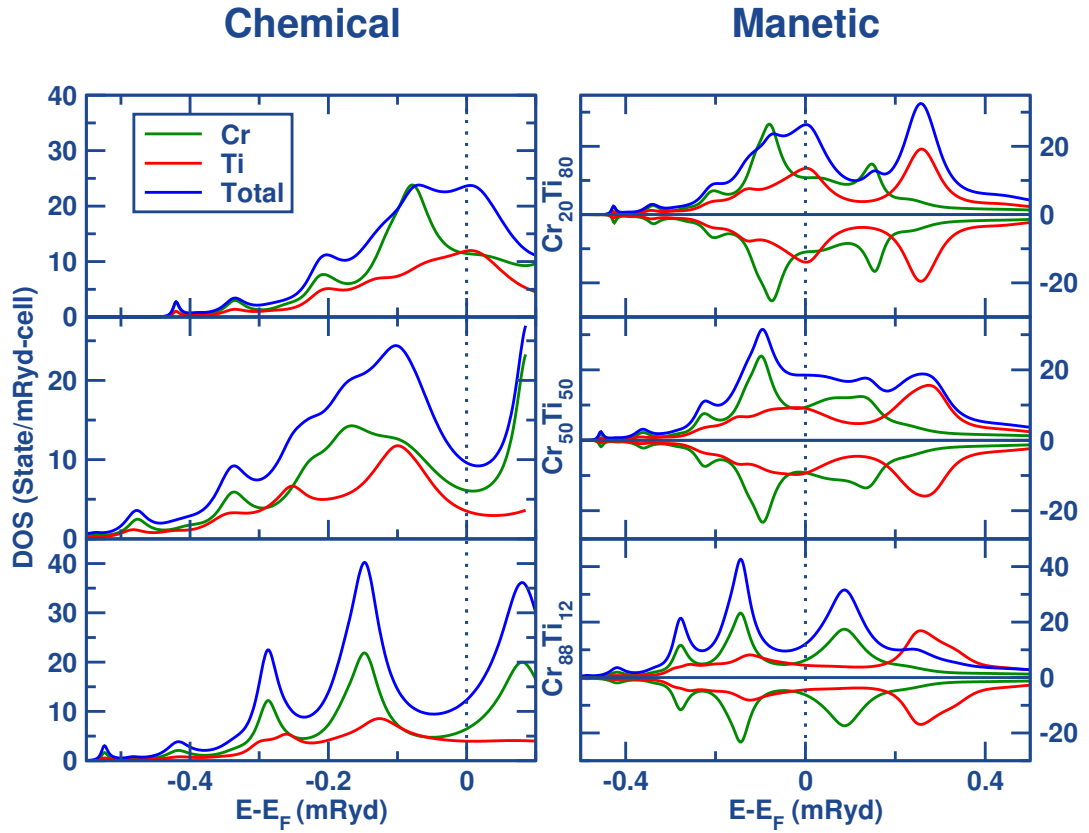


Figure 3.5: DOS for CrTi by ASR

tion of the lowest configurational energy for a specified alloy system. Models have been set up describing configurational energies in terms of effective multi-site interactions, in particular EPIs [Gon+87]. Within this approach, the analysis of alloy ordering tendencies and phase stabilities reduces to accurate and reliable determinations of these EPI. The simplest model which analyses the emergence of long ranged order from a disordered phase is the Ising model. So mapping of the energetics of the binary alloy problem onto an equivalent Ising model is often a natural way of addressing the problem. Once the effective multi-site interactions, in particular “effective pair energies” (EPE), is fairly accurately known, the standard statistical analysis of the Ising model can be employed to analyse the phase stabilities of alloys.

Traditionally there has been two different approaches of obtaining the effective cluster interactions. The first approach is to start with the electronic structure calculation and total energy determination of ordered super-structures of the alloy and to invert these total energies to get the effective duster interactions, namely, the CONNOLLY and WILLIAMS [CW83] method. The other approach is to start with a homoge-

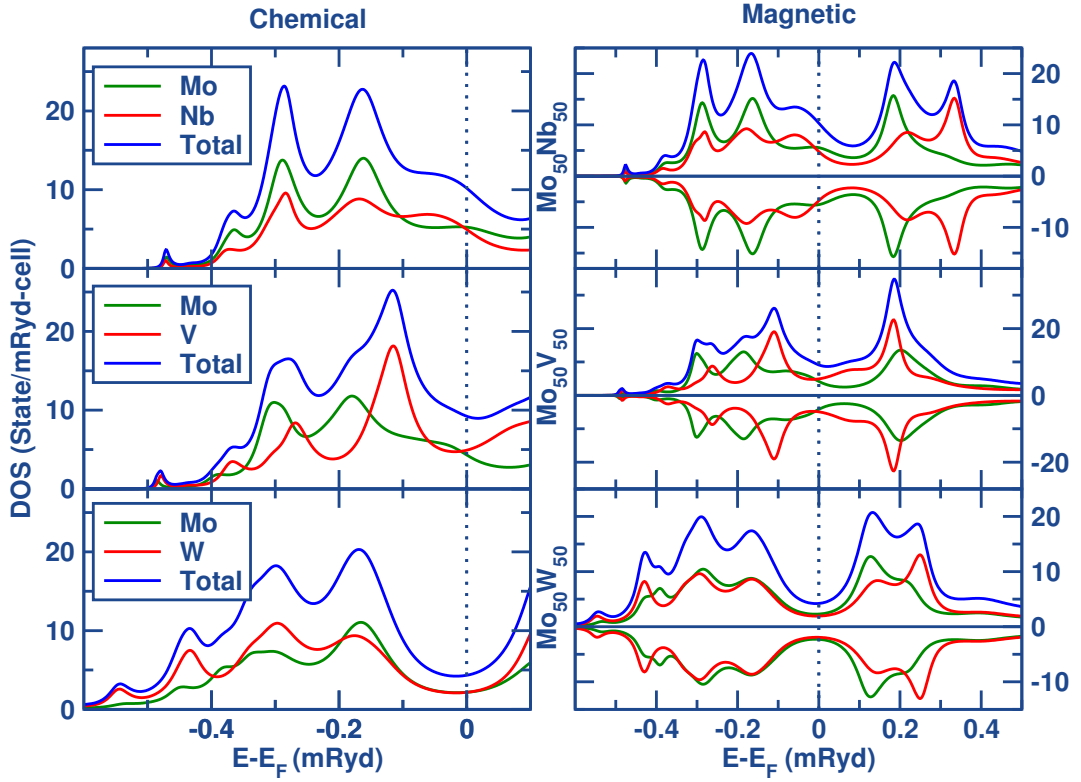


Figure 3.6: DOS for $\text{Mo}_{50}\text{Nb}_{50}$, $\text{Mo}_{50}\text{V}_{50}$ and $\text{Mo}_{50}\text{W}_{50}$ by ASR

neous, completely disordered phase, in it, set up a perturbation in the form of local concentration fluctuations associated with an ordered phase. One then decides, from the response, whether the alloy can sustain such a perturbation. At the critical point the response to such perturbations causes a divergent instability and order appears in the system. The amplification of a particular concentration wave indicates ordering in system. This approach includes the generalized perturbation method (GPM) [DG76], the embedded cluster method (ECM) [GG77; Gon+84] and the concentration wave approach [GS83]. All the latter three work are based on calculation within the frame-work of coherent potential approximation. Recently there has been combined attempt[Dre+89] to obtain effective pair interaction for each individual random configuration of the disordered alloy using recursion technique and then to obtain the configuration averaged pair interaction by direct configurational averaging (DCA). We used the GPM for the analysis.

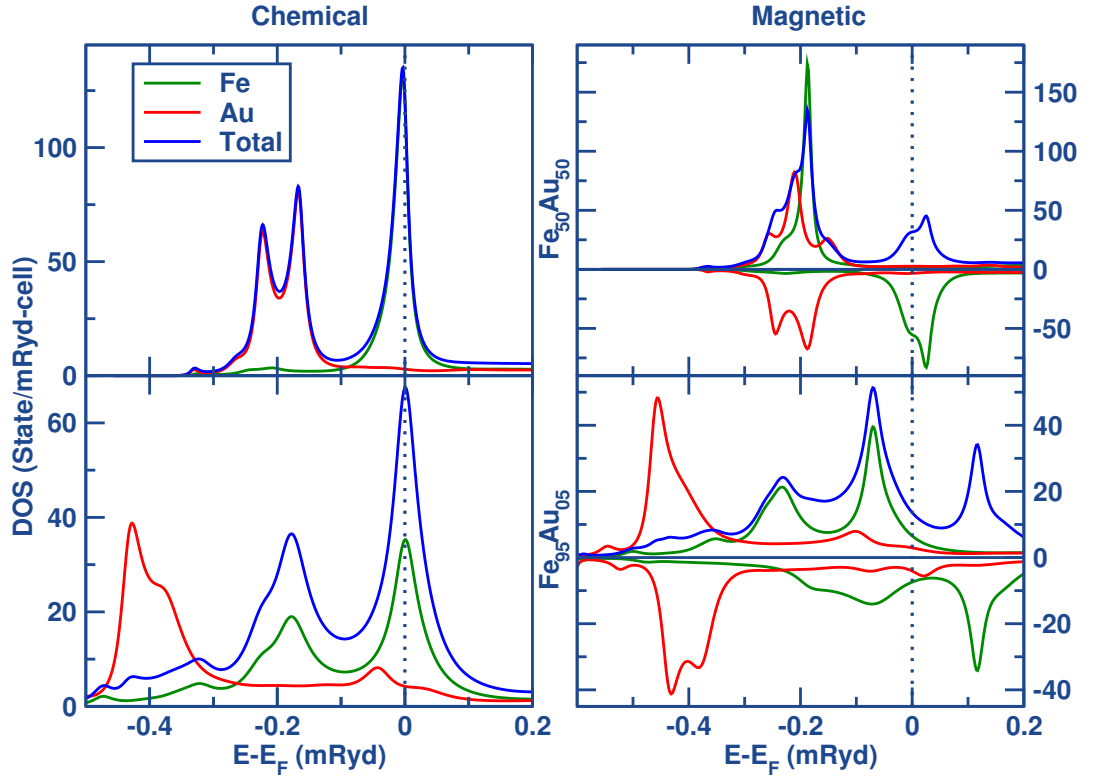


Figure 3.7: DOS for FeAu by ASR

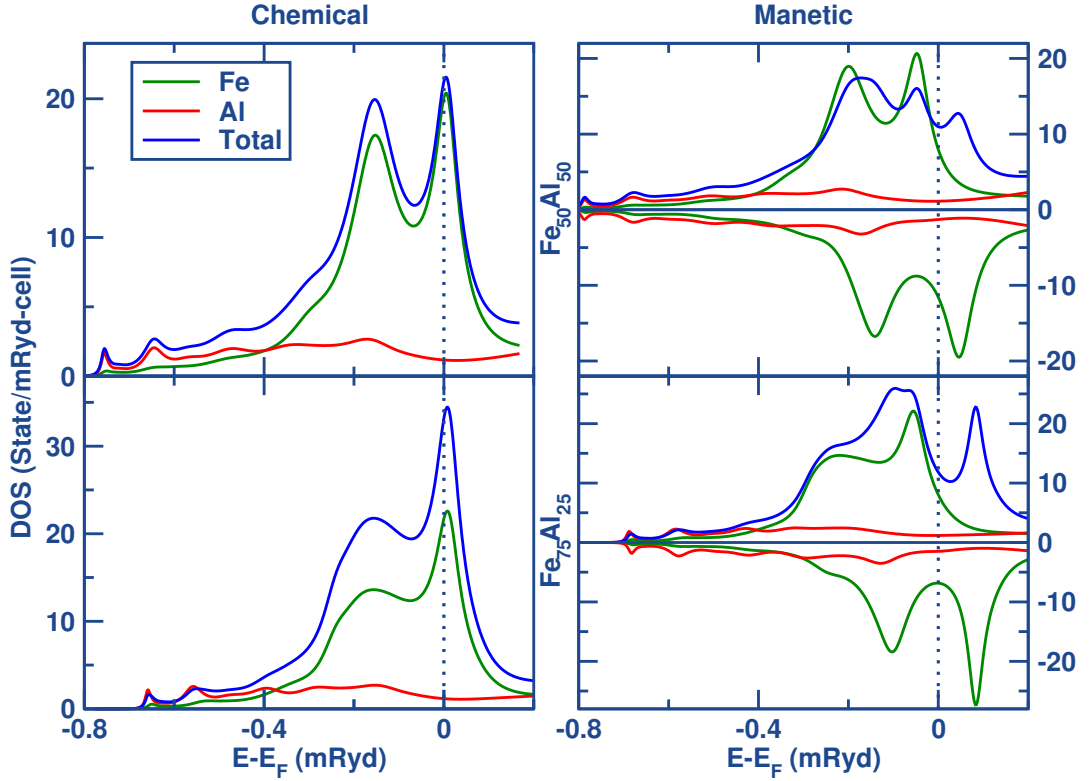
Generalized Perturbation Method(GPM): SANCHEZ and FONTAINE [SF78] shown that the set of multi-cite correlation function $\{\xi\}$ form a set of *complete* and *independent* variables in the thermodynamic configuration space. The correlation functions are formally defined as the ensemble average of products of the spin value n_i associated at lattice site i which take values $+1$ or -1 for A and B atoms, respectively.

$$\xi_{1,2,\dots,n} = \langle n_1 n_2 n_3 \cdots n_n \rangle$$

The state of order is described by the cluster probabilities x_{i_1, i_2, \dots, i_n} where i_1, i_2, \dots, i_n take values $+1$ or -1 for A and B atoms respectively. The cluster probabilities are inter-related and normalized. The correlation function and cluster probabilities are related by

$$x_{i_1, i_2, \dots, i_n} = \frac{1}{2^N} \left\{ 1 + \sum_l E(l; i_1, i_2, \dots, i_n) \cdot \xi_l \right\}$$

where $E(l; i_1, i_2, \dots, i_n)$ is, in general, a sum of l -order products involving the indices

Figure 3.8: DOS for $\text{Fe}_x\text{Al}_{1-x}$ by ASR

i_1, i_2, \dots, i_n and N is total number of indices.

As stated above, we have begun with a homogeneously disordered alloy A_xB_{1-x} , where every site is occupied by either an A or a B type of atom with probabilities proportional to their concentrations. We define the local ‘occupation’ variable $n(\vec{R}_i)$ to be a random variable which takes on the values 1 and 0 according to whether the lattice site \vec{R}_i is occupied by an A or a B atom. For a homogeneous perfect disorder the average $\langle n(\vec{R}_i) \rangle = x$, the atomic concentration of the component A in the alloy. In this homogeneously disordered system we now introduce fluctuations in the occupation variable at each site: $\delta n_{\vec{R}_i} = n_{\vec{R}_i} - x$. This perturbative approach expands the total electronic energy of a particular atomic configuration in terms of effective

renormalized cluster interactions $(E^{(0)}, E_{\vec{R}}^{(1)}, \dots)$ as follows:

$$\begin{aligned}
 E = & E^{(0)} + \sum_{\vec{R}_i} E_{\vec{R}_i}^{(1)} \delta n_{\vec{R}_i} + \sum_{\vec{R}_i} \sum_{\vec{R}_j} E_{\vec{R}_i \vec{R}_j}^{(2)} \delta n_{\vec{R}_i} \delta n_{\vec{R}_j} + \dots \\
 & \sum_{\vec{R}_i} \sum_{\vec{R}_j} \sum_{\vec{R}_k} E_{\vec{R}_i, \vec{R}_j, \vec{R}_k}^{(3)} \delta n_{\vec{R}_i} \delta n_{\vec{R}_j} \delta n_{\vec{R}_k} + \dots
 \end{aligned} \tag{3.10}$$

here,

- (i) $\vec{R}_n = \vec{R}_i - \vec{R}_j$ where $i \neq j$.
- (ii) $\delta n_{\vec{R}_i} = n_{\vec{R}_i} - x$ is the usual Flinn operator[Fli56] (or the spin-deviation operator in magnetism) and $\langle \delta n(\vec{R}_i) \rangle = 0$.
- (iii) in a homogeneously disordered alloy $\langle E \rangle = E_{dis} = E^{(0)}$.
- (iv) if $E_{\vec{R}_i}^Q$ is the configuration averaged total energy of a configuration in which any arbitrary site \vec{R}_i is occupied by a atom of the type Q and the other sites are randomly occupied, then:

$$E_{\vec{R}_i}^{(1)} = E_{\vec{R}_i}^A - E_{\vec{R}_i}^B \tag{3.11}$$

- (v) if $E_{\vec{R}_n}^{QQ'}$ is the averaged total energy of another configuration in which the sites \vec{R}_i and $\vec{R}_i + \vec{R}_n$ are occupied by atoms of the types Q and Q' respectively and all other sites are randomly occupied, then:

$$E_{\vec{R}_n}^{(2)} = E_{\vec{R}_n}^{BB} + E_{\vec{R}_n}^{AA} - E_{\vec{R}_n}^{AB} - E_{\vec{R}_n}^{BA} \tag{3.12}$$

- (iv) The single-site energy $E^{(1)}(\vec{R}_i)$ is unimportant for bulk ordered structures emerging from disorder. It is important for emergence of inhomogeneous disorder at surfaces and interfaces [DM96]. The pair energies $E^{(2)}(\vec{R}_n)$ dominantly govern the emergence of bulk ordering.
- (v) The multi-site energies $E^{(3)}(\vec{R}_i, \vec{R}_j, \vec{R}_k) \dots$ are usually too small to affect our conclusions qualitatively, except in cases of complex ordering. We shall ignore all such terms.

The interpretation of equation (3.12) leads us to note that although each of the terms $E^Q(\vec{R}_n)$ are of the $\mathcal{O}(10^3)$ Ry, the pair energy is of the order of mRy. The OP

formalism [Bur76] based on recursion [HHK72] was introduced by Burke precisely to calculate such small differences accurately, albeit in a different situation.

The total energy of a solid may be expressed in a generalised form as : $E = E_{\text{BS}} + E_{\text{Core}} + E_{\text{DC}} + E_{\text{Mad}}$, which can be separated in to two parts, the band term E_{BS} and an electrostatic term E_{ES} which, in turn, consists of : the Coulomb repulsion of the ion cores E_{Core} , the correction for double counting terms(E_{DC}) due to electron-electron interaction in E_{BS} , and a Madelung energy ($E_{\text{Mad}} = \frac{1}{2} \sum_{ij} M_{ij} q_i q_j$ where $M_{ij} = (1 - \delta_{ij}) / \vec{R}_{ij}$ is the Madelung matrix in atomic units) in case the model of the alloy has atomic spheres which are not charge neutral (q_i, q_j). The renormalized cluster interactions defined in Eq.3.10 should, in principle, include both E_{BS} and E_{ES} contributions. Since the renormalized cluster interactions involve the *difference* of cluster energies, it is usually assumed that the electrostatic terms which mainly has single-site character in charge neutral medium, cancel out and only the band contribution is important. Obviously, such an assumption is not rigorously true, but it has been shown to be approximately valid in a number of alloy systems[Tur+88]. We shall accept such an assumption and our stability arguments starting from the disordered side, will be based on the band structure contribution alone.

The Band energy E_{BS} is of the form:

$$E_{\text{BS}} = \int^{E_F} E n(E) dE = \frac{1}{2\pi i} \oint \text{Trace} [G(z)] z dz ,$$

where the density of states $n(E)$ is obtained from the resolvent $G(z) = (z - \hat{\mathcal{H}})^{-1}$ by

$$n(E) = -\frac{1}{\pi} \Im \text{Trace} [G(E + i\delta)] .$$

The direct evaluation of these large energies to obtain their differences is not advisable, instead we will find the Band energy combination as mentioned in Eqn.3.12 in an alternate and efficient way discussed in the proceeding section.

Orbital Peeling

Effective pair interactions are basically the cohesive energy differences obtained from ASR. The averaging of these EPIs has to be done with high precision and under the same class of treatments of disorder. The Orbital Peeling (OP) method is a real space prescription of direct calculation of the differences in energy moments of local dos

and avoids numerical instabilities due to subtractive cancellations. It is based on the same recursion method, which we have used to obtain the electronic structure, and in which we can control and estimate the errors systematically[Ehr80]. The effective pair interactions (3.12) can be related to the change in the configuration averaged local density of states :

$$E_{\vec{R}_n}^{(2)} = \int_{-\infty}^{E_F} dE (E - E_F) \Delta \langle n(E) \rangle \quad (3.13)$$

where $\Delta \langle n(E) \rangle$ is given by :

$$\Delta \langle n(E) \rangle = -\frac{1}{\pi} \Im m \sum_{QQ' \in AB} \text{Tr} \langle (EI - H^{(QQ')})^{-1} \rangle \xi_{QQ'}$$

$\xi_{QQ'} = 2\delta_{QQ'} - 1$, *i.e.*, is +1 or -1 according to whether $Q = Q'$ or $Q \neq Q'$, respectively. There are four possible pairs QQ' : AA, AB, BA and BB. $H^{(QQ')}$ is the Hamiltonian of a system where all sites are randomly occupied except \vec{R}_i and $\vec{R}_j = \vec{R}_i + \vec{R}_n$ which are occupied, respectively, by atoms of the type Q and Q' . This change in the averaged local density of states can be related to the generalized phase shift $\eta(E)$ through the equation :

$$\Delta \langle n(E) \rangle = \frac{d\eta(E)}{dE} = \frac{d}{dE} \left[\log \left\{ \frac{\det \langle G^{AA}(E) \rangle \det \langle G^{BB}(E) \rangle}{\det \langle G^{AB}(E) \rangle \det \langle G^{BA}(E) \rangle} \right\} \right]$$

$\langle G^{QQ'}(E) \rangle$ is the configuration averaged resolvent of the Hamiltonian $H^{(QQ')}$, *i.e.*, it describes the Green function with two atoms fixed at two positions and embedded in all possible combinations. The underlying complications of integral in Eq.3.13 lies in multivalued phases of $G^{QQ'}$ and prohibitive to employ standard routines (*e.g.*, Simpson's rule or Chebyshev polynomials). The generalized phase shift $\eta(E)$ can alternatively be calculated by the repeated application of the partition theorem on the Hamiltonian $H^{QQ'}$ as suggested by BURKE [Bur76], *albeit*, in a different context. Moreover, it is more efficient because the sub-block of effective augmented space Hamiltonian \tilde{H} relative only to the two sites of concerned atoms are affected and everything else remains unaltered. As our projected basis is also sub-spaced by a minimal set of orbitals, a more complete specification of the utilization of the Orbital peeling is to have the configuration averaged resolvent decomposed in terms of orbitals and sum all possible combinations of the two sites. The pair energy function is simply now defined in terms

of poles and zeroes of the Greens function, as :

$$\begin{aligned}
 F(\vec{R}_n, E) &= \sum_{QQ' \in AB} \sum_{\alpha=1}^{l_{max}} \xi_{QQ'} \int_{-\infty}^E dE' (E' - E) \log \langle G_{\alpha}^{QQ'}(E') \rangle \\
 &= \sum_{QQ' \in AB} \sum_{\alpha=1}^{l_{max}} \left[\sum_{k=1}^{p-1} Z_k^{\alpha, QQ'} - \sum_{k=1}^p P_k^{\alpha, QQ'} + \left(N_P^{\alpha, QQ'} - N_Z^{\alpha, QQ'} \right) E \right] \quad (3.14)
 \end{aligned}$$

where $\langle G_{\alpha}^{QQ'}(E) \rangle$ denotes the configuration averaged resolvent in which the orbitals from 1 to $(\alpha - 1)$ are deleted (peeled), hence the name. $Z_k^{\alpha, QQ'}(E)$ and $P_k^{\alpha, QQ'}(E)$ are its zeros and poles $\leq E$ and $N_Z^{\alpha, QQ'}(E)$ and $N_P^{\alpha, QQ'}(E)$ are the number of such zeros and poles of the relevant resolvent $\langle G_{\alpha}^{QQ'}(E) \rangle$ below E . The zeros and poles are obtained directly from the recursion coefficients for the averaged resolvent calculated from the TB-LMTO-ASR. This method of zeros and poles enables one to carry out the integration in equation (3.13) easily avoiding the multi-valuedness of the integrand involved in the evaluation of the integral by parts.

The effective pair energy (EPI) is then given by :

$$E_{\vec{R}_n}^{(2)} = F(\vec{R}_n, E_F). \quad (3.15)$$

In conclusion, we have projected our problem onto to an effective Ising model :

$$H^{\text{eff}} = -\frac{1}{2} \sum_{\vec{R}_i} \sum_{\vec{R}_n} J(\vec{R}_n) \sigma(\vec{R}_i) \sigma(\vec{R}_i + \vec{R}_n) \quad J(\vec{R}_n) = -2E^{(2)}(\vec{R}_n)$$

3.4 Statistical Analysis

We have discussed the development of *ab-initio* methods to study the ground state properties of many-body systems. Now extending these results to high temperature range is the real motivation of doing all these things as the application is never going to be used at 0°K. And then we have the obvious choice left that is doing a statistical analysis. Any equilibrium state is the most energetically favorable state available to the system. A system that is out of equilibrium will evolve toward equilibrium. The driving force for this transformation is derived from the requirement that the system minimize its free energy. The statistical mechanics of classical systems in thermal equilibrium starts with Ludwig Boltzmann: The statistical definition of the entropy, $S = k \log W$, provides a connection between the microscopic atomistic description of a many-body

system with macroscopic thermodynamics. Here W is the number of *micro states* of the system.

In statistical analysis the starting point is the configurational partition function which can be written as

$$Z = \sum_{states} \exp\left(-\frac{E_{state}}{kT}\right) = \sum_{\{n\}} g(\{n\}) \exp\left(\frac{E(\{n\})}{kT}\right),$$

where $g(\{n\})$ is the statistical weight of the configuration defined by the set of variables $\{n\}$.

3.4.1 Ordering Energy

Out of related mean-field based studies of Cowley[Cow50b], Krivoglaz [Kri69], and Clapp and Moss [CM66; CM68] emerges simple relationship between experimentally observed diffuse scattering and the Fourier transform of the effective pair interactions (EPI) $V(\vec{k})$. Known as the Krivoglaz-Clapp-Moss (KCM) formula, it treats the concentration fluctuations by the single site mean-field Bragg-Williams approximation. The inverse susceptibility or the diffuse intensity which measures the response of the disordered system to the concentration fluctuation perturbation described above, is

$$\chi^{-1}(\vec{k}) \propto 1 + x(1-x)\beta V(\vec{k}),$$

where \vec{k} is the wave vector of the fluctuation spectrum. The diffuse intensity has a maximum where $V(\vec{k})$ is minimum. This has been suggested by PHILHOURS and HALL [PH67], and CLAPP and MOSS [CM68] have formally shown that a sufficient (but not necessary) condition for a stable ground state is that the wave vector of concentration waves corresponding to an ordered phase lie in the positions of the minima of the Fourier transform of the pair energy function or the maxima of that of $J(\vec{R}_n)$:

$$V(\vec{k}) = \sum_{\vec{R}_n} \exp(i\vec{k} \cdot \vec{R}_n) J(\vec{R}_n) = -2 \sum_{\vec{R}_n} \exp(i\vec{k} \cdot \vec{R}_n) E^{(2)}(\vec{R}_n) \quad (3.16)$$

Finally, the EPIs also directly give the ground state ordering energies on a given lattice :

$$\Delta E_{ord} = \frac{1}{2} \sum_n E^{(2)}(\vec{R}_n) Q_n \quad (3.17)$$

where n is a n -th nearest neighbour of an arbitrarily chosen site (which we label 0) and $Q_n = (x/2)(N_n^{BB} - xN_n)$, N_n^{BB} is the number of BB pairs and N_n the total number of pairs in the n -th nearest neighbour shell of 0, x being the concentration of B -type atoms. It describes the difference between the considered state and a statistically uncorrelated arrangement.

3.4.2 Monte Carlo Simulation

Recently, with the development of computation power, increasingly more efforts has been made to understand order-disorder phenomena and other phase transitions in solids basing on the *ab-initio* calculations. The initial approach in every effort is to re-frame the Hamiltonian of the problem (order-disorder) to some theoretical model description like an open shell Ising type Hamiltonian of the form

$$\hat{\mathcal{H}} = \sum_{ij} J_{ij} S_i S_j + \sum_i h_i S_i, \quad (3.18)$$

where S_i is the spin variable associated to the i^{th} lattice site and h_i is the applied magnetic field of the system. The important average properties needed for description of the phase diagram are the average internal energy $\langle E \rangle$ and average magnetisation $\langle M \rangle$ as functions of temperature T . In the equivalence to the chemical transition in disordered alloys, for example, spin variables $\pm 1/2$ map on to alloy component type ± 1 (A/B) and then the magnetisation profile corresponds to the long range order parameter. The sub-critical region of reduced ferro or anti-ferromagnetic phase depicts the short ranged local ordering of the alloy. In this light, the solution of the Ising type Hamiltonian and the computation of the corresponding phase diagram is done with the following approximate methods :

- a. Mean-field (or Bragg-Williams)[Kik51] approximations and its variants (These are crudest of all but definitely the best start point to consider.),
- b. Renormalization group transformation (sophisticated analytical framework and hence has very limited application the simple systems only) and
- c. Monte Carlo simulations.

Monte Carlo simulation is a class of stochastic computer algorithms based on the use of sampling of random numbers and probability statistics to investigate problems, in general, with many degrees of freedom to obtain average properties. The history goes back to as early as 1949 when METROPOLIS and ULAM [MU49] in their paper

“Monte Carlo methods” suggested a statistical method using random numbers to solve a class of problems in Physics and Mathematics involving differential equations. This paper opened an era of possibility of natural emulation through computing devices, which, off course had to wait until the well supporting development of the computing power. Monte Carlo method employs a random distribution to simulate for nature to sample a probabilistic space for counting of states which is effectively integration in higher dimensions. Owing to it’s overweening usefulness in different fields of sciences, a corpus of Monte Carlo exists in literature. Our interest is concentrated here on the equilibrium Monte Carlo methods for random binary alloys. The details of this method with several useful applications are available in specialized texts[BH10; LB00; NB99]

For a statistical system in thermal equilibrium at temperature T , the probability distribution followed by the microscopic configurations (labelled by C) is the Boltzmann distribution (Gibbs measure)

$$P(C) = Z^{-1} \exp(-\beta E(C)). \quad (3.19)$$

We have used the usual notation, $\beta = 1/k_B T$ is the inverse temperature and $Z = \sum_{C \in \Omega} \exp(-\beta E(C))$ is the partition function and Ω represents the probability space of all configurations. The average value $\langle A \rangle$ of any general state function $A(C)$, without additive kinetic energy contributions, is thus (integration is necessarily replaced by a summation in discrete computational framework)

$$\langle A \rangle = \frac{\sum_{C \in \Omega} A(C) \exp(-\beta E(C))}{\sum_{C \in \Omega} \exp(-\beta E(C))} \quad (3.20)$$

The partition function is unknown and calculating it, is always the *difficult* part of the problem. In Monte Carlo simple sampling, one samples the whole phase space uniformly randomly using only a characteristic subset of phase space points $\{C_1, C_2, \dots, C_N\}$. But it is evident from Eq. 3.20, cf. Fig.3.9 that most of the significant regions of phase space are highly concentrated due to the *exponential* terms in the above sums. So rather than using a *crude* Monte Carlo, which becomes eventually impractical, one employs the *importance sampling* Monte Carlo which basically, as the name suggests, samples the relatively important area of the sum by a choicest probability distribu-

tion function($p(x)$) that closely and suitably follows the form of the function under consideration.

$$\langle A \rangle = \frac{\sum_{C \in \Omega} \frac{A(C)}{p(C)} \exp(-\beta E(C)) p(C)}{\sum_{C \in \Omega} \frac{\exp(-\beta E(C))}{p(C)} p(C)} \quad (3.21)$$

Now if one generates the configurations with probability $p(x)$, then

$$\langle A \rangle = \frac{\sum_{C \in p(C)} \frac{A(C)}{p(C)} \exp(-\beta E(C))}{\sum_{C \in p(C)} \frac{\exp(-\beta E(C))}{p(C)}} , \quad (3.22)$$

And it is the importance sampling of the given phase-space[MU49]. The choice of the pdf $p(x)$ is typical to the class of the problem. One widely accepted choice for $p(x)$, in statistical mechanics, is the Boltzman probability itself. Here one doesn't need to know the individual probability of any configuration, rather the transition probability is needed which additionally enables avoiding the calculation of the whole partition function Z . One has to choose configurations with a probability $p = \exp(-\beta E)$ and weight them evenly, like, for example, the estimate of A in the simulation is simply obtained as an arithmetic average

$$\langle A \rangle = \frac{1}{N} \sum_{i=1}^N A_i$$

as opposed to choosing configurations randomly and weighting them with $\exp(-\beta E)$ as done in *brute-force* Monte Carlo.

3.4.2.1 Detailed Balance

The probability distribution $P(C, t)$, in general, is a time-dependent property that describes the probability for the stochastic variable C of the system to have the value C . The stochastic variable can be any microscopic degrees of freedom *viz.*, the local concentration (η_i) of the alloy or local spin (S_i). Transitions from a configuration of the system described by C' to another state identified by C'' will change the corresponding

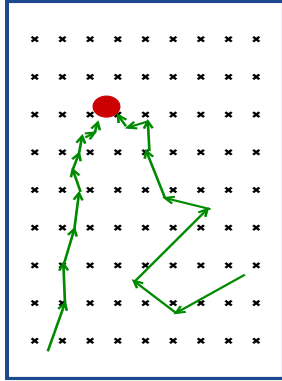


Figure 3.9: A schematic representation of phase space Ω as blue frame-box with a red disc corresponding to high probable region of states at a particular temperature T . Black cross marks are uniformly gridded/random simple sampling points. Many of these points are just negligibly contributing in the averaging (Eqn.3.20). A green line represents a **Markov chain** of importance sampling. Two different chains are shown to start at two arbitrary points and eventually converge to the important phase space region, with acceptable fluctuations.

occupations of $P(C', t)$ and $P(C'', t)$, as

$$dP(C', t) = -dP(C'', t) = P(C', t)T(C', C'') dt.$$

The summation over all possible transitions, for a discrete stochastic variable, results in a continuity relation known as the *master equation*

$$\frac{\partial}{\partial t}P(C, t) = \sum_{C \neq C'} [P(C', t)T(C', C) - P(C, t)T(C, C')] , \quad (3.23)$$

where $T(C, C')$ is the time independent transition probability distribution or transition rate for the transition of the system from state C to state C' . Thus follows the master equation for a stationary equilibrium probability-distribution function $P(C) \equiv P_{eq}(C)$

$$\sum_{C \neq C'} [P(C', t)T(C', C) - P(C, t)T(C, C')] = 0. \quad (3.24)$$

A stochastic process generating a series of configurations with time (not necessarily physical time) in which each transition only depends on the current configuration and not on the *history* is called a Markov process [LB00]. At each step of this fictitious time, the system is in one of all possible configurations comprising Ω . Successive configurations are generated by using the relative probabilities of the initial (C_i) and final (C_j) configurations called the transition probability T_{ij} . To depict a physical system, the transition probability matrix T must form a stochastic matrix, *i.e.*, satisfy following typical requirements: (i) The probabilities (matrix elements) must be positive. $T_{ij} \geq 0$ (ii) Total probability must be a definite or unity if normalized (rows sum up to unity). $\sum_j T_{ij} = 1$. The *irreducibility* (every configuration C_x is accessible from any con-

figuration C_y by some finite probability in some finite time steps) and *aperiodicity* (a configuration can be reversed in a single time step $T_{ii} > 0$) of the Markov chain ensures *ergodicity* of the system. The *stationary* and *reversible* master equation 3.24 can one way be satisfied term by term which poses as requiring the equilibrium be achieved both locally and globally. This equality is hence called the *principle of detailed balance* :

$$P(C_i)T_{ij} = P(C_j)T_{ji}. \quad (3.25)$$

This basically indicates that the evolution for a favourable configuration has come to an end with the state probability being limited to $P(C_j)$. Monte Carlo simulation produces a Markov chain of system configurations at equilibrium. What the simulation seeks for is a high probable equilibrium state of the system at some point down the chain. The choice of such transition probability is tactical though not unique.

3.4.3 Glauber dynamics

The goal is to construct a Markov chain of random walks through the phase space of the N-particle model system such that it has a desired stationary and converged distribution $P(C)$. One may simply consider a specific site on the lattice according to some rule, make a single spin flip with a certain probability, find the change in energy and accept the new configuration if it's energetically favoured. At equilibrium, Eq 3.25 is numerically sampled. This prescription of capturing the stochastic evolution is known as the Glauber dynamics[Gla63]. So one needs to find a suitable ergodic transition matrix constrained by the detailed balance condition. A move from a state C_i to a state C_j is proposed according to some proposal probability q_{ij} . It needs to be chosen in such a way that the Markov chain will be ergodic. The reverse transition from C_j to C_i is proposed with the same probability, *i.e.*, $q_{ij} = q_{ji}$. It ensures the ergodicity. By the detailed balance 3.25

$$\frac{T_{ij}}{T_{ji}} = \frac{P(C_j)q_{ji}}{P(C_i)q_{ij}}.$$

With $q_{ij} = q_{ji}$ and $P(C) = \exp(-\beta E(C))/Z$,

$$\frac{T_{ij}}{T_{ji}} = \exp(-\beta(E(C_j) - E(C_i))) = \exp(-\beta\Delta E).$$

According to Metropolis choice, $T_{ji} = 1$ and

$$T_{ij} = \begin{cases} \exp(-\beta\Delta E) & \text{if } \Delta E > 0 \\ 1 & \text{if } \Delta E \leq 0 \end{cases}.$$

It clearly satisfies the detailed balance condition Eq 3.25 by construction; Any spin configuration is obtainable from any other straightforwardly by the single flip method, so irreducibility and also aperiodicity are evident in this algorithm. This algorithm was introduced by METROPOLIS et al. [Met+53] in their classic paper; famously known as the Metropolis algorithm, is identifiably a flavour of Glauber dynamics with fast convergence. There exists several other update schemes, in addition to Metropolis, viz., Glauber, and heat-bath dynamics, but all update schemes, incumbent on the satisfying of the detailed balance, leads to much of the same results for equilibrium phenomena. Summarisingly, the state C_j is accepted as the next state of the chain with a probability $T_{ij}^{accept} = \min(1, \exp(-\beta\Delta E))$. When C_j is not accepted, the next state of the chain will again be C_i . In practice of coding, the implementation goes like this:

1. Generate a lattice as per the problem specifications. For simplicity we consider equal-sided d -dimensional (hyper)cubic lattice with each side length L and the total numbers of sites $N = L^d$. Populate the lattice with spins $+1$ or -1 randomly (hot start) or all spins either up or down (cold start).
2. Start from a site as beginning and go sequentially on up to the end of the lattice for checking following steps for each site.
 - Propose the spin flip and find out the change in energy ΔE resulting from the flip.
 - Accept the flip if $\Delta E \leq 0$.
 - Otherwise, generate a random number $r \in [0, 1]$ and accept the flip only if $r < \exp(-\beta\Delta E)$.

It's pertinent to mention that (a) unlike the method of choosing a random site, this book-keeping style choice tampers *ergodicity* slightly, especially, for small size systems and less number of repetitions(*sweeps*), but it has considerable advantages in computation (b) a single spin-flip ensures small change in energy thus larger acceptance probability.

3. Attempts covering all the N -sites usually considered as a unit of Monte Carlo steps called the *sweep* characterizes a non-deterministic time scale of the simulation. Quantities of interest are collected at each sweep and averaged to yield the ensemble average property. However, it should be noted that, the system is not under equilibrium from the very beginning of the simulation and hence one must identify and discard these non-equilibrium data. Due to correlations in the random numbers generated by a computer, the successive configurations may have high correlations leading to a non-Markovian nature of the simulation. Necessarily one has to avoid the memory of initial configuration and take only the asymptotic average value by dry-running several sweeps, a practice called the *thermalization or equilibration* of the system, and assess the results numerically using standard statistical techniques like autocorrelation and binning of data for convergence in order to identify the initial correlated fluctuations.
4. In the vicinity of the critical point in a system in equilibrium various quantities are characterized by power law singularities which are governed by some critical exponents. These exponents are however universal and do not depend on the details of the model and categorize the phase transitions as the so called universality class of the system. This universality helps us not to worry about the critical exponents and estimate the transition temperature fairly accurately.

3.4.4 Kawasaki dynamics

The transition rate is a key quantity from physical point of view. The choice is not unique and that gives a broader perspective to the simulation. Unlike in the last section, the rate can be chosen such as the order parameter is conserved. It is usually necessary in physically plausible descriptions of properties associated with transport phenomena such as diffusion, conduction, vacancy dynamics etc. If the order parameter is local concentration (spin) then it simulates a system in which the total concentration (magnetisation) is fixed. This is called the Conserved order parameter (COP) simulation. One widely used COP Markov chain in Ising configuration space is Kawasaki dynamics [Kaw66]. In Kawasaki dynamics the fundamental move is a flip of pair of opposite spins. The pair can be chosen at any distance randomly but to simulate the real physical system, choice of adjacent pair is preferred. Both Glauber and Kawasaki dynamics preserve the Boltzman distribution and have the same static critical exponents, But the addition of a conserved quantity makes the dynamic slower [Smi+08]

and the Kawasaki dynamics has different dynamic universality class characterized by the exponent associated with the correlation length. Hence we will use it only for the chemical ordering simulations.

3.4.5 Finite Size Effect

In principle, the errors can be made arbitrarily small if only enough computer time is invested. In practice sufficient accuracy is obtained for systems with fairly short-ranged interaction only. Phase transitions only occur in the thermodynamic limit. The fundamentally diverging quantities of phase transitions, *e.g.*, the correlation length, can not diverge in the limit of finite size of simulation owing to the limited memory and processing power of computer. These quantities scale with the linear size (L) of the system. The order parameter exhibits an unphysical long tail after the supposed transition, and the smoothness even precludes the identification of the order of the phase transition. With increasing L one observes a shift in the peak of any diverging thermodynamic quantity with simultaneous narrowing and thus the maxima of these quantities do not correspond to accurate T_C . A detailed and systematic analysis of this effect and deduction of conclusions for the thermodynamic limit by setting up proper scaling exponents is called the finite size scaling(FSS)[Kad+67]. In this finite size scale ansatz, regression of a chosen function of any finite size scaled quantity can determine the transition temperature T_C . The thermodynamic quantities can also empirically be extrapolated to an infinite system with these tunable parameters. One more elegant and useful theoretical tool to account for the high-temperature tail is the higher order cumulant approximation of BINDER [Bin97]. The cumulant method employs a Gaussian assumption to the order parameter distribution to characterize the order of the transition[CLB86] and provides finite size scaling all in one. It is formally shown that the fourth order cumulant of the order parameter is a constant w.r.t. L at the point of transition.

$$U_4(tL^{1/\nu}) = 1 - \frac{\langle M^4 \rangle}{3\langle M^2 \rangle^2}$$

and

$$\langle M^4 \rangle = \begin{cases} \langle M^2 \rangle^2 & \text{for } T < T_C \text{ So } U_L = \frac{2}{3} \\ 3\langle M^2 \rangle^2 & \text{for } T > T_C \text{ So } U_L = 0 \end{cases}$$

So the calculation of C_4 as a function of temperature for a range of L , through the intersection of resulting curves, provides a very precise estimation of the calculated

transition temperature of the simulation.

3.4.6 Boundary Conditions

Boundary conditions are necessary to curtail the edge effects on simulation and thus helps in preserving the symmetry of the lattice by mandating equal numbers of spin-spin interactions for all sites. The most intuitive and prevalent in use is the periodic boundary condition (pbc) in which the spins at the edge are made to interact with the corresponding spin at the geometrically opposite edge. The structure becomes a toroid in one dimension higher than that of the system itself. However, the simulation can be made more useful by choosing boundary conditions appropriate to the model studied, its physicality, the computational optimization of the calculations etc. Like a *free boundary condition* would be appropriate for surfaces while a *fixed* one would be more suited for trapped clusters. Even the anisotropic combinations thereof can be sometimes useful. The choice of boundary condition affects the finite size scaling of the system [Sel06], But the finite size scaled transition temperature is discordant to this choice [VS98].

We used the so called *skew-periodic* boundary condition, in which the spin of at the edge of one row is the neighbour to the spin at the beginning of the next row. In effect, the topology of any lattice of any dimension becomes a ring. This facilitates for considering one such ring for one *basis* in the *Bravais* lattice of the crystal. Like shown in Fig.3.10, the skew bc of a 2D square lattice with two rings for the square-corner and the square-centre positions, a 3D BCC lattice needs 2 rings and FCC, 4 rings for simulation. Multi-spin coding, which is very effective in reducing the computation requirement for 2d Ising model, is not suitable for simulations with interactions ranging beyond the nearest neighbour, due to the over-head of *bit*-manipulations. Resorting to vectorization of this kind, in this scenario, is quite instrumental. In addition, this extends the scope of the code for studying typical sub-lattice decomposed magnetism (anti-ferro) and chemical orderings of complex superstructures found in alloys.

3.4.7 Code Implementation and practicalities

A Monte Carlo (MC) program was developed in Fortran 90 computer language. All the discussions made earlier were taken into considerations and aimed at tackling the

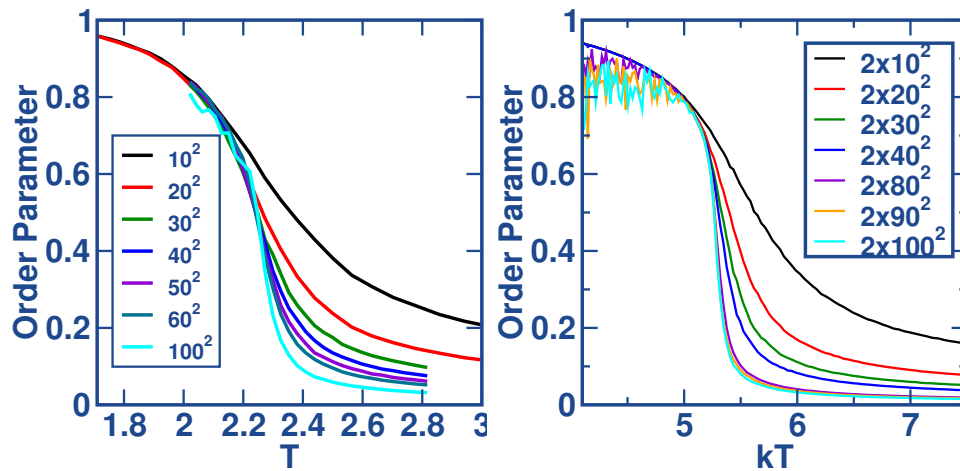


Figure 3.11: (left) The effect of lattice size is prominent for 2d-Ising model. (right) The order parameter for a denser (square-centred) 2d lattice.

value $T=2.27$. In the right panel, the result for a square-centred 2d Ising lattice the results is very similar. But in very low temperature region, magnetisation is seen to be increasingly fluctuating with the lattice size. This is due to the bi-modality of the probability distribution of the magnetisation parameter. At low temperature contiguous clusters of both up-spin and down-spin are formed and the change in energy at domain boundary is very little. So large sized systems, it needs more Monte Carlo time, even more than that as required to overcome the critical slowing down, to attain the ground state. We have deliberately performed the simulation for all sizes shown here, with equal sweeps and thermalization steps. This type of delayed equilibration at low temperature, albeit for a different reason of spin freezing, is crucial in spin-glass studies[BY85].

A slightly modified version of the *typewriter* updating sequence is the *checkerboard* scheme in which updating is done by regularly going from one site to its next nearest neighbour, effectively updating first one sub-lattice, then the other. The skew-periodic bc, in terms of computation, is more compatible with this type of updating, where instead of going to a distant memory location of the computer, every nearly located equivalent site of all the rings is tried for a flip first. This is not exactly the so called *multispin coding*(MSC) of CREUTZ, JACOBS, and REBBI [CJR79]. The MSC is very effective in size reduction and time optimization by assigning *spin* variable to the *bits* of computer *words* and then the operations like flip proposal and acceptance are performed using *logic operations* on those words. However, the gain is limited to the coordination of each spin considered in the simulation and for long ranged interac-

tions the overhead of these operations, in fact, slows down the simulation by several folds.[ZHR81] So this *pseudo-MS* is a kind of trade-off between conventional multi-dimensional array based MC coding and the MSC.

The utmost requirement of a MC simulation is a good random number generator(RNG). The generation and characterization of RNG, rather call it Pseudo-RNG (PRNG) in its true sense, is itself an active area of research now. A pragmatic discussion is inexorably found in all literature references. Routines for uniform PRNG are readily available. We have used a combined linear congruential generator. With cross calculations using compilers (gfortran & ifort™) provided generators, we verified the consistent nature of output.

The statistical error in Monte Carlo scales inversely with system size. The finite size scaling circumvents any confrontation to that in the determination of T_c . It is notable that systematic errors are expected to arise based on the methodologies, the choice of algorithms and boundary conditions etc. We have not tried to assess these errors, which are very difficult to quantify, because that's not imperative to our study.

3.5 Results and Discussion

The TB-LMTO-ASR-OP proposed by us will provide a unified recursion based technique to study problems of disorder-order transitions in binary alloys. Finally, a word about similar work done earlier using different methodologies. This is important in order to gauge the accuracy of our new approach against earlier results. The earliest work was that by BOSE et al. [Bos+97]. Their approach was by the LMTO-CPA using the Liechtenstein formula. In a later work by LONG and AKAI [LA07] the pair energies of $\text{Fe}_x\text{Al}_{1-x}$ was obtained using the KKR-CPA and the Lichtenstein formula. Curiously, there was no reference to the earlier work. We should also mention the works of DORFMAN [Dor99] and LIUBICH, DORFMAN, and FUKS [LDF02]. The authors treated the concentration dependencies of the pair energy functions both empirically from X-ray scattering data and from first principles LMTO-CPA. We shall compare our results with these works in a later section.

3.5.1 Density of states

Before we begin an analysis of the phase stability of the alloys, we shall first obtain the densities of states using our TB-LMTO-ASR and compare it with earlier work. This

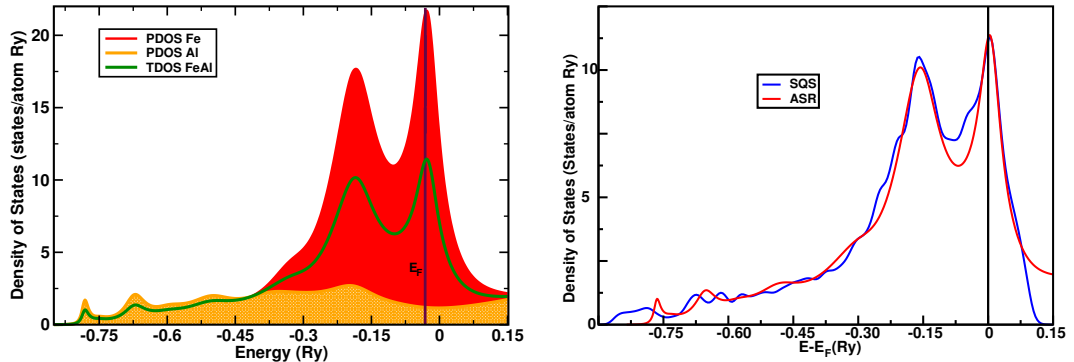


Figure 3.12: (left) Partial and total densities of states for the $\text{Fe}_{0.5}\text{Al}_{0.5}$ alloy (right) Total densities densities of states for $\text{Fe}_{0.5}\text{Al}_{0.5}$ alloy from SQS and ASR.

will be a yardstick of the accuracy of our method. In Fig. 3.12 left panel we show the partial densities of states (PDOS) for Fe and Al ($n_{\text{Fe}}(E)$ and $n_{\text{Al}}(E)$) and the total densities of states (TDOS) ($x n_{\text{Fe}}(E) + (1 - x) n_{\text{Al}}(E)$) for $\text{Fe}_{0.5}\text{Al}_{0.5}$. The component projected partial densities of states clearly indicate the s - p like states of Al (with $-0.04 \mu_{\text{B}}$) and the more localized d -states of Fe (with magnetic moment $0.76 \mu_{\text{B}}$).

We shall first compare our results with that of BOSE *et al.* [Bos+97]. This work was based on the LMTO-CPA and used the Barth-Hedin exchange functional. The Madelung energy was avoided by the use of neutral spheres for both Fe and Al. We have used the same exchange functional but used the idea suggested by RUBAN and SKRIVER [RS02] to estimate the Madelung effects. We compare the left hand panel of our Fig. 3.12 with the Fig. 1 of Bose *et al.*, and note that the agreement is more than satisfactory.

We also compare our ASR results with that obtained from the special quasi-random structures (SQS) based approach combined with the pseudo-potentials (PP) available in the VASP codes. The concept of SQS was proposed by Zunger *et al.*, [HDZ90; Jia+04; Wei+90; Zun+90], about which we will be discussing more in the next Chapter 4. The SQS, like the ASR, overcomes the limitations of the coherent potential approximation. The SQS also takes into account the distribution of distinct local environments, the average over which corresponds to the averaged properties of the random alloy. The right panel of Fig. 3.12 compares the ASR TDOS with that obtained from a 32-site SQS. Note that the super-cell technique used in the SQS leads to spurious fine structure in the TDOS. We have smoothed the TDOS using a small constant imaginary self-energy. The comparison shows remarkable agreement between the PP-SQS and TB-LMTO-ASR. This gives us confidence in the use of TB-LMTO-ASR. There

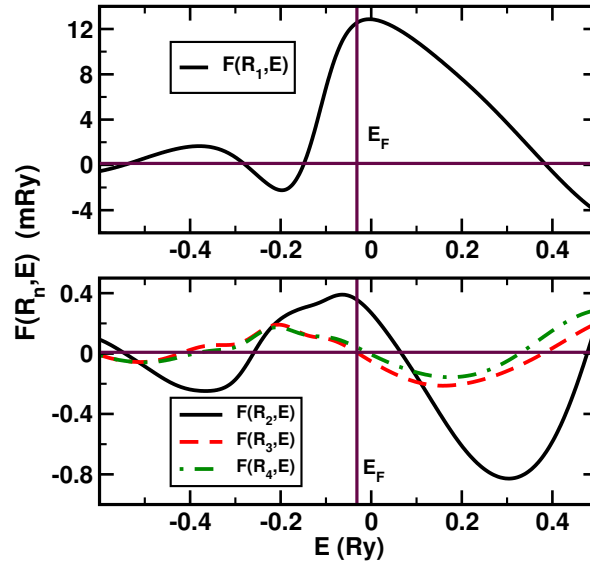


Figure 3.13: Pair energy functions at different neighbouring distances for $\text{Fe}_{50}\text{Al}_{50}$, calculated using TB-LMTO-ASR-OP. Variation is shown against energy. (top) Nearest neighbour pair function at a distance $\sqrt{3}a/2$, a being the equilibrium lattice parameter (bottom) second, third and fourth nearest neighbour pair functions at distances a , $\sqrt{2}a$ and $\sqrt{3}a$

are approximations in the use of ASA in TB-LMTO and in the ‘termination’ procedure in the recursion method. Nevertheless, the TB-LMTO-ASR remains accurate at least for $\text{Fe}_x\text{Al}_{1-x}$ alloys.

3.5.2 Pair Energies and stability analysis

We have calculated the composition dependent pair energy functions using the TB-LMTO-ASR coupled with the orbital peeling technique and the result for the equi-atomic composition is shown in Fig.3.13. The nearest neighbor pair energy function shows the characteristic shape of a positive lobe, indicating ordering, near the position of half filling, flanked by negative lobes indicating segregation near empty and full filling fractions.

Again, if we compare our Fig. 3.13 with the Fig. 2 of Bose *et al.*, we note the satisfactory agreement between the two. The pair energy functions of Bose *et al.*, were obtained via a LIECHTENSTEIN *et al.* [Lie+87] type formula involving the scattering t -matrices of the CPA. The self-consistent estimates for the dominant nearest neighbour effective pair interaction by Long and Akai [LA07] were ~ 10 and 12 mRy respectively

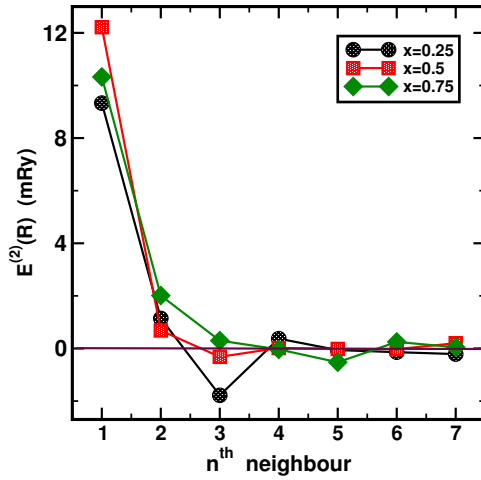


Figure 3.14: EPI calculated for $\text{Fe}_x\text{Al}_{1-x}$ as function of $|\vec{R}_n|$, for $x=0.25, 0.5$ and 0.75

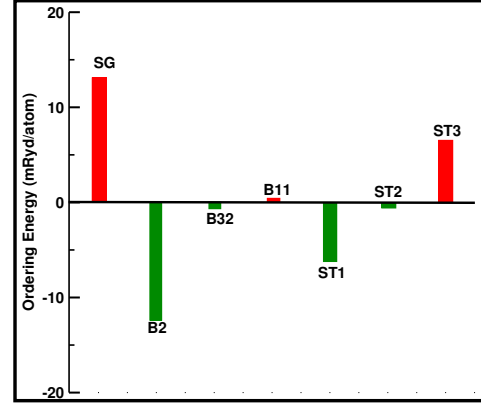


Figure 3.15: Ordering energies for seven different bcc based superstructures for FeAl (see Table 3.1).

for the 25-75 and 50-50 compositions. Bose *et al.*, [Bos+97] was ~ 18 mRy for the 50-50 compositions. Our estimates came out to be ~ 9.7 and 12.2 mRy respectively for the 35-75 and 50-50 compositions. Such a remarkable agreement convinces us of the accuracy of our orbital peeling technique, since the effective pair interactions are small energy differences which are very sensitive to the method of calculation and its approximations.

We should note here that both the pair energy function itself and the position of the Fermi energy depend upon the composition of the alloy. The position of the Fermi energy is also crucially related to band filling which is composition dependent. This is in contrast to some analyses (like the Connolly-Williams) which depend on similar, but composition independent, pair energy functions. The Fig.3.14 shows the pair energies $E^{(2)}(\vec{R}_n)$ as a function of n for three different compositions.

The behaviour of the pair energies change systematically as the concentration of Fe in the alloy increases. The sign of the dominant nearest neighbour pair energy does not change sign with Fe concentration, indicating ordering tendency throughout this composition range. The pair energies rapidly converge to zero with distance. In fact, although we have shown the pair energies up to the seventh nearest neighbour shells, their values beyond the fifth shell are smaller than the error bars of our calculational method and therefore these numbers are not really reliable. We also note that for the lower Fe concentrations the pair energies oscillate in sign with distance, leading to the

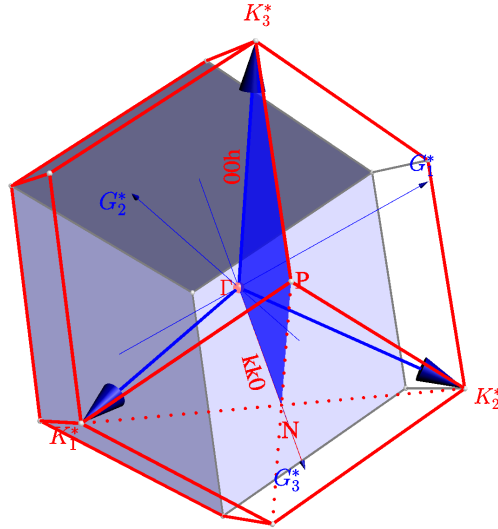


Figure 3.16: The plane bounded by the lines (00h) and (kk0) in reciprocal space within the bcc Brillouin zone

possibility of frustration.

Table 3.1: Weights for different neighbouring shells for seven different bcc based equi-atomic superstructures.

Structure	1	2	3	4	5
Segregated	1.00	0.75	1.50	3.00	1.00
B2	-1.00	0.75	1.50	-3.00	1.00
B32	0.00	-0.75	1.50	0.00	-1.00
B11	0.00	0.25	-0.50	0.00	-1.00
ST1	-0.50	0.25	0.00	0.50	0.00
ST2	0.000	-0.25	-0.50	0.00	1.00
ST3	0.50	0.25	-0.00	-0.50	0.00

The results of the ordering energies for seven different structures and super-structures based on the body-centered cubic lattice at 50-50 composition are shown in Fig. 3.15. We have calculated the ordering energies with contributions only up to the fifth neighboring shell. The Table 3.1 gives us the weights Q_n for the seven bcc based structures required to obtain the ordering energies in this alloy system. These superstructures are described in detail by Finel and Ducastelle [FD83]. We note that the segregated

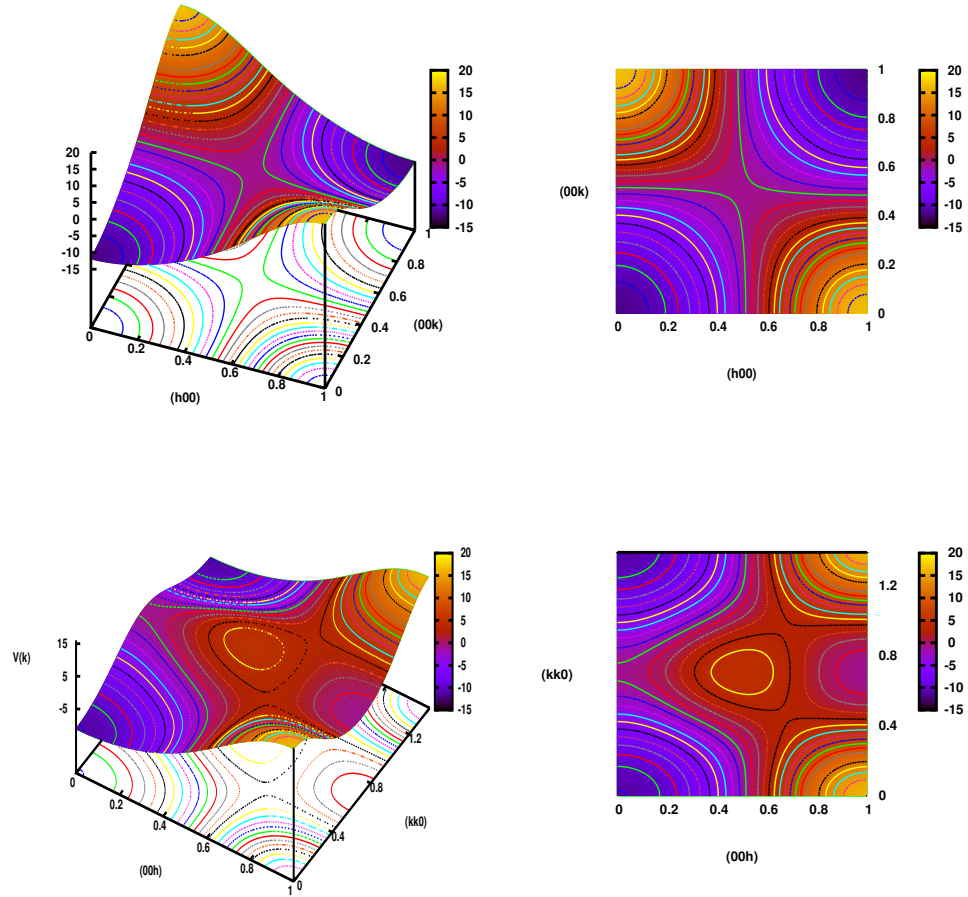


Figure 3.17: (left panels) $V(\vec{k})$ for $\text{Fe}_{25}\text{Al}_{75}$ shown as \vec{k} varies on the plane bounded by (top) (100) and (001) lines and (bottom) (001) and (110) lines (right panel) contour diagrams of the left panel projected onto the plane bounded by (top) (100) and (001) lines and (bottom) (001) and (110) lines.

phase and the two super-structures B11 and ST3 are unstable as low temperature phases. The B2 structure has the lowest ordering energy with a competition from the ST1 superstructure. This agrees with experimental observation of preferred transition from a disordered phase at high temperatures into an ordered B2 one on lowering the temperature.

Finally we shall examine the Fourier transform $V(\vec{k})$ of the pair energies and carry out a Clapp-Moss type of analysis. The behaviour of $V(\vec{k})$ for a 25-75 composition ($x = 0.25$) is shown in the left panels of Fig. 3.17 when \vec{k} sits on the plane in reciprocal space bounded by the lines (h00) and (00k) (shown on the top panel) and (00h) and (kk0) (shown on the bottom panel). The contours of $V(\vec{k})$ projected onto

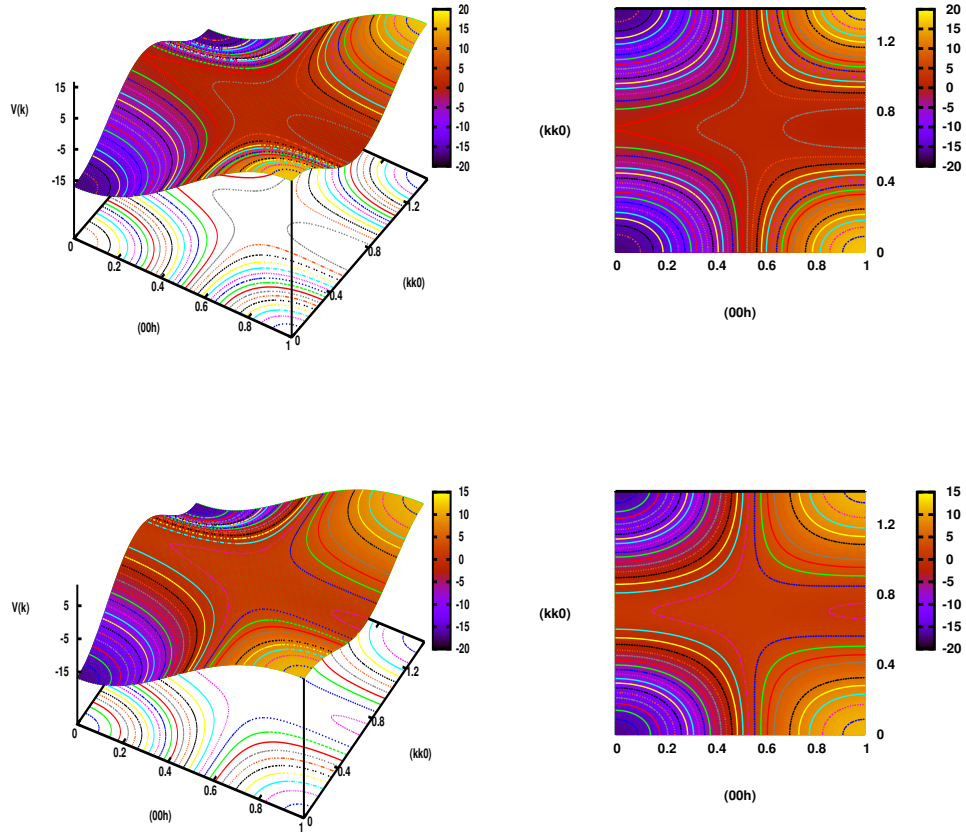


Figure 3.18: (left panels) $V(\vec{k})$ variation shown on the plane bounded by (001) and (110) in reciprocal space (top) 50-50 composition (bottom) 75-25 composition (right panels) projection of the left panel onto the plane bounded by (001) and (110) with contours.

these planes are shown in the right panels of Fig. 3.17. We note that in both the projections the maximum sits at the point (100) (and its symmetry equivalents) (in units of $2\pi/a$) which on a bcc lattice indicates B2 ordering. The projections in the bottom panels also show a minor peak at the point (0.5,0.5,0.5) which indicates an incipient short ranged ordering possibility. Projections of $V(\vec{k})$ on the plane bounded by (001) and (110) lines for two different compositions 50-50 and 75-25 are shown in the Fig.3.18. The dominant maximum at the point (001) persists throughout the composition range. However, the secondary maximum at (0.5,0.5,0.5) disappears and is replaced by a uniform ridge separating the two minima. The B2 structure is given to be the stable low temperature structure across the composition range and this agrees

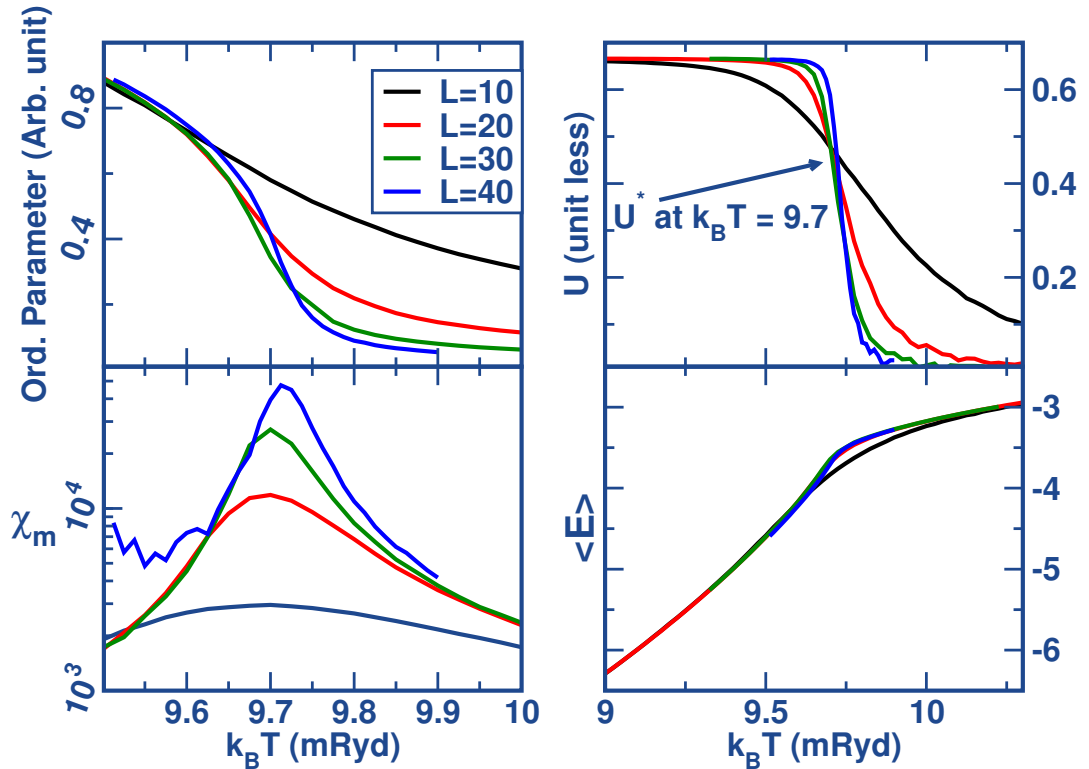


Figure 3.19: Monte Carlo results for $\text{Fe}_{50}\text{Al}_{50}$ showing transition around $T_C = 1250^\circ\text{C}$.

with experiment.

3.5.3 Monte Carlo simulation

For a phase-space integration of the fluctuating order parameters of the system of solids, Monte Carlo simulation is quite promising. In higher dimensionality it gives precise estimations. Random binary alloys magnetic spin and compositions are framed to a Ising like interacting Hamiltonian. Exchange Interaction between different types of atoms is averaged over the whole system as discussed earlier, and is obtained by the fitting of the alloy energy to a multi-site interaction expansion of the configuration. The magnetic exchange interactions can be direct or mediated through a non-magnetic species like here in the chosen case of FeAl alloys. With these interaction strengths the phase transition shown by Monte Carlo simulation is in well agreement with experimental data and more precise than the mean field estimations. In Fig.3.19, the variation of chemical order parameter in the transition region is shown for $\text{Fe}_{50}\text{Al}_{50}$ binary alloy. This MC simulation on the bcc lattice gives an anti-ferro type ordering at very high temperature which, necessarily, corresponds to a disordered A2 to or-

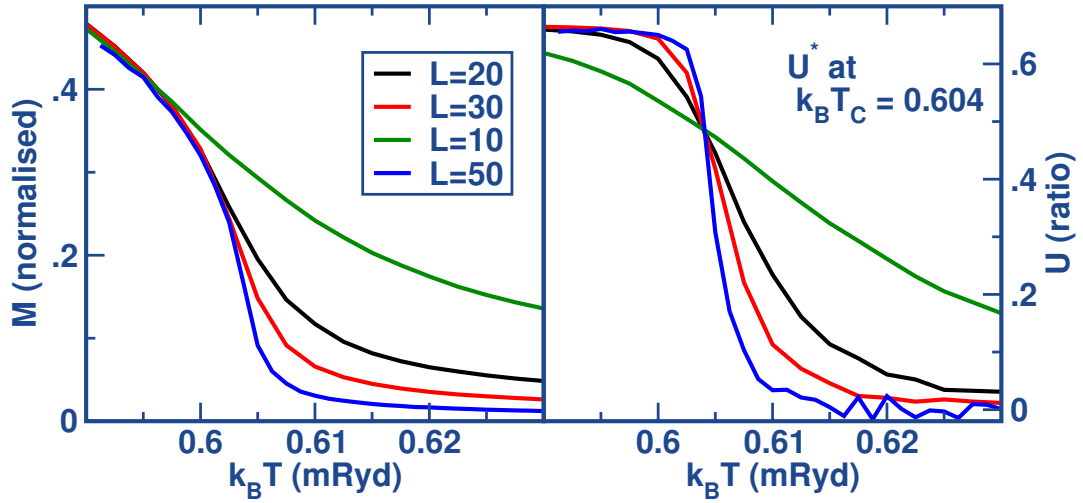


Figure 3.20: Monte Carlo simulation of magnetic interactions for $\text{Fe}_{50}\text{Al}_{50}$ showing a paramagnetic stability for temperature as low as $T_C = 95^\circ\text{K}$.

dered B2 chemical transition. In the different panels of the same figure is shown the temperature variations of fluctuations in the order parameter (equivalent to magnetic susceptibility), the equilibrium internal energy due to configurations, and the *Binder cumulant* with the expected nature for this class of transition. The MC simulation for magnetic interactions (Fig.3.20) of $\text{Fe}_{50}\text{Al}_{50}$ yields a very low temperature ($\sim 95^\circ\text{K}$) of transition to the ferromagnetic state. So the alloy in this atomic concentration region is a paramagnetic ordered solid solution in the room temperature as observed in the phase diagram (Fig. 3.1). Mechanical alloy formation of 1:1 stoichiometric $\text{Fe}_{50}\text{Al}_{50}$ ordered phase, due to high sensitive to environmental conditions, is prone to produce disordered solution in which the alloy shows ferro-magnetism coming out from the change in local coordination of Fe atoms [AG01; TJ58]. However in the model conditions of our calculations, the results show here yet another consistency. Explicit consideration of the interaction strengths, however, shows a Lattice-size independent behaviour due to the flattening of the transitions near critical region.

3.6 Conclusion & Future Plans

The suitability and accuracy of the Augmented Space Recursion (ASR) based Orbital Peeling (OP) method for the generation of pair energies is found to be prevalent. The phase stabilities of $\text{Fe}_x\text{Al}_{1-x}$ binary alloys based on these pair energies are in agreement with experimental evidence. The Monte Carlo code developed with all possi-

ble corrective measures is found to give plausible results in an optimized time scale and the whole computation process has become more robust and accessible. There are, however, several scopes to improve the efficiency of the code. The provision for more sampling the critical slowing down region, determination of the thermalisation requirement on the fly of simulation etc. are viable attractive improvements. Like the use of *variable step size* in particle transport MC, implementation of equivalent schemes to accelerate the simulation far from transition can also be useful. The recursion with ASR is now available with both relativistic corrections (including spin-orbit terms)[Hud+04] and non-collinear magnetism implementations [Gan+11]. Since earlier the ASR has been proposed as a analyticity preserving generalization of the single-site mean-field coherent potential approaches, this work provides an incentive to extend the use of the ASR to problems beyond the simple density of states calculations and in problems where relativistic corrections and non-collinear magnetism will play significant roles.

Short Range Ordering in FeCr Alloys

Introduction

Ferritic steels with BCC structure are most promising candidate structural materials for advanced fission and fusion reactors due to their low activation by irradiation. The properties to a first approximation are inherited mostly from the FeCr alloy, it being the parent alloy. In fact, the Cr concentration is responsible for the radiation tolerance of the system. The useful but unusual segregation of Cr at different locations and the complex behavior of magnetism in FeCr alloys has been attributed to its electronic structure. This has been studied in some detail [KDF06; OAW06]. These studies reveal that SRO plays an important role in this alloy system and changes from an ordering to a segregating behavior at a critical concentration of around 4-10 % of Cr [Hen83; MYM04]. This profoundly affects the thermodynamic behavior of this alloy [Ols+05]-[Bon+09]. Atomic SRO can have predominant effects on the magnetic properties of FeCr. Contributions of SRO to the chemical properties like free energy and enthalpy of mixing have been studied in detail by Lavrentiev et al. [Lav+07]. The structural phases of FeCr in the low Cr region has been found to have strong dependence on Cr clusters. The SRO effects substantially diminish for alloys with Cr concentration above 20%.

In a recent study, Lavrentiev *et al.*, [LDNM09] have employed cluster expansion to the magnetic moment and observed the effect of Cr concentration by fitting the cluster energy to that obtained by [ab-initio] calculations using DFT. Magnetic ordering showed inflation in the high Cr-concentration region subverted by the configurational disorder. There is a clear indication of direct relation between Cr-segregation and the magnetic transition. We will try to have some numerical quantification of the dependence. The electronic structure contribution of atomic short-range ordering in a disordered alloys has been extensively studied within the Augmented Space Formalism (ASF) [MP93] in the framework of TB-LMTO-Recursion and within a Non-Local

CPA based on KKR(KKR-NLCPA)[Row+05]. These ground state calculations capture the environment of alloy systems effect at 0 °K. But the correlation effects, as has been found experimentally, may extend to sufficiently high temperature ranges, depending on the atomic characteristics and the concentration. Though solving excited state quantum mechanical equations not possible, the statistical methods can be amalgamated with the ground state ab-initio calculations to proliferate the understanding.

4.1 Treatment of Short-range Ordering

Long range ordering(LRO) in alloy exists over a wider temperature range; And is much more palpable compared to the Short ranged ordering. In the case of existence of a perfect short range ordering(SRO), for example, in a binary alloy A_xB_{1-x} with simple cubic lattice and $x = 0.5$, every A -type atom has around it a B -type atom and *vice versa.*, long range order exists. But the LRO, responsible for the average properties of the alloy may not always conceal the occupational preference of individual atoms. Local ordering in these cases become crucial when the LRO vanishes above the critical temperature. SRO is the shortest length scale usually used to describe the structure of a material consists of an atom and its nearest neighbours, out to perhaps two or three atoms distant. Though, in principle, it can contain any of all possible correlations between the alloying atoms, a usual quantitative measure of SRO is the Warren-Cowley (WC) SRO parameter [Cow50a; SM98] restricted to pair-correlations only :

$$\alpha(x) = 1 - \frac{\text{Pr}(AB)}{1-x} = 1 - \frac{\text{Pr}(BA)}{x}$$

$\text{Pr}(AB)$ is the conditional probability of a site being occupied by B , given that its nearest neighbour is occupied by A . Here we have considered only the nearest neighbour sro, but it's easily generalized for higher shells (Being local ordering, it should not be more than 2-3 near neighbours) and specified directionality $\langle lmn \rangle$. SRO parameter is symmetric wrt exchange of A and B . For the binary alloy, then, all the probabilities are defined as:

$$\begin{aligned} \text{Pr}(AB) &= (1-\alpha)(1-x), & \text{Pr}(BA) &= (1-\alpha)x, \\ \text{Pr}(AA) &= 1-(1-\alpha)(1-x), & \text{Pr}(BB) &= 1-(1-\alpha)x. \end{aligned}$$

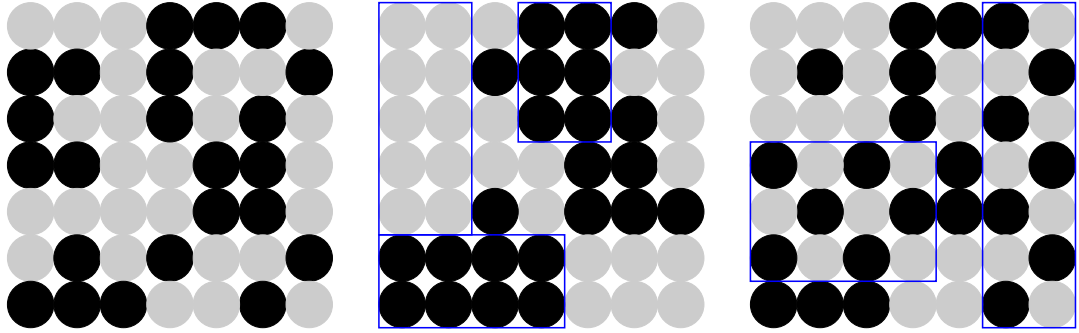


Figure 4.1: Schematic representation of short range ordering (left) Random binary alloy (middle) Positive correlation (right) Negative correlation

The value of SRO parameter α in real space gives the idea of local decomposition and ordering. In the absence of lro, very few sro parameters are non-zero. As shown schematically in Fig.4.1 negative *nearest neighbour* WC parameter indicates tendency to order, while its positive value leads to clustering or phase segregation. In the perfectly random disorder, SRO parameter is zero. Physically the occupation of i^{th} site by B -type atom is independent of whatever occupies its neighbour. And, thus, $\Pr(AB) = \Pr(B) = 1 - x$ irrespective of the local neighbouring.

SRO is directly obtainable from diffuse scattering intensities through mean-field approximations or Inverse Monte Carlo numerical simulations. It is possible because of understanding of the sro in terms of occupation variable n , in which the SRO parameter for p -th shell is

$$\alpha_p = \frac{\langle n_0 n_p \rangle - \langle n_0 \rangle^2}{1 - \langle n_0 \rangle^2},$$

where n_i is the occupation of i^{th} site, thence n_0 is the occupation of the origin and $\langle \dots \rangle$ represents the configuration averages. We note that these probabilities for BB , AA and AB pairs are $x^2 + x(1-x)\alpha_p$, $(1-x)^2 + x(1-x)\alpha_p$ and $x(1-x) - x(1-x)\alpha_p$, respectively.

The Warren-Cowley short range order parameter is explicitly related to the correlation functions of the cluster expansion[Mul03].

So far the effect of SRO on magnetic phase transitions had no precise method of study except through mean field approaches. We devise a technique which combines the Special Quasi-random structures proposed by Zunger *et al.*, [Wei+90; Zun+90] and Monte Carlo (MC) simulations to quantitatively study the effect of SRO on the magnetic phase transitions in FeCr. Zunger *et al.*, proposed a novel method of treating configuration averaging in a disorderd alloy. Structural models needed in calculations

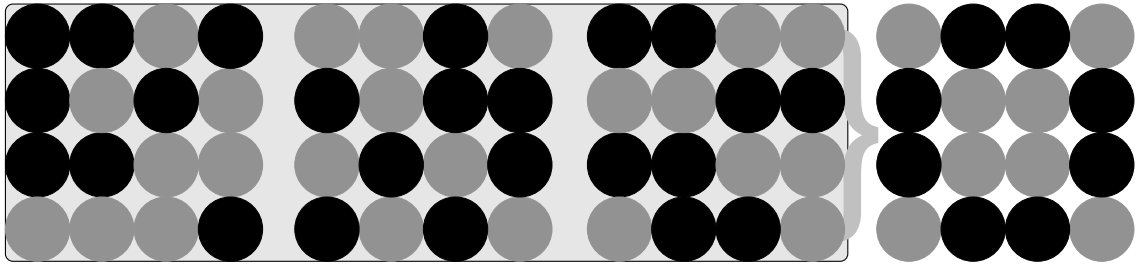


Figure 4.2: Schematic presentation of randomness of a small sqs cell (non-shaded) embodying average correlations of several apparently non-random configurations (shaded cells)

of properties of substitutionally random binary alloys A_xB_{1-x} are usually constructed by randomly occupying each of the N sites of a periodic super-cell by A or B atoms.

Zunger *et al.*, showed that it is possible to design “special quasirandom structures” (SQS’s) that mimic, even for small sizes ($N=8$), the first few, physically most relevant radial correlation functions of an infinite, random structure far better than the standard technique using random number generators do. These SQS’s are shown to be short-period super-lattices of 4 - 16 atoms/cell whose layers are stacked in rather nonstandard orientations. Since these SQS’s mimic the local atomic structure of the random alloy quite accurately, their electronic properties, calculated through first-principles techniques, provide a representation of the electronic structure of the alloy. The close agreement between the density of states calculated on a small SQS of size 16 and the much more elaborate calculation through Augmented Space Recursion method is already established in the Fig.3.12.

4.2 Cluster Expansion

The cluster expansion method (CE) is an effective statistical tool for the search of the thermodynamic ground state of a solid system. The concept is based on an Ising Hamiltonian for the lattice occupation. To model the alloy for study, for each lattice site i a fictitious spin variable S_i is assigned. In the context of random binary alloy $A_xB_{(1-x)}$, S_i takes value say -1 for i^{th} site occupied by A-type atom and $+1$ otherwise. The randomness in the alloy spans a configuration space, labelled by σ , containing 2^N possible elements where N is the number of lattice sites. [Wei+90] Any property, like the total energy ($E(\sigma)$) of the alloy, which depends on the topologically ordered configuration σ of lattice can be parametrized in terms of these discrete variables

as[SDG84]:

$$E_{CE}(\sigma) = J_0 + \sum_i J_i S_i(\sigma) + \sum_i \sum_{j < i} J_{ij} S_i(\sigma) S_j(\sigma) + \dots \quad (4.1)$$

Here J_i are configuration independent interaction energies. This equation can make use of the underlying lattice symmetry. For that one needs to rearrange the equation and introduce some terminologies. A particular spatial arrangement of number k of atoms(vertices) is called a 'geometrical-figure' f which is also characterized by the order m of neighbouring distance of separation and by the position l of the figure in the lattice. Many of such geometric-figures are related to each other by symmetry operation of the lattice and the group of all of them is identified as a figure F . The Correlation function is defined as the average of the spin products of all the symmetry equivalent figures.

$$\bar{\Pi}_F(\sigma) = \frac{1}{ND_F} \sum_{f \in F} (S_{f1}(\sigma) \cdots S_{fk}(\sigma)) \quad (4.2)$$

where $N \cdot D_F$ is the total number of symmetry related figures and the product of spin is taken over number of distinct k -sites ($f1, f2, \dots, fk$) in the cluster of the class F . Then Eq. 4.1 is written in terms of correlation functions as

$$E_{CE}(\sigma) = N \sum_F D_F V_F \bar{\Pi}_F(\sigma). \quad (4.3)$$

Then, the configuration averaged energy is

$$\langle E_{CE} \rangle = N \sum_F D_F V_F \langle \bar{\Pi}_F \rangle. \quad (4.4)$$

V_F , the configuration independent coefficients to represent the contribution of F to E , are known as the effective cluster interactions and are needed to be calculated by fitting with experimental or *ab initio* calculations. Correlation functions are invariant under permutation of site indices and under translation by a lattice vector. When the occupation is reversed, $A \leftrightarrow B$, the correlations among an even number of sites are invariant, and correlations among an odd number of sites have the same magnitude but the sign gets changed and to preserve the physical property of the alloy all odd coefficients are needed to be sign reversed. And also in the special case of 50 – 50 alloy, all odd-order coefficients vanish. $\{\bar{\Pi}_F\}$ forms a mathematically complete basis set. Hence theoretically the above equation in its full expansion (2^N -terms) gives the exact rep-

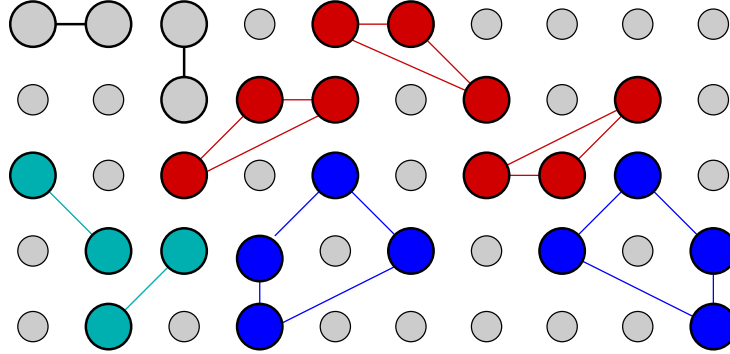


Figure 4.3: Illustration of ‘figures’ in a 2D lattice showing some pairs, triplets, and quadruplets with symmetric similitude in same colour

resentation of the physical property E for alloys, but practically one needs to consider only few preselected figures and chops off higher order ones to some approximations.

The cluster expansion is very useful in studying configuration dependent physical properties of alloys like structural order disorder transitions, exhaustive ground state searching, kinetics of defects and various surface and interface phenomena. In stead of the meticulous DFT calculations one quickly solves a coarse-grained but faster Hamiltonian to model macroscopic properties those have their origin in the atomic interactions. There exists extensive developments[Ler+09; WC02] in these regards, however, our approach here is radically different in the sense that we find the exchanges from *ab initio* calculations *apriori* and use the cluster expansion based special shells, as our proposal, to accelerate the time consuming Monte Carlo simulations. The SQS method proposed by Zunger *et al.*, lowers the computation burden of the existing direct configuration averaging techniques. In this method one constructs supercell to mimic the statistical characteristics of random alloys to a controllable accuracy. In other words, the correlation functions of the constructed SQS supercells can match the correlation functions of a random alloy with a selected error control.

The completeness of the orthonormal correlation function basis can be expressed in a generalised form as

$$\sum_{\sigma} \Pi_{k,m}(l, \sigma) \Pi_{k',m'}(l', \sigma) = 2^N \delta_{kk'} \delta_{mm'} \delta_{ll'}$$

where $\{k, m\} \equiv F$. The site averaged correlation function as discussed earlier is

$$\bar{\Pi}_F(\sigma) = \frac{1}{ND_F} \sum_l \Pi_F(l, \sigma) \quad (4.5)$$

For a random infinite alloy R , for any figure f ,

$$\langle S_{f_1} \cdot S_{f_2} \cdots S_{f_k} \rangle = \langle S \rangle^k$$

And thus the correlation functions can be expressed as follows [Wei+90]:

$$\bar{\Pi}_F(R) = \bar{\Pi}_{k,m}(R) = \langle \bar{\Pi}_{k,m} \rangle_R = (2x - 1)^k \quad (4.6)$$

The central idea of SQS approximation is to find or design a single N -atom periodic structure — ‘ S ’, whose distinct correlation functions $\bar{\Pi}_{k,m}(S)$ best matches the average of the random alloy. If $\langle E \rangle$ is the ensemble average of the *random alloy*, then the errors introduced by the use of the SQS can be represented by

$$\langle E \rangle - E(S) = \sum_{k,m} D_{k,m} [(2x - 1)^k - \bar{\Pi}_{k,m}(S)] V_{k,m}$$

The objective is to find S that minimizes the error.

4.2.1 Notes on Generation of SQS

The elegance of SQS as models for disordered medium is mathematically methodical elegant but the procedure to find such SQS is not prescribed, so not unique. One of the popularly used way is *based* on the idea of Reverse Monte Carlo(RMC), which have been used in this work. The difference of correlation functions $[(2x - 1)^k - \bar{\Pi}_{k,m}(S)]$ is the cost function in the SQS generation. RMC is general method of structural modelling based on experimental data. It is a variaation of standard Metropolis Monte Carlo method, originally developed to model structures of liquids and glasses, in consistence with available experimental constraints [MH92]. In RMC the mean square distance of the distribution *structure factors* plays the role of the *energy* of standard MC, where, the fluctuating field temperature equivalent is the *experimental error*. The generation of SQS, more or less, follows the same principle of modelling of distribution of atoms, though, on a perfectly crystalline lattice. Minimisation of the sro gap between the requisite and model structure, or an improved parameter such as the *cross-validation* score, here, characterises the equilibrium. However, the search is not Markovian and the convergence is thus slower or even not guaranteed at all. The obtained *structure* may not be *unique* but to the applicability of this modelling, all the arguments made for that of RMC by MCGREEVY [McG01] applies here so that once

a suitable SQS with desired correlations found, Zunger's methodology, as has been discussed earlier, preserves all their statistics non-typical to how we obtained them.

4.3 Computation of Magnetic Exchange Interactions

According to the *force theorem*[ARM80; WWD85], small changes in ground state total energy is reflected by the corresponding changes in the Kohn-Sham equations. For example, we could investigate small changes in volume to find the pressure. The force theorem is expressed by

$$\frac{dE}{dp} = \sum_{c,occ} \frac{\partial E_n}{\partial p}$$

and states that we only need to calculate the change in energy eigenvalues to obtain the lowest order change in energy. This holds only up to the linear changes in charge and the partial derivatives are *explicit* of capturing the change in energy eigenvalues as direct consequence of the change in external potential and ignore the change in energy eigenvalues due to the change in density.

In lower order change in magnetization densities due to small rotations of magnetic moments, the *force theorem* can be extended[Lie+87; LK84] to calculate the magnetic exchange interactions of collinear systems from the single particle band energies by *rigid spin approximation* which assumes the dependence of exchange correlation field on the magnetic orientation to be trivial. The *magnetic force theorem* (MFT)[Heine,SSP 35, 1, 1980][Osw+85] allows the evaluation of the Magnetic exchange interactions (MEI) from one collinear configuration which is usually ferromagnetic. So one doesn't need to calculate several magnetic configurations by hand and then fit the energy as is discussed earlier. Computationally, this method is thus very efficient. Assuming infinitesimal rotation angles of the magnetic moments, however, is necessary in this approach.

The total energy of the magnetic configuration of an alloy can be expanded as

$$E(\{\hat{\mu}\}) = E_0 + \sum_i E_i^{(1)}(\hat{\mu}_i) + \sum_{ij} (\hat{\mu}_i, \hat{\mu}_j) + \dots ,$$

where $\hat{\mu}_i$ is the unit magnetic moment vector at i^{th} site.

By the application of the magnetic force theorem, a small directional perturbation

to the moment is approximated as

$$E(\{\hat{\mu} + \delta\hat{\mu}\}) - E(\{\hat{\mu}\}) \sim E_{band}(\{\hat{\mu} + \delta\hat{\mu}\}) - E_{band}(\{\hat{\mu}\}) = \delta E_{band}(\delta\mu)$$

In KKR formalism, the formulation of Liechtenstein *et al.*, directly follows from Lloyd's formula. The change in energy accompanied to the interactions of two μ s at sites i and j is, hence, obtainable by

$$\delta E_{band}(\delta\hat{\mu}_i, \delta\hat{\mu}_j) \sim \frac{1}{\pi} \Im \text{Tr} \int^{\epsilon_F} d\epsilon \delta t_i^{-1}(\epsilon) \mathcal{T}_{ij}(\epsilon) \delta t_j^{-1}(\epsilon) \mathcal{T}_{ji}(\epsilon)$$

This energy can be mapped to an effective Heisenberg model

$$E(\{\delta\hat{\mu}\}) = \frac{1}{2} \sum_{ij} J_{ij} \delta\hat{\mu}_i \cdot \delta\hat{\mu}_j$$

and the exchanges can be extracted.

In the Green function method using the Tight-binding linear muffin-tin orbital basis with the effective medium of Coherent Potential Approximation, the exchanges are

$$J^{QQ'}(\vec{R}_i - \vec{R}_j) = \frac{1}{4\pi} \int_{-\infty}^{E_F} dE \Im m \text{Tr} \left\{ \Delta_{\vec{R}_i}^Q T^{\uparrow\uparrow}(\vec{R}_i - \vec{R}_j) \Delta_{\vec{R}_j}^{Q'} T^{\downarrow\downarrow}(\vec{R}_j - \vec{R}_i) \right\} \quad (4.7)$$

Here Q, Q' refer to the constituents Fe or Cr. $\Delta_{\vec{R}} = t_{\vec{R},Q}^{-1} - t_{\vec{R},Q'}^{-1}$, t is the scattering t -matrix and $T^{\sigma\sigma'}(\vec{R}_i - \vec{R}_j)$ is the path operator related to the off-diagonal element of the Green's function.

The left panel of Fig.4.4 shows the nearest neighbor exchange energies for the different constituents. We note that the exchange energies are composition dependent and the Fe-Fe exchange dominates over the other two. The right panel shows that the exchange energies are damped oscillatory typical of disordered itinerant systems.

4.4 Results and Discussion

We generated the SQS structures and performed MC simulation on the magnetic distributions, initially distributed on the SQS. The standard Metropolis single flip dynamics was used on the derived Hamiltonian. For random initialization, it is usual to take statistics of thermodynamic properties from multiple initialized configurations to

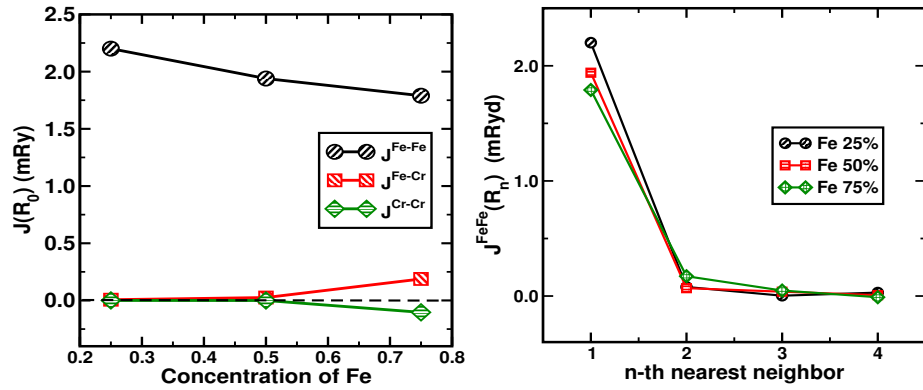


Figure 4.4: (left panel) Nearest neighbor exchange energies. Fe-Fe exchanges are much stronger compared to Fe-Cr and Cr-Cr exchanges over the entire concentration range. (right panel) Fe-Fe exchange as a function of distance.

avoid trapping in local minima. This marriage between the SQS and MC saves us an order of magnitude in computation time. Also it is enough to consider only one SQS structure, because it intrinsically ensures the correct energy path of the simulation. Another great advantage is that any degree of SRO, measured by the Warren-Cowley parameter α can be built into the SQS. In this way perfectly random alloys as well as alloys with requisite definite SRO can be mimicked by small super-cell structures and we may couple this with a MC analysis and the computation can be done over a rather short time scale. A maximum of 65536 Monte Carlo steps were considered for each case from which 32768 steps were discarded for achieving thermalisation.

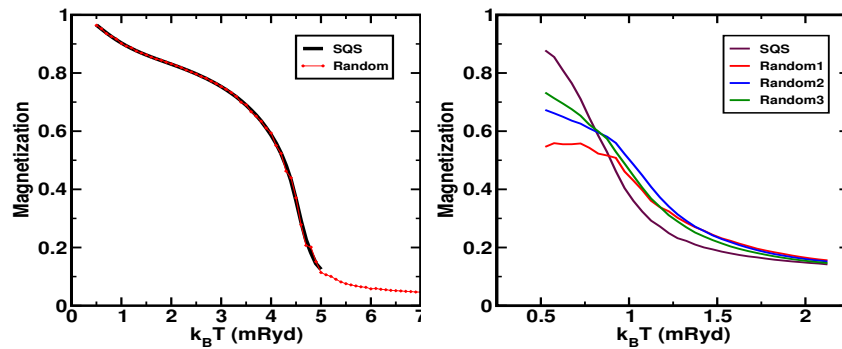


Figure 4.5: Temperature variation of the Order parameter (left) for strongly ferromagnetic $\text{Fe}_{75}\text{Cr}_{25}$ shows equivalent natures for Monte Carlo runs from generated random structures and the adapted method of Monte Carlo simulation on SQS structures. For both structures super-cells of 1024 sites were considered. (right) For $\text{Fe}_{25}\text{Cr}_{75}$ the agreement is less than the previous case.

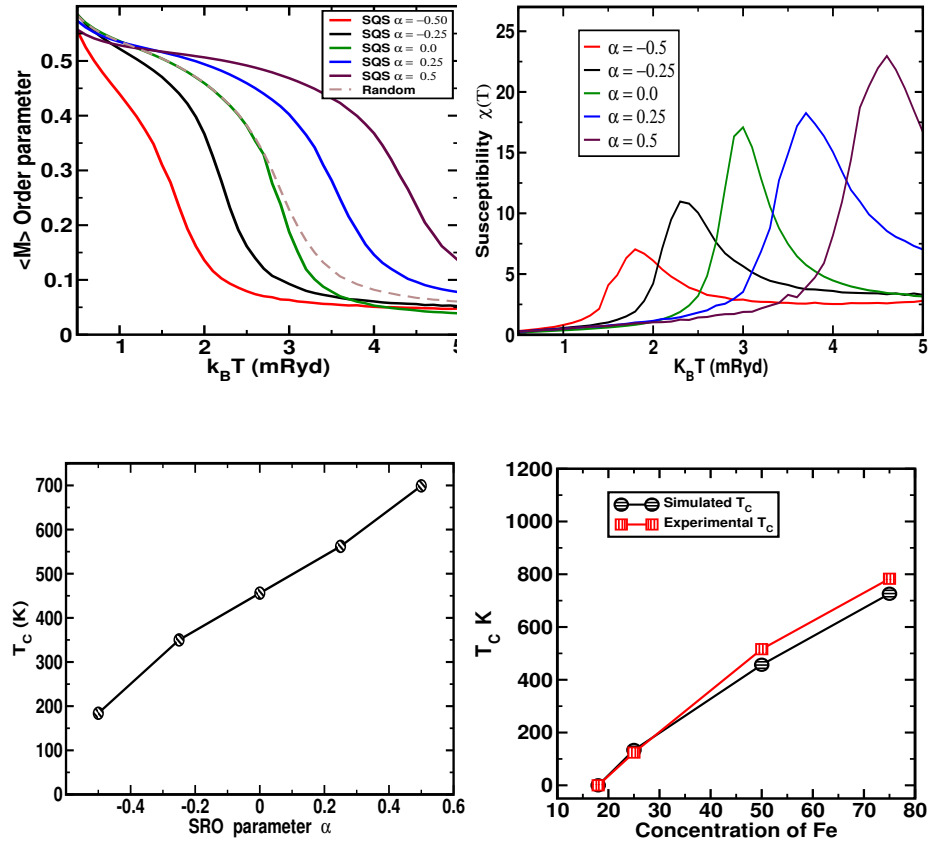


Figure 4.6: (Top left panel) Effect of SRO on the temperature variation of magnetization for the alloy $Fe_{50}Cr_{50}$. (Top right panel) Effect of SRO on the temperature variation of susceptibility. (Bottom left panel) Variation of T_C with SRO for the 50-50 alloy. (Bottom right panel) The variation of T_C with composition, and comparison with experimental data [Bur+83].

In the region of strong magnetic exchanges and weak chemical SRO, the dynamics of the simulations of systems initialized by random structures and the SQS cell with $\alpha = 0$ almost fall on top of each other as in the left panel of Fig. 4.5. However, when the Fe concentration is as low as 25%, in spite of having almost equal strength of $Fe - Fe$ exchanges, the numbers of such $Fe - Fe$ pairs is rather low and the SRO-effect dominates. We observe such effects in $Fe_{25}Cr_{75}$ shown in the right panel of Fig. 4.5 where for equal number of Monte Carlo sampling for every structure, SQS initialization becomes more efficient.

As we already have pointed out that in this way we can simulate magnetic properties of alloys having definite chemical SRO embedded in it. In Fig. 4.6 the results of the simulations for observing the variation of magnetic transitions due to the chemical orderings quantified by the SRO are shown.

Fig.4.6 shows clearly the dependence of T_c on SRO. Box size of simulation was 432 atoms. Finally we compared the transition temperatures for the disordered FeCr. We have chosen the SRO parameter to be the oft-quoted 0.2 around 50-50 composition. The values of transition temperature are comparable to the earlier experimentally reported values [Bur+83].

4.5 Conclusions & Future Plan

The effect of atomic sro is substantially influential on the magnetic properties of the alloy. The novel concoction of MC and SRO suggested in this chapter has been successful in capturing this effect. In addition it is advantageous in terms of simulation experiments that incorporation of SRO in a SQS can be carried out in a controlled manner. In MC simulation, random initialization of the atoms is often necessary for statistical correctness. In that respect the combination of Monte-Carlo and SQS comes out even more powerful in saving computation time without the loss of any exactitude. Rather than carrying out multiple simulations over many randomly generated configurations, we needed to perform Monte-Carlo on single reasonably small SQS with equal accuracy. However, the generation of sqs with requisite sro is not very easy, but this difficulty is easily circumvented by the fact that the sqs are inherently reusable and once a database is created one doesn't need to spend time on this part.

Inter-biasing of Multiple Ordering in Alloys

Introduction.

In the last chapter, we looked at an alloy system where the chemical SRO substantially affected the magnetic ordering. Both the chemical and the magnetic ordering are prominent properties of any alloy system and impart usefulness to it. Many of the earlier theories of phase transitions focused on either magnetic or chemical ordering and assumed that they were independent of each other [BL67; BV71; Kik+80; KS74; The74; TK72; VB73]. However, the two fields existing in the same alloy leads to the possibility of profound influence of one on the other [BVC78; HS75; TkK77]. There has been several experimental observations [Han65; Hou63; MF74; OC77] regarding this. Morán-López and co-workers [MH+85; MLF80; MLUML81] argued that for many alloys both of whose components were magnetic, ignoring this inter-dependence can lead to results at variance with experiment. SCHMID [Sch92] using the interaction parameters from scattering experiments have studied Fe-rich narrow region of $\text{Fe}_x\text{Al}_{1-x}$ phase diagram in which better agreement is found by taking the chemical interactions renormalized by the magnetic interactions. The chemical order-disorder transitions at a critical temperature T_0 go side by side with magnetic transitions at the Curie or Néel temperatures T_c if one or more of alloy constituents are magnetic. This motivates for searching a method that characterizes one transition by the other.

FeCo is an alloy system having all these typical peculiarities in its phase diagram we have discussed. The magnetic Curie temperature of the bcc phase of FeCo increases from 770 °C for pure iron to about 930 °C at 14.5 at%Co, beyond which the magnetic transition temperatures coincide with the *bcc* – *fcc* structural transition. In the bcc region, chemical ordered super-lattice of the CsCl type exists which has a peak transition temperature of about 730 °C around the equi-atomic composition. The order-disorder

and the magnetic transitions show the same pattern wrt the composition. So, we consider Fe_xCo_y alloy as the suitable candidate of our study.

In this chapter we shall first discuss a mean-field approach where both transitions are addressed in the same footing. Several earlier workers have studied this alloy both from mean-field [MH+85] and renormalization group [RC80] approaches. In all these works the Hamiltonian parameters were taken as parameters fitted to experiment. In our approach we shall derive these parameters from the first-principles density functional based approach we have already discussed. Unlike the empirical parameters we shall find that the chemical pair-energies and the magnetic exchange energies will be both long ranged and composition dependent. The starting point is a suitable Hamiltonian as suggested by Tahir [TkK77]. A mean-field numerical analysis rapidly becomes insufficient for real materials. However, the trend is predicted quite well. We shall follow this up by treating the Hamiltonian with coupled order parameters with a Monte Carlo (MC) study. The combined MC has to be of a mixed type : the chemical transition with conserved order parameters has to be studied with Kawasaki dynamics while the magnetic transition has to be addressed with the Metropolis algorithm.

5.1 Mean-field Analysis

In order to study the phenomenon, we choose a Hamiltonian similar to that proposed by Tahir-Kheli [TK72] :

$$H = H_{\text{mag}} + H_{\text{ord-dis}} \quad (5.1)$$

The Ising-like Hamiltonian is divided basically into two parts H_{mag}^0 and $H_{\text{ord-dis}}^0$. The coupling is actually included in the magnetic component of the Hamiltonian which is of the form

$$H_{\text{mag}} = - \sum_{\vec{R}_i \vec{R}_j} \sum_{QQ'} J^{QQ'}(\vec{R}_i - \vec{R}_j) S^Q(\vec{R}_i) S^{Q'}(\vec{R}_j) n^Q(\vec{R}_i) n^{Q'}(\vec{R}_j) \quad (5.2)$$

where $n^Q(\vec{R}_i)$ are local variables which describe the occupation of the site labelled \vec{R}_i by the species $Q = A$ or B .

$$n^Q(\vec{R}_i) = \begin{cases} 1 & \text{if species } Q \text{ occupies site labelled } \vec{R}_i \\ 0 & \text{if not} \end{cases} \quad (5.3)$$

The chemical part of the Hamiltonian contains only the occupation variables

$$H_{(\text{ord-dis})} = -\frac{1}{2} \sum_{\vec{R}_i, \vec{R}_j} \sum_{QQ'} V^{QQ'}(\vec{R}_i - \vec{R}_j) n^Q(\vec{R}_i) n^{Q'}(\vec{R}_j) \quad (5.4)$$

In the first step we transform the occupation variables to pseudo-spins $C(\vec{R})$:

$$n^A(\vec{R}) = \frac{1}{2} + C(\vec{R}) \quad n^B(\vec{R}) = \frac{1}{2} - C(\vec{R})$$

In the next step, since we wish to describe chemical ordering, we separate the system into two inter-penetrating lattices. Let the positions on the sublattices be labelled by α and β . Since we are considering in the purview of studying a binary alloy in mean-field approach, it is reasonable to expect that the coupled interactions giving rise to ordering will have major contributions from the lower order inter-sublattice interactions.

$$\begin{aligned} H = & \sum_{\vec{R} \in \alpha, \vec{R}' \in \beta} \left[V^{(1)}(\vec{R} - \vec{R}') C(\vec{R}) C(\vec{R}') - V^{(2)}(\vec{R} - \vec{R}') \left\{ C(\vec{R}) + C(\vec{R}') \right\} \right. \\ & - \frac{1}{2} \sum_{QQ'} J^{QQ'}(\vec{R} - \vec{R}') \eta_{QQ'} S^Q(\vec{R}) S^{Q'}(\vec{R}') \left(\eta_{QQ'} + 4C(\vec{R}) C(\vec{R}') \right) \\ & + \left\{ J^{BB}(\vec{R} - \vec{R}') S^B(\vec{R}) S^B(\vec{R}') - J^{AA}(\vec{R} - \vec{R}') S^A(\vec{R}) S^A(\vec{R}') \right\} \left\{ C(\vec{R}) + C(\vec{R}') \right\} \\ & \left. + J^{AB}(\vec{R} - \vec{R}') \left\{ S^A(\vec{R}') S^B(\vec{R}) - S^A(\vec{R}) S^B(\vec{R}') \right\} \left\{ C(\vec{R}) - C(\vec{R}') \right\} \right] \quad (5.5) \end{aligned}$$

where $V^{(1)}(\vec{R} - \vec{R}') = V^{AA}(\vec{R} - \vec{R}') + V^{BB}(\vec{R} - \vec{R}') - 2V^{AB}(\vec{R} - \vec{R}')$ is the chemical effective-pair interaction, $V^{(2)}(\vec{R} - \vec{R}') = -\frac{1}{2} \left(V^{AA}(\vec{R} - \vec{R}') - V^{BB}(\vec{R} - \vec{R}') \right)$ is the chemical potential strength of A -type over B -type of species and $\eta_{QQ'} = 2\delta_{QQ'} - 1$.

In the Hamiltonian 5.5, for the choices $Q \in \{A, B\}$ and sublattices $\in \{\alpha, \beta\}$, we have six degrees of freedom. The order parameters emerging from the thermally equilibrated spin variables are the sublattice magnetizations :

$$\langle S_\xi^Q \rangle = M_\xi^Q = \{M_\alpha^A, M_\alpha^B, M_\beta^A, M_\beta^B\}.$$

The two pseudo-spin variables C_α and C_β are not independent of each other as the chemical composition of the alloy is fixed. The thermal averages $\rho_\alpha = \langle C_\alpha \rangle$ and $\rho_\beta = \langle C_\beta \rangle$ are the sublattice concentrations, and analogous to a solid-liquid phase, the

order parameter, here, is defined as the difference in these concentrations.

$$L = \langle C_\alpha \rangle - \langle C_\beta \rangle = \rho_\alpha - \rho_\beta \quad (5.6)$$

L is not local, rather a long range order parameter. In terms of the site occupation variable n , the linearly dependent chemical order parameters are defined as $p_\xi^Q \equiv \langle n_\xi^Q \rangle$, and p_ξ^Q is the concentration of Q -type of atom in ξ sublattice. In more explicit form all the p 's are related as :

$$\begin{aligned} p^A + p^B &= 1, \\ p_\alpha^A + p_\alpha^B &= 1, \quad p_\alpha^A + p_\beta^A = 2p^A, \\ p_\beta^A + p_\beta^B &= 1, \quad p_\alpha^B + p_\beta^B = 2p^B, \end{aligned}$$

where p^A and p^B are the atomic concentrations of the two constituents in the alloy. Given these constraints, the long-ranged chemical ordering parameter L in a physically more relevant form is :

$$L = \frac{1}{2} \{ (p_\alpha^A - p_\beta^A) - (p_\alpha^B - p_\beta^B) \} .$$

As for any mean-field theory, the spatial correlations between the spins on lattices leading to magnetizations are ignored so that $\langle S_\alpha^Q S_\beta^{Q'} \rangle = M_\alpha^Q M_\beta^{Q'}$. The pseudo spin of chemical interactions are decoupled as:

$$C(\vec{R})C(\vec{R}') = C(\vec{R})\langle C(\vec{R}') \rangle + \langle C(\vec{R}) \rangle C(\vec{R}') - \langle C(\vec{R}) \rangle \langle C(\vec{R}') \rangle .$$

With the omission of the irrelevant constant energy shifts in the Hamiltonian and assumption that the nearest neighbour exchange predominantly contributes to the energetics, the mean-field Hamiltonian is obtained in the form:

$$H_{MF} = - \sum_\alpha \sum_\beta \left[E_\alpha C_\alpha + E_\beta C_\beta + \frac{1}{2} E_{\alpha\beta} \right]$$

where

$$\begin{aligned}
E_\alpha &= -V^{(2)} \rho_\beta + (2\rho_\beta + 1)(J_{\alpha\beta}^{AA} M_\alpha^A M_\beta^A - J_{\alpha\beta}^{AB} M_\alpha^B M_\beta^A) \\
&\quad + (2\rho_\beta - 1)(J_{\alpha\beta}^{BB} M_\alpha^B M_\beta^B - J_{\alpha\beta}^{AB} M_\alpha^A M_\beta^B) \\
E_\beta &= -V^{(2)} \rho_\alpha + (2\rho_\alpha + 1)(J_{\alpha\beta}^{AA} M_\alpha^A M_\beta^A - J_{\alpha\beta}^{AB} M_\alpha^A M_\beta^B) \\
&\quad + (2\rho_\alpha - 1)(J_{\alpha\beta}^{BB} M_\alpha^B M_\beta^B - J_{\alpha\beta}^{AB} M_\alpha^B M_\beta^A) \\
E_{\alpha\beta} &= \rho_\alpha \rho_\beta [V^{(2)} + 2J_{\alpha\beta}^{AB} (M_\alpha^A M_\beta^B + M_\beta^A M_\alpha^B) - J_{\alpha\beta}^{AA} M_\alpha^A M_\beta^A - J_{\alpha\beta}^{BB} M_\alpha^B M_\beta^B]
\end{aligned} \tag{5.7}$$

The partition function of the system is

$$\begin{aligned}
\mathcal{Z} &= \text{Trace} [\exp(-H/k_B T)]_{\{C\}} \\
&= 4 \exp(zN E_{\alpha\beta}/k_B T) [\cosh(zE_\alpha/2k_B T) \cosh(zE_\beta/2k_B T)]^{N/2}
\end{aligned} \tag{5.8}$$

Here $z = 8$ is the coordination number for bcc lattice and $N_\alpha = N_\beta = N/2$. In this coupled system the free energy $F \equiv F(L, M, p^A, T)$ and its minima in these parameter space are the stable statistical configurations. Eqn.5.8 is the mean-field partition function for the system with fixed magnetic moments and concentration. The free energy per atom is

$$f = -\frac{1}{2} \left[E_{\alpha\beta} + k_B T \ln \cosh \left(\frac{E_\alpha}{2k_B T} \right) + k_B T \ln \cosh \left(\frac{E_\beta}{2k_B T} \right) \right]. \tag{5.9}$$

Minimizing with respect to the chemical order parameters we get the transcendental self-consistent equations for the chemical order parameter $L(p^A, M, T)$:

$$L = \frac{1}{2} (4p^A p^B - L^2) \tanh \left(\frac{\Delta}{2kT} \right), \tag{5.10}$$

where

$$\Delta = 2zJ^{AB} (M_\alpha^A M_\beta^B - M_\alpha^B M_\beta^A) + zL \left[V - 2 \sum_{QQ'} J^{QQ'} \eta_{QQ'} M_\alpha^Q M_\beta^{Q'} \right] \tag{5.11}$$

The decoupling scheme for the spin variables $S^Q(\vec{R})$ –

$$S^Q(\vec{R}) S^{Q'}(\vec{R}') = S^Q(\vec{R}) \langle S^{Q'}(\vec{R}') \rangle + \langle S^Q(\vec{R}) \rangle S^{Q'}(\vec{R}') - \langle S^Q(\vec{R}) \rangle \langle S^{Q'}(\vec{R}') \rangle$$

for $Q \neq Q'$ and $\vec{R} \neq \vec{R}'$ – having been re-employed in Eq.5.5, the corresponding free energy minimization leads to a set of homomorphic equations for the magnetic order parameters :

$$M_{\mu}^Q = \frac{1}{2}(2S^Q + 1) \coth \left((2S^Q + 1) \frac{\Gamma_{\mu}^Q}{2kT} \right) - \frac{1}{2} \coth \left(\frac{\Gamma_{\mu}^Q}{2kT} \right), \quad (5.12)$$

where

$$\Gamma_{\mu}^Q = 2Z \left(\sum_{Q'} J^{QQ'} M_{\beta}^{Q'} p_{\mu'}^{Q'} \right) \quad (5.13)$$

The order parameters are coupled and Eqns. (5.10-5.13) constitute the mean-field equations. There are two possibilities in the physical scenario: case-I Chemical transition occurs at a higher temp. than the magnetic one so that $m_{\xi} = 0$ during transition. The chemical transition (T_0) in this case is obtained from lower order approximations of Eqn. 5.10 as $k_B T_0 = p^A p^B V$.

case-II Magnetic transition occurs in a disordered medium ($L=0$). And the transition temperature, with A -type magnetic only, is given by $2k_B T_c = \frac{v^A}{4} \sum_{QQ'} J^{QQ'} \eta_{QQ'}$.

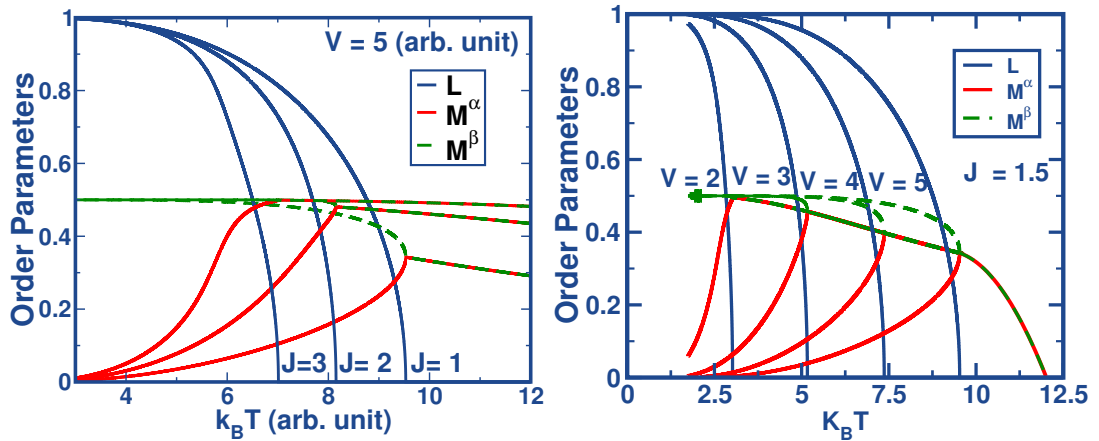


Figure 5.1: The mean-field behaviour of magnetic and chemical order parameters coupled. One of 50-50 alloy constituent is non-magnetic. (left panel) V is fixed and J is varied. Increasing J suppresses order-disorder transition temperature T_0 . (right panel) Here J is fixed and V is varied. With increasing V the magnetic critical temperature T_c is elevated.

5.1.1 Mean-Field Solution

Let us first solve the mean-field equations for a model case where only one of the constituents is magnetic and the lattice, chosen here to be the body-centred cubic, is exactly bi-partite. This means that $M_\alpha^B = M_\beta^B = 0$, $N_A = N_B = N/2$. We shall also consider simply nearest neighbour exchange energies. Referring to Eqn.5.4 we appropriately choose $V < 0$ so that we have ordering rather than a phase segregation. We shall fix parameters such that the magnetic transition takes place at a higher temperature than the order-disorder transition. The left panel of Fig. 5.1 shows the behaviour of the coupled order parameters where we fix V and vary $J = J^{AA}$. Once the magnetic transition has taken place at $k_B T > 10$ (T_c is higher for larger J) initially the alloy is still disordered and the two sub-lattice magnetizations are equal and increase as we lower the temperature. At a critical temperature $T_0 < T_c$ ordering begins and the magnetic constituent A begins to segregate to the sub-lattice labelled β and non-magnetic B segregates into the sub-lattice α . The magnetic moment (per atom) in the sub-lattice saturates at $T = 0$ to the value 0.5 ($N_A = N/2$), while that in the other goes to zero. We also note that for a fixed value of V , the order disorder transition temperature goes down with increasing J . In the right panel we show the coupled behaviour of the order parameters with a fixed value of J and varying V . The behaviour of sub-lattice magnetic moments is similar to the first example and, as expected, the ordering temperature goes down with decreasing V . The ordering temperature is therefore suppressed below its value for $M = 0$ as J increases.

The next example is one in which both the constituents are taken to be magnetic. Slightly off-stoichiometric compositions : 40-60 and 60-40 were considered. This means that even at $T = 0$ one sub-lattice will be filled with one type of atoms while the other sub-lattice must have some 10% of *wrong* type of atoms. The exchange energies were fixed at $V = 2.5$, $J^{AA} = 2.0$, $J^{BB} = 1.5$, $J^{AB} = 1.8$. As we shall see later in our study, this choice is not inappropriate for Fe_xCo_y alloys. The results are shown in Fig.5.2. Now, even after ordering begins since both the sub-lattices get populated by magnetic atoms, the magnetic moment of both the sub-lattices increase and attain saturation at $T = 0$. In this example, too, the ordering transition is suppressed below its value in the absence of magnetism. This spontaneous outcome is the main message of the coupled problem.

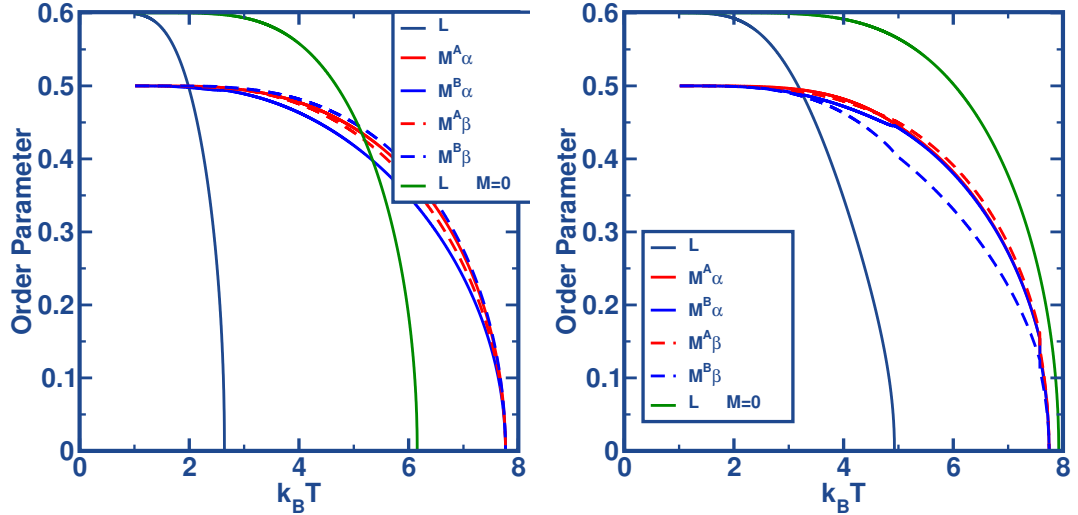


Figure 5.2: Here both the constituents are magnetic. We show the behavior of the coupled magnetic and chemical order parameters at two compositions (left) 40-60 and (right) 60-40.

5.2 Computation of Exchanges

When the lattice is divided to sub-lattices ($\xi = \alpha, \beta \dots$) quantities like $p_\xi^Q = N_\xi^Q / (N/2)$, with $Q=A/B$, represent the lro of the simulated lattice whereas the quantities $\sigma_{AB}^{\alpha\beta}$ (the probability that a specified nearest-neighbour position of an A atom on α sub-lattice is occupied by a B-atom) calculated by counting the number of AB pairs, are the short-range order parameters. Here A & B are generalised variables, can be atoms or spins. For the given values of exchanges and concentration, the degree of order at temperature T is completely characterised by these order-parameters.

The Fe_xCo_y alloy system with a body-centred cubic crystal structure undergoes a paramagnetic to ferromagnetic transition in the disordered phase at around 1250K followed by an ordering transition to a B2 structure at a lower temperature of around 1000K [Han65]. Experimental data on this alloy is available [BVC78; OC77]. Herring [Her66] showed that the magnetism in this alloy is of the itinerant type, therefore describing it in terms of an Ising model will require justification [MLF80].

We shall begin with an electronic structure determination of the valence electrons of Fe_xCo_y . Disorder fluctuations in the alloy are local. Therefore, a tight-binding basis will be the most suitable in describing such disorder. We shall choose the tight-binding, linear muffin-tin orbitals technique (TB-LMTO)[AJ84] as our basic methodology. To

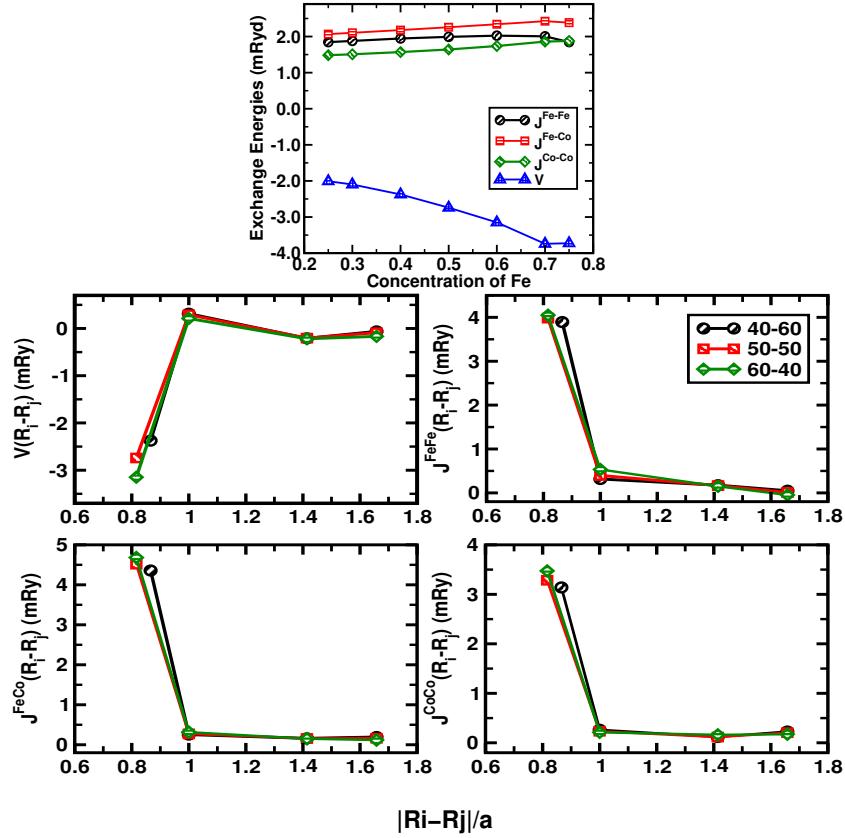


Figure 5.3: (left) Estimates of the nearest neighbour exchange energies $J^{QQ'}(R_0)$ and $V(R_0)$ for FeCo alloys obtained from the Lichtenstein formula implemented within the LMTO-CPA. (right) The spatial extent of the exchange energies.

describe disorder we shall use the the coherent potential approximation (CPA).

Once we understand how the itinerant electrons provide each atomic sphere with a magnetic moment, we note that these moments interact with one another leading to (in this case) a ferromagnetic pattern. We shall describe the ordering phenomenon following the generalized perturbation method (GPM) proposed by Ducastelle and Gautier[DG76]. We start with a perfectly random arrangement of up or down moment carrying atomic spheres of Fe and Co. Then we introduce local configuration fluctuations as perturbations into the system. The total energy in GPM is written as:

$$E = E_0 + \sum_{\vec{R}_i} E^{(1)}(\vec{R}_i) \delta n_{\vec{R}_i} + \frac{1}{2} \sum_{\vec{R}_i} \sum_{\vec{R}_j} E^{(2)}(|\vec{R}_i - \vec{R}_j|) \delta n_{\vec{R}_i} \delta n_{\vec{R}_j} + \dots \quad (5.14)$$

where $\delta n_{\vec{R}_i}$ is the perturbation in the occupation variable: depending on the orientation of moment at the site \vec{R}_i , these take the values ± 1 .

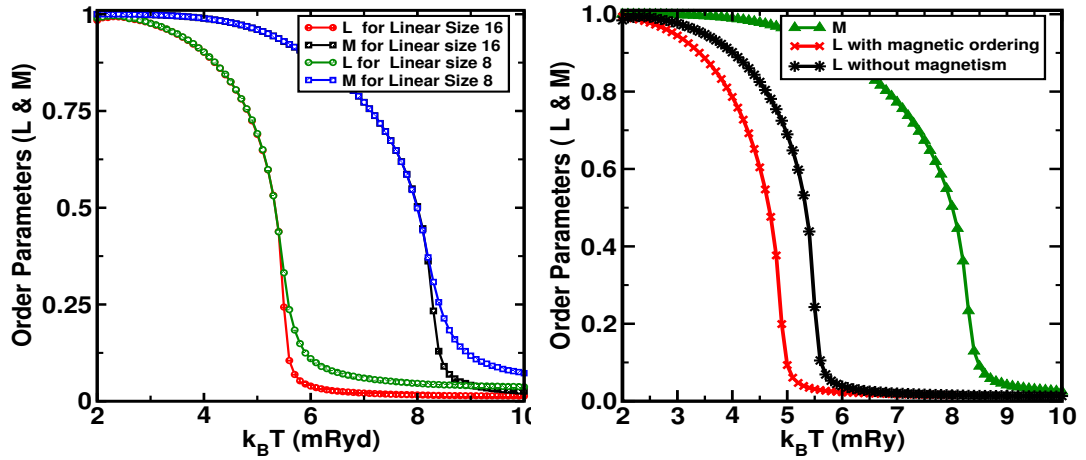


Figure 5.4: (left) Finite size effect of two order parameters with system size $\text{Fe}_{50}\text{Co}_{50}$. (right) The shift of the ordering temperature caused by magnetic ordering for $\text{Fe}_{50}\text{Co}_{50}$.

The first two terms play no role in the emergence of ordering in the bulk. The the third term $E^{(2)}$ is the required exchange interaction which maps our problem onto the equivalent Ising model of our system. The magnetic exchange interactions are calculated by the magnetic force theorem of Lichtenstein *et al.*, [Lie+87; LK84] and the chemical effective pair interactions within the GPM.

The exchange energies are shown in Fig. 5.3. We note that in contrast to earlier works with parameterized exchange couplings our first-principles approach indicates that they are explicitly composition dependent. Although all exchange energies are dominated by the nearest neighbor terms, they are also reasonably long ranged and damped. For our Monte Carlo calculations we have retained both the composition dependence and exchange energies up to the fourth nearest neighbour on the body-centred cubic lattice.

5.3 Inadequacies of Mean-field calculations

The mean-field solutions obtained earlier for model situations are indeed indicative of a strong inter-dependence. However, for the real exchanges obtained from the *ab-initio* calculations, the self-consistent equations 5.10–5.13 are numerically unstable with multiple divergences. So the transitions are not characterised properly. Furthermore, the estimation is limited to first neighbour interaction only. Though the successive exchange interactions are substantially lower compared to the first neighbour interaction, the effect of sign change up to few neighbours has to be included.

	Φ_1	Φ_2	Φ_4	Φ_8
Φ_1	2	3	5	9
Φ_2	3	4	6	10
Φ_4	5	6	8	12
Φ_8	9	10	12	16

Figure 5.5: The way all possibilities(up/down and A/B) are numbered in MC code

These inadequacies drives us for consideration of an explicit numerical simulation free from such restrictions.

5.4 Monte Carlo Set up

We shall now carry on a Monte Carlo simulation analysis with the coupled order-parameter Hamiltonian given by Eqn.(5.1) with our calculated exchange energies up to the fourth nearest neighbours on a body-centred cubic lattice. The magnetization, being a non-conserved parameter, is treated with the conventional Metropolis algorithm. On the other hand, the chemical order parameter is conserved since the global composition of the alloy remains unchanged throughout. The updating of chemical orderings has to follow Kawasaki dynamics [Kaw66]. In the Kawasaki update we exchange only nearest neighbour atoms with a probability $\min \{1, \exp -\Delta E/k_B T\}$, where ΔE is the energy cost of the interchange. The sweeps are now repeated consecutively till thermal equilibrium is achieved.

In the code, this dual degrees of freedom of a site invites additional slowing down effects. In order to streamline the incorporation to already developed code, we enlist all the four possibilities as different variables, as shown in Fig.5.5, so that any two-spin interaction is a distinct number in the array. Corresponding interaction energy is stored in a table for quick access thereby refraining from carrying out repeated floating-point operations . For each Monte Carlo step the entire lattice was updated as per the details mentioned in Ch.3. However, One Monte Carlo Step(MCS) here refers a first sweep over the lattice with one single-spin flip Metropolis updating for the magnetization

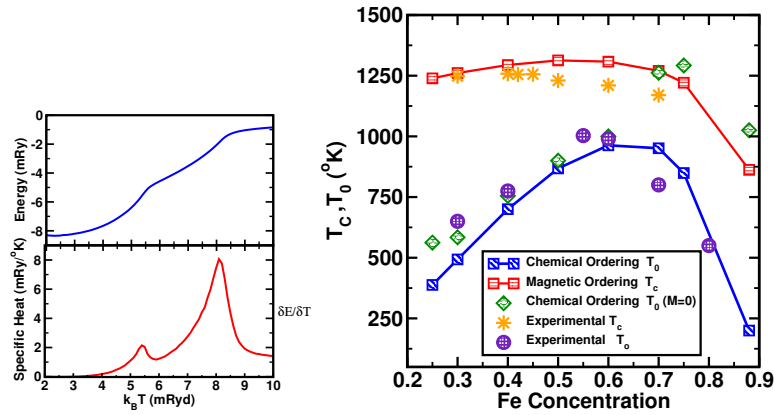


Figure 5.6: (left) Two bumps in total energy for $Fe_{50}Co_{50}$ corresponding to two peaks in the specific heat which in turn indicates the two transitions taking place. (right) Variation of the Magnetic and Ordering transition temperatures of $Fe_{50}Co_{50}$ with composition. The experimental data has been taken from HANSEN [Han65] and OYEDELE and COLLINS [OC77].

followed by a second sweep with Kawasaki updating for chemical ordering.

5.5 MC Results

In the Monte Carlo simulation, a total of 65536 steps were tried from which initial 32768 attempts were discarded before getting averages of properties. In order to avoid the possibility of getting trapped in local energy minima, we started with multiple random configurations and averaging was carried out over all of them. To get the estimates of transition temperature we carried out Monte Carlo on different cell-sized lattices and obtained the transition temperature using the universality property of the fourth order Binder cumulant [Bin81] at T_c over the finite size of the cell of the simulation. The left panel of Fig.5.4 shows the size effect on the two (scaled) order parameters. The right panel of Fig.5.4 shows the suppression of the ordering temperature because of the coupling with magnetic ordering. The left top panel of Fig.5.6 shows the internal energy variation with temperature showing the two characteristic inflection points corresponding to the two phase transitions. This is better reflected in the two peaks in the specific heat. Such a behavior was predicted also in the mean-field approach of M3ran-Lop3ez and Falicov [MLF80]. These results are for the stoichiometric 50-50 composition.

We have carried out Monte Carlo analysis for compositions across the range and

the composite results for the transition temperatures are shown in the right panel of Fig.5.6. For comparison we have also shown the experimental results from Hansen [Han65] and Oyedele and Collins [OC77]. We first note that our Monte-Carlo analysis based on our first-principles evaluation of the exchange energies for the magnetic transition agree excellently well with experimental data. In the Co rich part of the phase diagram, the magnetic and chemical transition temperatures are well separated, and the coupled and uncoupled solutions for the chemical transition temperatures agree with each other and with the experimental data. However for alloys with Fe content greater than 60%, magnetism and chemical orderings are strongly coupled with the former suppressing the latter to lower temperatures. Fig.5.6 right panel shows that the coupled solution for T_0 and experimental data agree appreciably well. The uncoupled solution is way off the mark.

5.6 Conclusion & Future Plans

We observed that the two types of transitions, magnetic and chemical order-disorder, in alloys can be interdependent on each other. Our study confirms the suppression of the chemical ordering temperature caused by a magnetic transition at a higher temperature in FeCo alloys. In the combined way of Monte Carlo simulation we devised, results obtained are in close agreement with experiments. And this agreement confirms the proposed underlying understanding of the interdependence. This general method of simulation can also be useful in combining any such interactions supposed to be inter-influential. In this study, we conclude that for studies of alloy magnetism it is imperative to take this coupling into account.

In the thesis we conducted studies on chemical and magnetic properties of disordered alloys arising from electronic interactions. We discussed the methods on disorder averaging and focussed on assessment of spontaneously manifested natural properties from *ab-initio* methods. The ground-state calculations based on DFT is utilised and combined with statistical approaches for finite temperature predictions. Reasonable agreements with experimental results were always sought for and eventually observed. Nonetheless, opportunities for improvements is never limited to predicaments. The simulation, as there always would be, has many scopes for improvements to improve the fineness of understanding.

References

- [AG01] E APINANIZ and JS GARITAONANDIA. “Influence of disorder on the magnetic properties of FeAl alloys: theory”. *Journal of Non-Crystalline* 287 (2001), pp. 302–307.
- [AHS99] VP ANTROPOV et al. “Aspects of spin dynamics and magnetic interactions”. *J. Magn. Magn. Mater.* 200.1-3 (1999), pp. 148–166.
- [AJ84] O. K. ANDERSEN and O. JEPSEN. “Explicit, First-Principles Tight-Binding Theory”. *Phys. Rev. Lett.* 53.27 (1984), pp. 2571–2574.
- [AK71] O. ANDERSEN and R. KASOWSKI. “Electronic States as Linear Combinations of Muffin-Tin Orbitals”. *Phys. Rev. B* 4.4 (1971), pp. 1064–1069.
- [And75] O. KROGH ANDERSEN. “Linear methods in band theory”. *Phys. Rev. B* 12.8 (1975), pp. 3060–3083.
- [ARM80] O. K. ANDERSEN A. R. MACKINTOSH. “Electrons at the Fermi Surface”. In: ed. by M. SPRINGFORD. Cambridge University Press, 1980. Chap. The electronic structure of transition metals.
- [Ber+88] A BERERA et al. “A direct method for obtaining effective pair interactions in binary alloys”. *J. Phys F: Met. Phys.* 18.4 (Apr. 1988), pp. L49–L55.
- [BH10] KURT BINDER and DIETER HEERMANN. *Monte Carlo Simulation in Statistical Physics: An Introduction (Graduate Texts in Physics)*. Springer, 2010.
- [Bin81] K BINDER. “Finite size scaling analysis of ising model block distribution functions”. *Zeitschrift fur Physik B Condensed Matter* 43.2 (1981), pp. 119–140.
- [Bin97] K. BINDER. “Applications of Monte Carlo methods to statistical physics”. *Reports on Progress in Physics* 487 (1997).

- [BL67] ARTHUR BIENENSTOCK and JOAN LEWIS. “Order-Disorder of Nonstoichiometric Binary Alloys and Ising Antiferromagnets in Magnetic Fields”. *Phys. Rev.* 160.2 (1967), pp. 393–403.
- [Blö29] FELIX BLÖCH. “Über die Quantenmechanik der Elektronen in Kristallgittern”. *Zeitschrift für Physik* 52.7-8 (July 1929), pp. 555–600.
- [BO27] M. BORN and R. OPPENHEIMER. “Zur Quantentheorie der Molekeln”. *Annalen der Physik* 389.20 (1927), pp. 457–484.
- [Bon+09] G. BONNY et al. “The influence of short range order on the thermodynamics of Fe-Cr alloys”. *Modelling Simul. Mater. Sci. Eng.* 17.2 (2009), p. 025006.
- [Bos+92] S. K. BOSE et al. “Electronic structure of ordered and disordered $\text{Cu}_x\text{Pd}_{1-x}$ alloys via the linear-muffin-tin-orbitals method”. *Phys. Rev. B* 45 (15 1992), pp. 8272–8282.
- [Bos+97] S. K. BOSE et al. “Theoretical study of ordering in Fe-Al alloys based on a density-functional generalized-perturbation method”. *Phys. Rev. B* 55.13 (1997), pp. 8184–8193.
- [BP84] N. BEER and D. PETTIFOR. *The Electronic Structure of Complex Systems*. Plenum Press, New York, 1984.
- [Bur+83] S K BURKE et al. “The evolution of magnetic order in CrFe alloys. II. Onset of ferromagnetism”. *Journal of Physics F: Metal Physics* 13.2 (1983), pp. 451–470.
- [Bur76] N.R. BURKE. “A Tight-Binding theory of the interactions between transition metal adatoms adsorbed on a transition metal substrate”. *Surf. Sci.* 58 (1976), pp. 349–373.
- [BV71] F. BROUERS and A.V. VEDYAYEV. “On the magnetic properties of substitutional disordered ferromagnets”. *Sol. St. Comm.* 9.17 (1971), pp. 1521–1524.
- [BVC78] L BILLARD et al. “Short-range and long-range ordering in ferromagnetic binary alloys”. *J. Phys. C: Solid State Phys.* 11.13 (1978), pp. 2815–2822.
- [BY85] R. BHATT and A. YOUNG. “Search for a Transition in the Three-Dimensional $\pm J$ Ising Spin-Glass”. *Phys. Rev. Lett.* 54.9 (1985), pp. 924–927.

- [CJR79] MICHAEL CREUTZ et al. “Experiments with a Gauge-Invariant Ising System”. *Phys. Rev. Lett.* 42.21 (1979), pp. 1390–1393.
- [CLB86] MURTY CHALLA et al. “Finite-size effects at temperature-driven first-order transitions”. *Phys. Rev. B* 34.3 (1986), pp. 1841–1852.
- [CM01] A. CHAKRABARTI and A. MOOKERJEE. “Augmented-space recursion for partially disordered systems”. *J. Phys.: Condens. Matter* 13.45 (2001), pp. 10149–10157.
- [CM66] PHILIP CLAPP and SIMON MOSS. “Correlation Functions of Disordered Binary Alloys. I”. *Phys. Rev.* 142.2 (1966), pp. 418–427.
- [CM68] PHILIP CLAPP and S. MOSS. “Correlation Functions of Disordered Binary Alloys. II”. *Phys. Rev.* 171.3 (1968), pp. 754–763.
- [Cow50a] J. COWLEY. “An Approximate Theory of Order in Alloys”. *Phys. Rev.* 77.5 (1950), pp. 669–675.
- [Cow50b] JM COWLEY. “X-Ray Measurement of Order in Single Crystals of Cu₃Au”. *J. Appl. Phys.* 21.1 (1950), pp. 24–30.
- [CS+88] D. CONTRERAS-SOLORIO et al. “Modeling of the Fe-Al phase diagram”. *Phys. Rev. B* 38.16 (1988), pp. 11481–11485.
- [CS35] E. U. CONDON and G. H. SHORTLEY. *The Theory of Atomic Spectra*. Cambridge University Press, 1935.
- [CW83] J. CONNOLLY and A. WILLIAMS. “Density-functional theory applied to phase transformations in transition-metal alloys”. *Phys. Rev. B* 27.8 (1983), pp. 5169–5172.
- [DB87] B. DÜNWEG and K. BINDER. “Model calculations of phase diagrams of magnetic alloys on the body-centered-cubic lattice”. *Phys. Rev. B* 36.13 (1987), pp. 6935–6952.
- [DG76] F. DUCASTELLE and F. GAUTIER. “Generalized perturbation theory in disordered transitional alloys: Applications to the calculation of ordering energies”. *J. Phys, F: Met. Phys.* 2039 (1976).
- [DM96] I. DASGUPTA and A. MOOKERJEE. “An augmented-space recursive method for the study of concentration profiles at CuNi alloy surfaces”. *J. Phys.: Condens. Matter* 8.23 (1996), pp. 4125–4137.

- [Dor99] S. DORFMAN. “Concentration dependencies of energy parameters in Fe-Al alloy”. *Solid State Commun.* 113.1 (1999), pp. 53–57.
- [Dre+89] H. DREYSSÉ et al. “Determination of effective-pair interactions in random alloys by configurational averaging”. *Phys. Rev. B* 39.4 (1989), pp. 2442–2452.
- [Ehr80] HENRY EHRENREICH, ed. *Solid State Physics: Advances in Research and Applications*. Vol. 35. Academic Press, 1980.
- [ES76] H. EHRENREICH and L.M. SCHWARTZ. “The Electronic Structure of Alloys”. In: *Solid State Physics*. Ed. by H. EHRENREICH et al. Vol. 31. Academic Press, 1976, pp. 149–286.
- [Fau82] J.S. FAULKNER. “The modern theory of alloys”. *Prog. Mater Sci.* 27.1-2 (1982), pp. 1–187.
- [FD83] A. FINEL and F. DUCASTELLE. “Ordered Structures on the BCC Lattice with First, Second, Third and Fifth Neighbour Interactions”. *MRS Proceedings, Cambridge University Press (CUP)* 21 (1983).
- [Fli56] P. FLINN. “Electronic Theory of Local Order”. *Phys. Rev.* 104.2 (1956), pp. 350–356.
- [Foc30] V. FOCK. “Näherungsmethode zur Lösung des quantenmechanischen Mehrkörperproblems”. *Z. Angew. Phys.* 61.1-2 (1930), pp. 126–148.
- [Gan+11] S. GANGULY et al. “Augmented space recursion formulation of the study of disordered alloys with noncollinear magnetism and spin-orbit coupling: Application to MnPt and Mn₃Rh”. *Phys. Rev. B* 83.9 (2011), pp. 1–10.
- [GDM97] SUBHRADIP GHOSH et al. “Convergence of the augmented-space recursion”. *J. Phys.: Condens. Matter* 9.48 (1997), pp. 10701–10714.
- [GG77] A. GONIS and J. GARLAND. “Multishell method: Exact treatment of a cluster in an effective medium”. *Phys. Rev. B* 16.6 (1977), pp. 2424–2436.
- [Gia95] STEFANO GIALANELLA. “FeAl alloy disordered by ball-milling”. *Intermetallics* 3.1 (1995), pp. 73–76.
- [Gla63] ROY J. GLAUBER. “Time-Dependent Statistics of the Ising Model”. *Journal of Mathematical Physics* 4.2 (1963), p. 294.

- [Gon+84] A. GONIS et al. "Local-environment fluctuations and densities of states in substitutionally disordered alloys". *Phys. Rev. B* 29.2 (1984), pp. 555–567.
- [Gon+87] A. GONIS et al. "Configurational energies and effective cluster interactions in substitutionally disordered binary alloys". *Phys. Rev. B* 36.9 (1987), pp. 4630–4646.
- [GP00] G. GROSSO and G.P. PARRAVICINI. *Solid state physics*. San Diego: Academic Press, 2000.
- [GS83] B. GYORFFY and G. STOCKS. "Concentration Waves and Fermi Surfaces in Random Metallic Alloys". *Phys. Rev. Lett.* 50.5 (1983), pp. 374–377.
- [GTP76] N.S. GOLOSOV et al. "Theory of order-disorder and order-order transformation in binary alloys with BCC lattice-III.: Atomic ordering in Fe-Al system". *J. Phys. Chem. Solids* 37.3 (1976), pp. 273–277.
- [Han65] MAX HANSEN. *Constitution of Binary Alloys*. McGraw-Hill, 1965.
- [Har28a] D. R. HARTREE. "The Wave Mechanics of an Atom with a Non-Coulomb Central Field. Part I. Theory and Methods". *Mathematical Proceedings of the Cambridge Philosophical Society* 24.01 (1928), pp. 89–110.
- [Har28b] D. R. HARTREE. "The Wave Mechanics of an Atom with a Non-Coulomb Central Field. Part II. Some Results and Discussion". *Math. Proc. Camb. Phil. Soc.* 24.01 (1928), p. 111.
- [Har28c] D. R. HARTREE. "The Wave Mechanics of an Atom with a non-Coulomb Central Field. Part III. Term Values and Intensities in Series in Optical Spectra". *Math. Proc. Camb. Phil. Soc.* 24.03 (1928), p. 426.
- [Har29] D. R. HARTREE. "The Wave Mechanics of an Atom with a Non-Coulomb Central Field. Part IV. Further Results relating to Terms of the Optical Spectrum". *Math. Proc. Camb. Phil. Soc.* 25.03 (1929), p. 310.
- [Has80] MASAYUKI HASAKA. "Ordering and Phase Separation in the Fe-Al Alloy". *Transactions of the Japan Institute of Metals* 21.10 (1980), pp. 660–666.
- [HDZ90] K. HASS et al. "Electronic structure of random Al_{0.5}Ga_{0.5}As alloys: Test of the "special-quasirandom-structures" description". *Phys. Rev. B* 42.6 (1990), pp. 3757–3760.

- [Hen83] M. HENNION. “Chemical SRO effects in ferromagnetic Fe alloys in relation to electronic band structure”. *J. Phys. F: Met. Phys.* 2351 (1983).
- [Her66] C. HERRING. “Exchange Interactions Among Itinerant Electrons”. In: *Magnetism*. Ed. by T. RADO and H. SUHL. Vol. 4. New York, USA: Academic Press, 1966.
- [HHK72] R. HAYDOCK et al. “Electronic structure based on the local atomic environment for tight-binding bands”. *J. Phys. C: Solid State Phys.* 5.20 (1972), pp. 2845–2858.
- [HK64] P. HOHENBERG and W. KOHN. “Inhomogeneous Electron Gas”. *Phys. Rev.* 136.3B (1964), B864–B871.
- [Hou63] CR HOUSKA. “A theoretical treatment of atomic configurations found in some iron-aluminum solid solutions”. *J. Phys. Chem. Solids* 24 (1963), pp. 95–107.
- [HS75] B. HUBERMAN and W. STREIFER. “Coupled order parameters, lattice disorder, and magnetic phase transitions”. *Phys. Rev. B* 12.7 (1975), pp. 2741–2746.
- [Hud+04] AIN-UL HUDA et al. “Spin-orbit coupling: a recursion method approach”. *Physica B: Condensed Matter* 351.1-2 (2004), pp. 63–70.
- [Ike+01] O. IKEDA et al. “Phase equilibria and stability of ordered BCC phases in the Fe-rich portion of the Fe-Al system”. *Intermetallics* 9.9 (2001), pp. 755–761.
- [Jia+04] CHAO JIANG et al. “First-principles study of binary bcc alloys using special quasirandom structures”. *Phys. Rev. B* 69.21 (2004), p. 214202.
- [Kad+67] L. KADANOFF et al. “Static Phenomena Near Critical Points: Theory and Experiment”. *Reviews of Modern Physics* 39.2 (1967), pp. 395–431.
- [Kaw66] KYOZI KAWASAKI. “Diffusion Constants near the Critical Point for Time-Dependent Ising Models. I”. *Phys. Rev.* 145.1 (1966), pp. 224–230.
- [KDF06] T. P. C. KLAVER et al. “Magnetism and thermodynamics of defect-free Fe-Cr alloys”. *Phys. Rev. B* 74 (9 2006), p. 094435.
- [KG76] THEODORE KAPLAN and L. GRAY. “Elementary excitations in random substitutional alloys”. *Phys. Rev. B* 14.8 (1976), pp. 3462–3470.

- [Kik+80] R. KIKUCHI et al. “Theoretical calculation of the Cu-Ag-Au coherent phase diagram”. *Acta Metallurgica* 28.5 (1980), pp. 651–662.
- [Kik51] RYOICHI KIKUCHI. “A Theory of Cooperative Phenomena”. *Phys. Rev.* 81.6 (1951), pp. 988–1003.
- [Koj85] NORIMICHI KOJYO. “Coherent Cluster Theory for Static and Dynamic Disordered Systems on Bethe Lattices”. *J. Phys. Soc. Jpn.* 54.4 (1985), pp. 1486–1496.
- [Kor47] J KORRINGA. “On the calculation of the energy of a Bloch wave in a metal”. *Physica* X.6 (1947), pp. 392–400.
- [Kor94] J KORRINGA. “Early history of multiple scattering theory for ordered systems”. *Phys. Rep.* 238.6 (1994), pp. 341–360.
- [KR54] W. KOHN and N. ROSTOKER. “Solution of the Schrödinger Equation in Periodic Lattices with an Application to Metallic Lithium”. *Phys. Rev.* 94.5 (1954), pp. 1111–1120.
- [Kri69] M.A. KRIVOGLAZ. *Theory of X-ray and thermal-neutron scattering by real crystals*. Plenum Press, 1969.
- [KS65] W. KOHN and L. SHAM. “Self-Consistent Equations Including Exchange and Correlation Effects”. *Phys. Rev.* 140.4A (1965), A1133–A1138.
- [KS74] RYOICHI KIKUCHI and HIROSHI SATO. “Characteristics of superlattice formation in alloys of face centered cubic structure”. *Acta Metallurgica* 22.9 (1974), pp. 1099–1112.
- [LA07] N H LONG and H AKAI. “First-principles KKR-CPA calculation of interactions between concentration fluctuations”. *J. Phys.: Condens. Matter* 19.36 (2007), p. 365232.
- [Lav+07] M. YU. LAVRENTIEV et al. “Monte Carlo study of thermodynamic properties and clustering in the bcc Fe-Cr system”. *Phys. Rev. B* 75 (2007), p. 014208.
- [LB00] DAVID P. LANDAU and KURT BINDER. *A Guide to Monte Carlo Simulations in Statistical Physics*. Cambridge University Press, 2000.
- [LDF02] VLAD LIUBICH et al. “Non-empirical study of phase competition in A2-B2 mixture in Fe-Al alloy”. *Computational Materials Science* 24.1-2 (2002), pp. 268–272.

- [LDNM09] M.YU. LAVRENTIEV et al. “Magnetic cluster expansion simulations of FeCr alloys”. *J. Nucl. Mater.* 386-388 (2009), pp. 22–25.
- [Ler+09] D LERCH et al. “UNCLE: a code for constructing cluster expansions for arbitrary lattices with minimal user-input”. *Modelling and Simulation in Materials Science and Engineering* 17.5 (2009), p. 055003.
- [Lev79] MEL LEVY. “Universal variational functionals of electron densities, first-order density matrices, and natural spin-orbitals and solution of the v-representability problem”. *PNAS* 76.12 (1979), pp. 6062–6065.
- [Lie+87] A.I. LIECHTENSTEIN et al. “Local spin density functional approach to the theory of exchange interactions in ferromagnetic metals and alloys”. *J. Magn. Mater.* 67.1 (1987), pp. 65–74.
- [Lie83] ELLIOTT H. LIEB. “Density functionals for coulomb systems”. *Int. J. Quant. Chem.* 24.3 (1983), pp. 243–277.
- [LK84] AI LIECHTENSTEIN and MI KATSNELSON. “Exchange interactions and spin-wave stiffness in ferromagnetic metals”. *J. Phys. F: Met. Phys* 125 (1984).
- [LN87] M U LUCHINI and C M M NEX. “A new procedure for appending terminators in the recursion method”. *J. Phys. C: Solid State Phys.* 20.21 (1987), pp. 3125–3130.
- [Lou67] T. L. LOUCKS. *Augmented Plane Wave Methods*. Benjamin, New York, 1967.
- [Mar04] R. MARTIN. *Electronic structure : basic theory and practical methods*. Cambridge, UK New York: Cambridge University Press, 2004.
- [McG01] R L MCGREEVY. “Reverse Monte Carlo modelling”. *J. Phys.: Condens. Matter* 13.46 (2001), R877–R913.
- [Met+53] NICHOLAS METROPOLIS et al. “Equation of State Calculations by Fast Computing Machines”. *The Journal of Chemical Physics* 21.6 (1953), p. 1087.
- [MF74] T.W. MCDANIEL and C.L. FOILES. “Paramagnetic curie temperature in dilute magnetic alloys: Influence of order-disorder transitions”. *Solid State Commun.* 14.9 (1974), pp. 835–839.

- [MH+85] F. J. MARTÍNEZ-HERRERA et al. “Theory of phase equilibria in Co-Fe alloys”. *Phys. Rev. B* 31 (1985), pp. 1686–1688.
- [MH92] R L MCGREEVY and M A HOWE. “RMC: Modeling Disordered Structures”. *Annu. Rev. Mater. Sci.* 22.1 (1992), pp. 217–242.
- [MLF80] J L MORÁN-LÓPEZ and L M FALICOV. “Ferromagnetism and spatial long-range order in binary alloys”. *J. Phys. C: Solid State Phys.* 13.9 (1980), pp. 1715–1723.
- [MLUML81] F. MEJÍA-LIRA et al. “Order-disorder transformations in ferromagnetic binary alloys”. *Phys. Rev. B* 24.9 (1981), pp. 5270–5276.
- [Moo02] A. MOOKERJEE. “Electronic Structure of Alloys, Surfaces and Clusters”. In: ed. by A. MOOKERJEE and D. D. SHARMA. CRC Press, 2002. Chap. 3, p. 71.
- [Moo73a] A MOOKERJEE. “A new formalism for the study of configuration-averaged properties of disordered systems”. *J. Phys. C: Solid State Phys.* 6.10 (1973), p. L205.
- [Moo73b] A MOOKERJEE. “Averaged density of states in disordered systems”. *J. Phys. C: Solid State Phys.* 6.8 (1973), p. 1340.
- [MP93] ABHIJIT MOOKERJEE and RAJENDRA PRASAD. “Generalized augmented-space theorem for correlated disorder and the cluster-coherent-potential approximation”. *Phys. Rev. B* 48.24 (1993), pp. 17724–17731.
- [MR78] R. MILLS and P. RATANAVARARAKSA. “Analytic approximation for substitutional alloys”. *Phys. Rev. B* 18 (10 1978), pp. 5291–5308.
- [MU49] NICHOLAS METROPOLIS and S. ULAM. “The monte carlo method”. *J. Am. Stat. Assoc.* 44.247 (1949), pp. 335–341.
- [Mul03] STEFAN MULLER. “Bulk and surface ordering phenomena in binary metal alloys”. *J. Phys.: Condens. Matter* 15.34 (2003), R1429–R1500.
- [MV93] G. MÜLLER and V.S. VISWANATH. *The User-friendly Recursion Method*. Troisième cycle de la physique en Suisse romande. Université, Bâtiment des sciences physiques, M.D. Reymond, 1993.
- [MYM04] A. A. MIRZOEV et al. “Calculation of the Energy of Mixing for the Fe-Cr Alloys by the First-Principles Methods of Computer Simulation”. *The Physics of Metals and Metallography* 97.4 (2004), p. 336.

- [NB73] BERNIE NICKEL and WILLIAM BUTLER. “Problems in Strong-Scattering Binary Alloys”. *Phys. Rev. Lett.* 30.9 (1973), pp. 373–377.
- [NB99] M. E. J. NEWMAN and G. T. BARKEMA. *Monte Carlo methods in statistical physics*. Oxford New York: Clarendon Press Oxford University Press, 1999.
- [OAW06] P. OLSSON et al. “Electronic origin of the anomalous stability of Fe-rich bcc Fe-Cr alloys”. *Phys. Rev. B* 73 (2006), p. 104416.
- [OC77] J. OYEDELE and M. COLLINS. “Composition dependence of the order-disorder transition in iron-cobalt alloys”. *Phys. Rev. B* 16.7 (1977), pp. 3208–3212.
- [Ols+05] PÄR OLSSON et al. “Two-band modeling of α' -phase formation in Fe-Cr”. *Phys. Rev. B* 72 (2005), p. 214119.
- [Osw+85] A OSWALD et al. “Interaction of magnetic impurities in Cu and Ag”. *Journal of Physics F: Metal Physics* 15.1 (1985), pp. 193–212.
- [Pea72] W. B. PEARSON. *The crystal chemistry and physics of metals and alloys*. New York: Wiley-Interscience, 1972.
- [Pet72] DG PETTIFOR. “First principle basis functions and matrix elements in the H-NFE-TB representation”. *J. Phys. C: Solid State Phys.* 5 (1972), p. 97.
- [PH67] JOEL PHILHOURS and GEORGE HALL. “Ordering Conditions. I. For Alloys Represented by Generalized Ising Models”. *Phys. Rev.* 163.2 (1967), pp. 460–462.
- [PK59] JAMES PHILLIPS and LEONARD KLEINMAN. “New Method for Calculating Wave Functions in Crystals and Molecules”. *Phys. Rev.* 116.2 (1959), pp. 287–294.
- [Pra92] R. PRASAD. “KKR Approach to Random Alloys”. In: *Lectures on Methods of Electronic Structure Calculations*. Ed. by V. KUMAR et al. World Scientific, 1992, pp. 211–230.
- [RC80] ZOLTÁN RÁCZ and MALCOLM F. COLLINS. “Effect of three-body interactions on the ordering of bcc binary alloys”. *Phys. Rev. B* 21 (1980), pp. 229–237.

- [Row+05] D. ROWLANDS et al. “Effect of short-range order on the electronic structure of disordered metallic systems”. *Phys. Rev. B* 72.045101 (2005), pp. 1–8.
- [RS02] A. RUBAN and H. SKRIVER. “Screened Coulomb interactions in metallic alloys. I. Universal screening in the atomic-sphere approximation”. *Phys. Rev. B* 66.2 (2002), pp. 1–15.
- [Sah+03] KAMAL KRISHNA SAHA et al. “Symmetry reduction in the augmented space recursion formalism for random binary alloys”. *J. Phys.: Condens. Matter* 16.8 (2003), p. 18.
- [Sch92] F SCHMID. “Modelling order-disorder and magnetic transitions in iron-aluminium alloys”. *J. Phys.: Condens. Matter* 4 (1992).
- [SDG84] J. SANCHEZ et al. “Generalized cluster description of multicomponent systems”. *Physica A: Statistical and Theoretical Physics* 128.1-2 (1984), pp. 334–350.
- [SDM94] T SAHA et al. “An augmented-space recursive technique for the calculation of electronic structure of random binary alloys”. *J. Phys.: Condens. Matter* 6.17 (1994), L245–L251.
- [Sel06] W. SELKE. “Critical Binder cumulant of two-dimensional Ising models”. *The European Physical Journal B* 51.2 (2006), pp. 223–228.
- [SF78] J. SANCHEZ and D. de FONTAINE. “The fee Ising model in the cluster variation approximation”. *Phys. Rev. B* 17.7 (1978), pp. 2926–2936.
- [SK54] J. C. SLATER and G. F. KOSTER. “Simplified LCAO Method for the Periodic Potential Problem”. *Phys. Rev.* 94.6 (1954), pp. 1498–1524.
- [Skr11] HANS L. SKRIVER. *The LMTO Method: Muffin-Tin Orbitals and Electronic Structure*. Springer, 2011.
- [Skr85] H. L. SKRIVER. “Crystal structure from one-electron theory”. *Phys. Rev. B* 31.4 (1985), pp. 1909–1923.
- [Sla37] J. SLATER. “Wave Functions in a Periodic Potential”. *Phys. Rev.* 51.10 (1937), pp. 846–851.
- [SM96] TANUSRI SAHA and ABHIJIT MOOKERJEE. “The effects of local lattice distortion in non-isochoric alloys: CuPd and CuBe”. *J. Phys.: Condens. Matter* 8.17 (1996), 2915–2927.

- [SM98] N. SAUNDERS and A. P. MIODOWNIK, eds. *CALPHAD (Calculation of Phase Diagrams): A Comprehensive Guide*. Vol. 1. Pergamon Materials Series, 1998.
- [Smi+08] THOMAS H R SMITH et al. “Interfaces in confined Ising models: Kawasaki, Glauber and sheared dynamics”. *J. Phys.: Condens. Matter* 20.49 (2008), p. 494237.
- [SO80] H. SAGANE and K. OKI. “Equilibria on the Ordered Phase Fe₃Al”. *Transactions of the Japan Institute of Metals* 21.12 (1980), pp. 811–818.
- [Sov67] PAUL SOVEN. “Coherent-Potential Model of Substitutional Disordered Alloys”. *Phys. Rev.* 156.3 (1967), pp. 809–813.
- [Sov70] PAUL SOVEN. “Application of the Coherent Potential Approximation to a System of Muffin-Tin Potentials”. *Phys. Rev. B* 2.12 (1970), pp. 4715–4722.
- [Sun+09] BO SUNDMAN et al. “An assessment of the entire Al-Fe system including DO₃ ordering”. *Acta Materialia* 57.10 (2009), pp. 2896–2908.
- [SW80] PRABODH SHUKLA and MICHAEL WORTIS. “Spin-glass behavior in iron-aluminum alloys: A microscopic model”. *Phys. Rev. B* 21.1 (1980), pp. 159–164.
- [The74] A. THEUMANN. “Generalized CPA approach to the disordered Heisenberg ferromagnet”. *J. Phys. C: Solid State Phys.* 7 (1974), p. 2328.
- [TJ58] A. TAYLOR and R.M. JONES. “Constitution and magnetic properties of iron-rich iron-aluminum alloys”. *J. Phys. Chem. Sol.* 6.1 (1958), pp. 16–37.
- [TK72] RAZA TAHIR-KHELI. “Spatially Random Heisenberg Spins at Very Low Temperatures. I. Dilute Ferromagnet”. *Phys. Rev. B* 6.7 (1972), pp. 2808–2825.
- [TkK77] RAZA TAHIR-KHELI and TATUO KAWASAKI. “Simultaneous occurrence of magnetic and spatial long-range order in binary alloys”. *J. Phys. C: Solid State Phys.* 10.1977 (1977), p. 2207.
- [Tur+88] P. TURCHI et al. “First-principles study of ordering properties of substitutional alloys using the generalized perturbation method”. *Phys. Rev. B* 37.10 (1988), pp. 5982–5985.

- [VB73] C.M. VAN BAAL. “Order-disorder transformations in a generalized Ising alloy”. *Physica* 64.3 (1973), pp. 571–586.
- [VS98] THOMAS VOJTA and MICHAEL SCHREIBER. “Differences between regular and random order of updates in damage-spreading simulations”. *Phys. Rev. E* 58 (6 1998), pp. 7998–8000.
- [Wan+91] J.C. WANG et al. “The positron study of the process of heat-treatments of three important $\text{Fe}_x\text{Al}_{1-x}$ alloys”. *Scripta Metallurgica et Materialia* 25.11 (1991), pp. 2581–2583.
- [WC02] A. WALLE and G. CEDER. “Automating first-principles phase diagram calculations”. *J. Phase Equilib.* 23.4 (2002), pp. 348–359.
- [Wei+90] S.-H. WEI et al. “Electronic properties of random alloys: Special quasirandom structures”. *Phys. Rev. B* 42.15 (1990), pp. 9622–9649.
- [Wik14] WIKIPEDIA. *Adiabatic theorem* — *Wikipedia, The Free Encyclopedia*. [Online; accessed 14-August-2014]. 2014.
- [Wol+93] C. WOLVERTON et al. “Ab initio determination of structural stability in fcc-based transition-metal alloys”. *Phys. Rev. B* 48.2 (1993), pp. 726–747.
- [WS34] E. WIGNER and F. SEITZ. “On the Constitution of Metallic Sodium. II”. *Phys. Rev.* 46.6 (1934), pp. 509–524.
- [WWD85] M. WEINERT et al. “Total-energy differences and eigenvalue sums”. *Phys. Rev. B* 32.4 (1985), pp. 2115–2119.
- [ZHR81] R. ZORN et al. “Tests of the multi-spin-coding technique in Monte Carlo simulations of statistical systems”. *Comp. Phys. Comm.* 23.4 (1981), pp. 337–342.
- [Zun+90] ALEX ZUNGER et al. “Special quasirandom structures”. *Phys. Rev. Lett.* 65.3 (1990), pp. 353–356.